THE S-MATRIX FORMULATION OF QUANTUM STATISTICAL MECHANICS, WITH APPLICATION TO COLD QUANTUM GAS

A Dissertation

Presented to the Faculty of the Graduate School

of Cornell University

in Partial Fulfillment of the Requirements for the Degree of

Doctor of Philosophy

by

Pye Ton How

August 2011

THE S-MATRIX FORMULATION OF QUANTUM STATISTICAL MECHANICS, WITH APPLICATION TO COLD QUANTUM GAS

Pye Ton How, Ph.D.

Cornell University 2011

A novel formalism of quantum statistical mechanics, based on the zero-temperature S-matrix of the quantum system, is presented in this thesis. In our new formalism, the lowest order approximation ("two-body approximation") corresponds to the exact resummation of all binary collision terms, and can be expressed as an integral equation reminiscent of the thermodynamic Bethe Ansatz (TBA). Two applications of this formalism are explored: the critical point of a weakly-interacting Bose gas in two dimensions, and the scaling behavior of quantum gases at the unitary limit in two and three spatial dimensions. We found that a weakly-interacting 2D Bose gas undergoes a superfluid transition at $T_c \approx 2\pi n/[m \log(2\pi/mg)]$, where n is the number density, m the mass of a particle, and g the coupling. In the unitary limit where the coupling g diverges, the two-body kernel of our integral equation has simple forms in both two and three spatial dimensions, and we were able to solve the integral equation numerically. Various scaling functions in the unitary limit are defined (as functions of μ/T) and computed from the numerical solutions. For bosons in three spatial dimensions, we present evidence that the gas undergoes a strongly interacting version of Bose-Einstein condensation at $n\lambda_T^3 \approx 1.3$, where n is the number density and λ_T is the thermal wavelength. Finally, we look at the ratio of shear viscosity to entropy density η/s of the unitary quantum gas, which has a conjectured lower bound of $\eta/s \geq \hbar/4\pi k_b$ based on the AdS/CFT correspondence of a strongly coupled Yang-Mills theory.

BIOGRAPHICAL SKETCH

Pye Ton How was born on February 16, 1981 in Pulau Pinang, Malaysia. His family moved to Taiwan a few months later, and he grew up and went to school there.

The family moved back to Malaysia once again when he was sixteen. After two years of high school in Malaysia, he went on to attend the University of Cambridge in the United Kingdom. He was a member of Selwyn College, elected college scholar twice, and a fellow of the Cambridge Commonwealth Society.

He obtained the Bachelor of Art (Honor first class) and the Master of Natural Sciences from University of Cambridge in June 2002, but decided to stay one more year and attend what is known as the Part III of the Mathematical Tripos. He received the Certificate of Advanced Studies in Mathematics (CASM) with distinction in June 2003.

After leaving Cambridge, he became a research associate for one year under Professor Fun Hoong Kun in the School of Physics, Universiti Sains Malaysia. He joined the Physics graduate program of Cornell University in August 2004.

ACKNOWLEDGEMENTS

First and foremost, I owe my deepest gratitude to my advisor Prof. André LeClair for patiently guiding me through all these years of grad school.

I would also like to thank Mr. John Miner and Prof. Jeevak Parpia. If not for your great patient, understanding, and continual support, I would not have made it.

I thank Prof. Erich Mueller for his sometimes harsh, but always to-the-point and extremely useful criticism to my work.

To all of the undergraduate students I have taught as a TA: thank you all for putting up with my badly designed quizzes and those ill-prepared sections. The positive feedbacks I occasionally received really made me happy.

And finally, to all Physics graduate students: I really enjoyed my time here, and it's all thanks to you guys.

TABLE OF CONTENTS

LIST OF FIGURES

CHAPTER 1

INTRODUCTION

1.1 Non-perturbative method in quantum field theories

With the exception of the exactly solvable models, the only known method of quantizing a field theory is through perturbative expansion [37, 11]. Given a classical filed theory action S, it must first be separated into two parts:

$$S = S_0 + S_1, \tag{1.1}$$

where S_0 is quadratic in the field degrees of freedom and admits (classically) plane-wave solutions, while S_1 is treated as a small perturbation. This way of quantizing a field theory has a very intuitive interpretation: the plane-wave solutions of S_0 describe freely moving particles, and S_1 adds to it interaction between particles. Then the perturbation theory is an expansion in the powers of the interaction parameter.

The initial application of this perturbative quatization scheme to the quantum electrodynamics (QED) was a spectacular success [37], thanks to the existence of a small parameter, the fine structure constant $\alpha \approx 1/137$. However, it soon became evident that not all problems can be treated within this scheme.

It is conceivable that a problem may be without a truly small parameter that allows for an expansion. There are also cases where the desired result has a non-analytic dependent in the interaction parameter, rendering any truncated power series qualitatively incorrect.

To tackle such problems theoretically, one may invent an alternative small

parameter and derive an expansion around it. The semi-classical expansion in powers of $\hbar$, the large-N expansion, and the ϵ expansion are a few examples. On the other hand, one may attack the problem more directly by explicitly resumming an infinite subset of terms in the perturbation series.

A well-known example of such resummation, though not necessarily known to all in field-theoretic form, is the Thomas-Fermi screening of the electrostatic potential in a Fermi liquid [39].

The field theory for a Fermi liquid consists of electron and hole excitations near the Fermi surface, and the $1/r$ electrostatic potential as a perturbation. In momentum space, we may use solid lines to represent electrons and holes, and dashed line to represent $\tilde{U}(k)$, the Fourier transform of the potential. See Fig. 1.1(a).

The lowest-order correction to the interaction potential is represented by the Feynman diagram 1.1(b). The loop integral, however, diverges in this case. Thus it becomes necessary to sum over diagrams of the form Fig. 1.1(c) to all order. The result is simple:

$$\begin{aligned} \tilde{U}_{eff}(k) &= \tilde{U}(k) \sum_{n=0}^{\infty} \left(\tilde{U}(k) \int (\text{loop}) \right) \\ &= \frac{\tilde{U}(k)}{1 - \tilde{U}(k) \int (\text{loop})}, \end{aligned} \tag{1.2}$$

and is vanishingly small due to the diverging denominator. As one can see, the interaction potential $\tilde{U}$ ends up in the denominator of the full expression. This type of behavior can't be captured by any truncated expansion.

Another example of non-perturbative phenomena in field theory is the self-energy of a scalar particle at finite temperature in four dimensional spacetime [27]. Assuming that the scalar field theory has a quartic interaction as allowed by

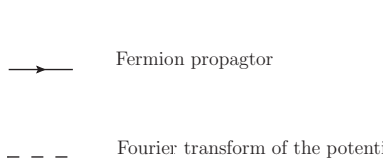

(a) Feynman rule for a Fermi liquid.

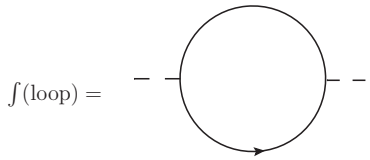

(b) The one-loop correction to interaction.

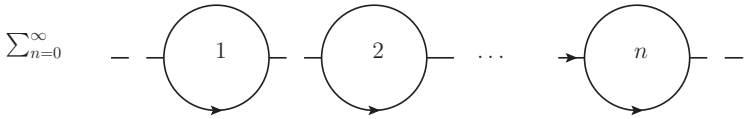

(c) The diagrams that needs to be re-summed.

Figure 1.1: The Feynman diagrams related to Thomas-Fermi screening.

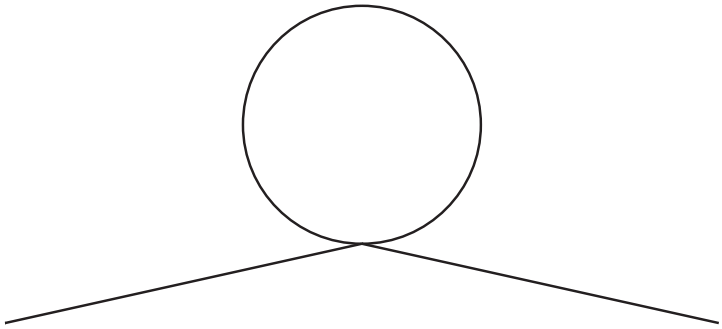

Figure 1.2: The lowest order correction to self energy of a scalar ϕ^4 theory. The next order correction comes from imposing a self-consistent condition on this diagram.

symmetry, with coupling strength g, the leading order correction is given by the simple bubble diagram 1.2, and is linear in g. However, the sub-leading term is known to be of order $g^{3/2}$. This result is obtained by imposing a self-consistent condition on the self-energy. Clearly no truncated expansion in powers of g can yield such a result.

In this thesis, we will develop an alternative representation of the free energy of an interacting quantum field theory, based on its zero-temperature S-matrix. Each term in our expansion contains an infinite number of Feynman diagrams.

Therefore the lowest order, or "two-body" approximation already corresponds to an infinite resummation of the Feynman perturbative series. We will then apply our formalism to the problem of unitary quantum gas, where the interaction parameter diverges, and a straightforward perturbative expansion is doomed to failure.

1.2 Motivation

The motivation of our new formalism is two-folded. First, we seek a higher-dimensional generalization of the thermodynamics of integrable models in $1+1$ dimensions; second, we wish to achieve the separation of thermal and quantum effects in a given problem, much like the classical kinetic theory of gas.

The Thermodynamic Bethe Ansatz (TBA) was introduced by Yang and Yang[51, 25]. It builds on the Bethe Ansatz solution of a one-dimensional quantum spin chain, due to Bethe himself, and allows the exact computation of thermodynamic properties of some integrable models in $1+1$ dimensions.

The "prototype" TBA was formulated for a gas of non-relativistic bosons, interacting with a δ-function potential. The solution is contained in the Yang-Yang equation:

$$\epsilon(k) = k^2 - \mu - \frac{1}{2\pi\beta}\int_{-\infty}^{\infty} K(k,p)\log\left(1-e^{-\beta\epsilon(p)}\right). \tag{1.3}$$

Here ϵ is the so-called pseudo-energy, and can be considered as the single-particle energy in the background of all the other particles interacting with it. The kernel $K(k,p)$ is the derivative of the scattering phase when two particles, with momenta k and p respectively, scattered in vacuum.

TBA relies on the integrable structure of the theory, and does not generalize to

higher dimensions. Thacker showed that the factorizability of the S-matrix directly leads to the TBA [48, 49]. But, unlike the many models in 1+1 dimensions without known Lagrangian formulations, the interacting boson gas has a clear generalization to higher dimensions. It is then natural to ask: is there an approximation scheme in the higher dimensions, that is a parallel, or a "generalization" of the TBA in $1+1$ dimensions?

Dashen *et. al.* [8] gives the partition function of a quantum field theory model in terms of its S-matrix. Based on their result, it should be possible to organize an expansion that mimics the TBA. However, the S-matrix of a non-integrable theory does not factorize, and the expansion quickly becomes complicated beyond the lowest order. Nevertheless, for a dilute gas, the resummation of all two-body terms, corresponds to an exact treatment of binary collisions, may serve as a useful approximation intrinsically different from other methods.

Building on the result of Dashen, we derived an integral equation for the pseudo-energy of a quantum gas:

This integral equation is, of course, only an approximation, since the higher-dimensional model is not integrable. But we hope that this alternative treatment would grant us insights otherwise inaccessible via simple perturbation theory.

In the view of the kinetic theory, the microscopic degrees of freedom interact and evolve according to their microscopic, zero-temperature equations of motion. They do not directly know about the temperature of the system; rather the temperature comes in through the distribution of the background particles.

In our integral equation, all "quantumness" of the problem is confined within the kernel, and all thing thermal is kept in the filling fraction f, reflecting the

background distribution. In a sense, the kernel can be understood as the analogy of the collision integral in the classical kinetic theory. Having a different type of interaction amounts to plugging in a different kernel to the same integral equation, with the same temperature dependence. This separation of thermal and quantum parts is in stark contrast with the usual Matsubara or Keldysh formalism, where the temperature is directly built into the quantum propagators.

Thus, like the kinetic theory of gas, we also expect the integral equation to hold in the dilute limit, where it forms a quantum analogy of binary collision approximation.

1.3 Phase transition of a Bose gas in two dimensions

In two spatial dimensions, the famous Mermin-Wagner-Hohenberg theorem states that a true long-range order is not possible [31, 17]. As a consequence, a non-interacting Bose gas does not undergo Bose-Einstein condensation (BEC) in two dimensions. This result can also be shown directly as followed. A non-interacting Bose gas undergoes BEC at zero chemical potential. In d spatial dimensions, the critical density is

$$\begin{aligned} n_c &= \int \frac{d^d k}{(2\pi)^d} \frac{1}{e^{\beta \frac{k^2}{2m}} - 1} \\ &= \left(\frac{2m}{4\pi\beta} \right)^{d/2} \zeta(d/2) \end{aligned} \tag{1.4}$$

where ζ is the Riemann zeta-function.

When $d = 3$, $\zeta(3/2)$ is finite, and the gas undergoes BEC at a finite critical density. On the other hand, $\zeta(2)$ is divergent when $d = 2$, meaning the normal state of a two-dimensional Bose gas can support an arbitrarily large density, and

there exists no critical point.

Nevertheless, a two-dimensional system can undergo a Berezinsky-Kosterlitz-Thouless (BKT) transition, and its correlation function decays as power-law rather than exponentially [41, 12, 42]. The computation of this critical point in Chapter 5 will be the first application of our integral equation formalism.

1.4 Unitary gas

The method to optically trap neutral atoms and to cool the trapped atomic gas to a temperature in the nano-Kelvin range was developed in the 1990s [40]. This development opened up the entire exciting new field of ultra-cold quantum gas.

Ultra-cold quantum gas attracts considerable attention for various reasons. From the stand point of physics of strongly interacting system, it is an ideal testing ground of new theoretical ideas due to its controllability. Across a Feshbach resonance, the s-wave scattering length a between two atoms can in principle be tuned to any arbitrary value between negative infinity and infinity by varying the external magnetic field [5, 23, 6, 35]. In three spatial dimensions, the atoms in such a gas can be modeled as integrating via a δ-function pseudo-potential whose coefficient is the scattering length [11]. The cold quantum gas therefore presents us an experimental realization of a system, whose interaction strength is can be arbitrarily and easily tuned to any desired value!

It has long been postulated [10, 34] that, in three spatial dimensions, the Bardeen-Cooper-Schriefer (BCS) superconductor phase and the Bose-Einstein condensation (BEC) phase are connected smoothly as the interaction varies from re-

pulsive to attractive, with a crossover at infinite scattering length, the so-called unitary limit. This crossover has recently been realized experimentally in cold quantum gas, thanks to the Feshbach resonance technique [1, 9, 14, 35].

With a diverging s-wave scattering length, there is no length scale in the low-energy theory of a unitary quantum gas. The low-energy properties of such a unitary gas is thus believed to be scale-invariant and *universal* [33]. On the other hand, the absence of a small parameter makes theoretical treatments difficult.

We believe that our integral equation approach is well-suited for exploring the unitary limit. It will be shown that the two-body kernel in our approach remains well-behaved as the scattering length diverges– in fact, the structure of the kernel is drastically simplified in this limit.

The cold quantum gas is a metastable state: the stable equilibrium state is the crystalline phase. However, in order to form a crystal, bonds must form between atoms as the first step. Yet the formation of a bounded pair requires at least three atoms in the process, one to take away the excess energy as dictated by energy and momentum conservation. Since binary collision between atoms is by far the most frequent events, the quantum gas can "equilibrate" while staying as a gas. Collision processes involving more than two atoms contribute to particle loss from the gas, and the gas would eventually solidify.

Given that the gas reaches its (pseudo) equilibrium state through binary collisions, we believe that our integral equation approach, which treats two-body processes exactly, can be a useful description for such quantum gas, even in the unitary limit.

1.5 The road map

This thesis consists of works previously published by the author in three separate papers [19, 20, 21].

The layout of this thesis is as followed. In Chapter 2, we shall developed the so-called S-matrix formulation of quantum statistical mechanics. A diagrammatic expansion will be given so that one may write down the partition function or the free energy density of an interacting system to arbitrary order of the scattering kernel.

In Chapter 3, the formulation will be developed further, and we shall specialize in the two-body approximation, which leads to an integral equation similar to the Yang-Yang equation of TBA (1.3).

In Chapter 4, we turn our attention to the field theoretic model of quantum gas. In particular, we shall derive the explicit forms of the two-body kernel in various spatial dimensions.

We take a break from the development of the theoretical framework in Chapter 5, and applies the formalism to the weakly interacting Bose gas in three dimensions. The correction to the critical density of the Bose-Einstein condensation due to interaction is computed.

The field-theoretic analysis resumes in Chapter 6. There we will attempt to interpret the unitary limit, in the context of the interaction kernel introduced in Chapter 2, in terms of renormalization group flow. The scaling functions at the unitary limit are also defined in this chapter.

The results of our numerical calculation at the unitary limit, in two and three

spatial dimensions, are detailed in Chapter 7 and Chapter 8 respectively.

In Chapter 9, the shear viscosity to entropy ratio of unitary quantum gas is computed using our integral equation, and compared with the conjectured lower bound in certain supersymmetric gauge theory. We found that our result is in good agreement with recent experimental finding by Cao *et. al* [4].

1.6 Notations and conventions

Throughout this thesis, we will choose our units such that $k_B = \hbar = 1$ unless explicitly stated otherwise.

We assume that any system discussed has a (second-quantized) Hamiltonian $H = H_0 + V$, where H_0 is the "free" part and V is an interaction term. We further assume that the spectrum of H_0 has a free-particle interpretation.

We denote the N-particle eigenstate of H_0, where the individual particles have momentum $\mathbf{k}_1, \cdots \mathbf{k}_N$ respectively, by

$$|\mathbf{k}_1, \cdots \mathbf{k}_N\rangle. \tag{1.5}$$

Throughout the thesis d shall denote the number of spatial dimensions. Also we define as a shorthand integration measure in the Fourier space:

$$(d\omega) = \frac{d\omega}{2\pi} \tag{1.6}$$

$$(d\mathbf{k}) = \frac{d^d\mathbf{k}}{(2\pi)^d} \tag{1.7}$$

It will be necessary at times to keep track of the particle statistics. We define

the quantity s by:

$$s = \begin{cases} +1 & \text{for Bosons} \\ -1 & \text{for Fermions} \end{cases} \tag{1.8}$$

Throughout this thesis we shall primarily consider quantum gases with a single species of particles. However, a fermionic degree of freedom necessarily has two components due to its spin, and this may affect the symmetry factor of a Feynman diagram in the standard perturbation theory. We define the numerical factor α as a book-keeping tool:

$$\alpha = \begin{cases} 1 & \text{for Bosons} \\ \frac{1}{2} & \text{for Fermions.} \end{cases} \tag{1.9}$$

CHAPTER 2

QUANTUM STATISTICAL MECHANICS: THE S-MATRIX APPROACH

2.1 Partition function in terms of the S-matrix

Given a quantum mechanical system with Hamiltonian H, its partition function is defined as

$$Z(\mu, \beta) = \operatorname{Tr} e^{-\beta(H-\mu N)}, \tag{2.1}$$

where $\beta = 1/T$ is the inverse temperature, and μ is the chemical potential.

Following the work of Dashen [8], we shall now recast Z into a different form:

$$\begin{aligned} Z &= \operatorname{Tr} e^{-\beta(H-\mu N)} \\ &= \int dE e^{-\beta E} \operatorname{Tr} \delta\left(E - (H - \mu N)\right) \\ &= \int dE e^{-\beta E} \frac{1}{2\pi i} \operatorname{Tr} \left[\frac{1}{E - (H - \mu N) - i0^+} - \frac{1}{E - (H - \mu N) + i0^+} \right] \end{aligned} \tag{2.2}$$

Here we have used the identity $\lim_{\eta \to 0^+} \operatorname{Im}\left(i\pi/(x + i\eta)\right) = \delta(x)$ to formally express the δ-function in a more tractable form. We shall now relate this expression to the S-matrix in the scattering theory.

We follow the usual prescription of splitting the Hamiltonian H into the "free" part H_0 and the interaction part V. Our convention of the S-matrix is

$$S(E) = 1 + 2\pi i \delta\left(E - H_0\right) T(E). \tag{2.3}$$

Also we define:

$$\begin{aligned} G(E) &= \lim_{\eta \to 0^+} \frac{1}{E - H + i\eta} \\ G_0(E) &= \lim_{\eta \to 0^+} \frac{1}{E - H_0 + i\eta}. \end{aligned} \tag{2.4}$$

The S-matrix is then related to G and G_0 by

$$S = G_0^*(G^*)^{-1}GG_0^{-1}. \tag{2.5}$$

See appendix for the proof.

Now we claim that $\operatorname{Tr} S^{-1}\partial_E S = -\operatorname{Tr}[(G - G_0) - (G * -G_0*)]$. Using the fact that $\partial_E G = -G^2$ and $\partial_E(G^{-1}) = 1$, it is easily shown:

$$\begin{aligned}
\operatorname{Tr} S^{-1}\partial_E S &= \operatorname{Tr}\left(\left[G_0 G^{-1} G^* (G_0^*)^{-1}\right]\partial_E\left[G_0^*(G^*)^{-1}GG_0^{-1}\right]\right) \\
&= \operatorname{Tr}\left[(G_0^*)^{-1}\partial_E G_0^* + G^*\partial_E(G^*)^{-1} + G^{-1}\partial_E G + G_0\partial_E(G_0)^{-1}\right] \\
&= -\operatorname{Tr}\left[(G - G_0) - (G^* - G_0^*)\right].
\end{aligned} \tag{2.6}$$

Inserting this result into (2.2), we see that the partition function becomes

$$\begin{aligned}
Z &= \frac{1}{2\pi i}\int dE e^{-\beta E}\left(\operatorname{Tr}(S^{-1}(E)\partial_E S(E)) - \operatorname{Tr}(G_0(E) - G_0^*(E))\right) \\
&= Z_0 + \frac{1}{2\pi i}\int dE e^{-\beta E}\operatorname{Tr}(S^{-1}(E)\partial_E S(E)),
\end{aligned} \tag{2.7}$$

where $Z_0 = \operatorname{Tr} e^{-\beta H_0}$ is the partition function of the free theory.

Using the cyclic property of the trace, we may write $\operatorname{Tr}(S^{-1}(E)\partial_E S(E)) = \partial_E \operatorname{Tr}\log S(E)$. Furthermore we can integrate by part and move the derivative ∂_E onto $e^{-\beta E}$. So we arrived at the expression for partition function that we will be working with:

$$Z = Z_0 - i\beta\int \frac{dE}{2\pi}e^{-\beta E}\operatorname{Tr}\log S(E) \tag{2.8}$$

Since $\log S(E) \propto \delta(E - H_0)$, we may factor the energy-conserving δ-function out, and define the operator W by

$$\operatorname{Im}\log S(E) \equiv 2\pi\delta(E - H_0)W(E). \tag{2.9}$$

Insert this definition into (2.8), and integrate by part, one obtains:

$$Z = \int dE\ e^{-\beta E}\,\mathrm{Tr}\left[\delta(E - H_0)\left(W(E)\beta + 1\right)\right]. \tag{2.10}$$

For simplicity of the notation, we further define

$$\hat{U} = W\beta + 1 \tag{2.11}$$

2.2 Cluster decomposition

One can take the principle of cluster decomposition as an axiom of any well-defined quantum field theory [50]. It is a necessary condition for the field theory being local.

Take two electrons scattering off two atomic nuclei for example. Formally the incoming quantum state is a two-electron state, and the S-matrix connects this state to a two-electron outgoing state.

However, suppose now we are talking about two identical copies of experiments, each involving a single electron scattering off a single nucleus, being performed at locations miles away from each other. Certainly we do not expect any correlation between the two experiments. In this case, the (formal) two-body S-matrix must be just the tensor product of two one-body S-matrices.

On the other hand, when the two sets of experiment are brought closed to each other, quantum interference must take place, and the S-matrix is no longer a product of two independent pieces.

Mathematically, we write:

$$\langle e_1', e_2'|S|e_1, e_2\rangle = \langle e_1'|S|e_1\rangle\langle e_2'|S|e_2\rangle_c + s\langle e_1'|S|e_2\rangle\langle e_2'|S|e_1\rangle_c + \langle e_1', e_2'|S|e_1, e_2\rangle_c. \tag{2.12}$$

The subscript c denotes "connected", meaning the piece cannot be further decomposed into a tensor product of smaller matrices. The quantity s arises from particle statistics: $s = +1$ for bosons, and $s = -1$ for fermions.

In our previous example, for the two experiments performed far away to not affect each other, the connected two-body S-matrix must vanish as the distance between the two incoming electrons increases. This is in fact a general property of any connected matrix elements of a physical observable from a local field theory.

It is therefore not surprising that, in the present context, the clustering property of the S-matrix ensures the extensivity of the free energy, since the later is a consequence of the locality.

For any operator X, the cluster decomposition can be expressed as follows:

$$\langle\Psi'|X|\Psi\rangle = \sum_{\text{partitions}} s^p \ \langle\Psi_1'|X|\Psi_1\rangle_c\langle\Psi_2'|X|\Psi_2\rangle_c\langle\Psi_3'|X|\Psi_3\rangle_c\cdots \tag{2.13}$$

where the sum is over partitions of the state $|\Psi\rangle$ into clusters $|\Psi_1\rangle, |\Psi_2\rangle, ...$ (The number of particles in $|\Psi_i\rangle$ and $|\Psi_i'\rangle$ is not necessarily the same.) The above formula essentially *defines* what is meant by the connected matrix elements $\langle X\rangle_c$.

In order for the free energy to be extensive, $\hat{U}$ must cluster properly, as we now describe. Introducing the short-hand notation $|\mathbf{12}\cdots\rangle = |\mathbf{k}_1\mathbf{k}_2\cdots\rangle$, for the

operator $\hat{U}$ the above equation reads

$$\begin{aligned}
\langle \mathbf{1}'|\hat{U}|\mathbf{1}\rangle &= \langle \mathbf{1}'|\hat{U}|\mathbf{1}\rangle_{\mathbf{c}} \\
\langle \mathbf{1}'\mathbf{2}'|\hat{U}|\mathbf{1}\mathbf{2}\rangle &= \langle \mathbf{1}'\mathbf{2}'|\hat{U}|\mathbf{1}\mathbf{2}\rangle_c + \langle \mathbf{1}'|\hat{U}|\mathbf{1}\rangle_c\langle \mathbf{2}'|\hat{U}|\mathbf{2}\rangle_c + s\langle \mathbf{2}'|\hat{U}|\mathbf{1}\rangle_c\langle \mathbf{1}'|\hat{U}|\mathbf{2}\rangle_c \\
\langle \mathbf{1}'\mathbf{2}'\mathbf{3}'|\hat{U}|\mathbf{1}\mathbf{2}\mathbf{3}\rangle &= \langle \mathbf{1}'\mathbf{2}'\mathbf{3}'|\hat{U}|\mathbf{1}\mathbf{2}\mathbf{3}\rangle_c \\
&\quad + \Big[\langle \mathbf{1}'|\hat{U}|\mathbf{1}\rangle_c\langle \mathbf{2}'\mathbf{3}'|\hat{U}|\mathbf{2}\mathbf{3}\rangle_c + \text{permutations}\Big]_9 \\
&\quad + \Big[\langle \mathbf{1}'|\hat{U}|\mathbf{1}\rangle_c\langle \mathbf{2}'|\hat{U}|\mathbf{2}\rangle_c\langle \mathbf{3}'|\hat{U}|\mathbf{3}\rangle_c + \text{permutations}\Big]_6
\end{aligned} \tag{2.14}$$

etc. The subscript $[*]_9$ denotes the number of terms within the bracket, so that for three particles there is a total of $1 + 9 + 6 = 16$ terms on the right hand side of the above equation. The connected matrix elements are characterized by being proportional to a *single* overall δ-function.

When $\{\mathbf{k}'\} = \{\mathbf{k}\}$, the above cluster expansion leads to another specialized type of cluster expansion that is suited to the computation of the partition function. From eq. (2.14) we define $\hat{w}_N(\mathbf{k}_1, ..., \mathbf{k}_N)$ as factors that cannot be written as a product of separate functions of disjoint subsets of the $\mathbf{k}_i$:

$$\begin{aligned}
\langle \mathbf{1}|\hat{U}|\mathbf{1}\rangle &= \langle \mathbf{1}|\hat{U}|\mathbf{1}\rangle_c = \hat{w}_1(\mathbf{k}_1) \\
\langle \mathbf{1}\mathbf{2}|\hat{U}|\mathbf{1}\mathbf{2}\rangle &= \hat{w}_2(\mathbf{k}_1, \mathbf{k}_2) + \hat{w}_1(\mathbf{k}_1)\hat{w}_1(\mathbf{k}_2) \\
\langle \mathbf{1}\mathbf{2}\mathbf{3}|\hat{U}|\mathbf{1}\mathbf{2}\mathbf{3}\rangle &= \hat{w}_3(\mathbf{k}_1, \mathbf{k}_2, \mathbf{k}_3) + [\hat{w}_2(\mathbf{k}_2, \mathbf{k}_3)\hat{w}_1(\mathbf{k}_1) + \hat{w}_2(\mathbf{k}_1, \mathbf{k}_3)\hat{w}_1(\mathbf{k}_2) + \hat{w}_2(\mathbf{k}_1, \mathbf{k}_2)\hat{w}_1(\mathbf{k}_3)] \\
&\quad + \hat{w}_1(\mathbf{k}_1)\hat{w}_1(\mathbf{k}_2)\hat{w}_1(\mathbf{k}_3)
\end{aligned} \tag{2.15}$$

etc.

The above definition implies that the $\hat{w}_N$ are sums of terms involving the con-

nected matrix elements of $\hat{U}$. For instance:

$$\begin{aligned}\hat{w}_2(\mathbf{k}_1,\mathbf{k}_2) &= \langle \mathbf{12}|\hat{U}|\mathbf{12}\rangle_c + s\langle \mathbf{2}|\hat{U}|\mathbf{1}\rangle_c\langle \mathbf{1}|\hat{U}|\mathbf{2}\rangle_c \\ \hat{w}_3(\mathbf{k}_1,\mathbf{k}_2,\mathbf{k}_3) &= \langle \mathbf{123}|\hat{U}|\mathbf{123}\rangle_c + \Big[s\langle \mathbf{2}|\hat{U}|\mathbf{1}\rangle_c\langle \mathbf{13}|\hat{U}|\mathbf{23}\rangle_c + \text{perm.}\Big]_6 \\ &\quad + \Big[\langle \mathbf{3}|\hat{U}|\mathbf{1}\rangle_c\langle \mathbf{1}|\hat{U}|\mathbf{2}\rangle_c\langle \mathbf{2}|\hat{U}|\mathbf{3}\rangle_c + \text{perm.}\Big]_2\end{aligned} \tag{2.16}$$

A combinatoric argument then shows:

$$\log Z = \sum_{N=1}^{\infty} \frac{z^N}{N!} \int (d\mathbf{k}) \cdots \mathbf{k}_N \; e^{-\beta \sum_{i=1}^{N} \omega_i} \; \hat{w}_N(\mathbf{k}_1, ..., \mathbf{k}_N) \tag{2.17}$$

where $z \equiv e^{\beta\mu}$ and $\omega_i = \omega_{\mathbf{k}_i}$.

All of the $\hat{w}$ are proportional to an overall $(2\pi)^d \delta^{(d)}(0) = V$, so let us factor out the volume V and define:

$$\hat{w}_N(\mathbf{k}_1, ..., \mathbf{k}_N) \equiv V \, w_N(\mathbf{k}_1, ..., \mathbf{k}_N) \tag{2.18}$$

The free energy density is then completely determined by the functions w_N:

$$\mathcal{F} = -\frac{1}{\beta V} \log Z = -\frac{1}{\beta} \sum_{N=1}^{\infty} \frac{z^N}{N!} \int (d\mathbf{k}_1) \cdots (d\mathbf{k}_N) \; e^{-\beta \sum_i \omega_i} \; w_N(\mathbf{k}_1, ..., \mathbf{k}_N) \tag{2.19}$$

For free particles, the only non-zero connected matrix element is the one-particle to one-particle one: $\langle 2|\hat{U}|1\rangle = \langle 2|1\rangle$. This still implies $\hat{w}_N$ is non-zero for any N:

$$\hat{w}_N(1, 2, .., N) = s^{N-1}(N-1)! \, \langle \mathbf{N}|\mathbf{1}\rangle\langle \mathbf{1}|\mathbf{2}\rangle\langle \mathbf{2}|\mathbf{3}\rangle \cdots \langle \mathbf{N-1}|\mathbf{N}\rangle \tag{2.20}$$

Note that although $\hat{w}_N$ is a product of N δ-functions, it only has a single $\delta(0)$. All but one $\mathbf{k}$ integral is saturated by δ-functions at each N and one obtains the well-known free-particle result:

$$\mathcal{F}_0 = \frac{s}{\beta} \int (d\mathbf{k}) \; \log\left(1 - sze^{-\beta\omega_{\mathbf{k}}}\right) \tag{2.21}$$

2.3 Diagrammatic description

In the interacting case, terms involving the one-particle factors $\langle \mathbf{2}|\hat{U}|\mathbf{1}\rangle_c$ can be easily summed over as in the free particle case. We assume that $|\mathbf{k}\rangle$ is a stable one-particle eigenstate of H with energy $\omega_{\mathbf{k}}$:

$$\langle \mathbf{k}'|\hat{U}|\mathbf{k}\rangle_c = \langle \mathbf{k}'|\mathbf{k}\rangle = (2\pi i)^d \delta^{(d)}_{\mathbf{k},\mathbf{k}'} \tag{2.22}$$

Consider for example the $\hat{w}_3$ contribution coming from the second terms in eq. (2.16):

$$\log Z = ...+\frac{z^3}{3!}\int (d\mathbf{k}_1)(d\mathbf{k}_2)(d\mathbf{k}_3)\, e^{-\beta\sum_{i=1}^3\omega_i}\, \Big(s\langle \mathbf{2}|\hat{U}|\mathbf{1}\rangle_c\langle \mathbf{13}|\hat{U}|\mathbf{23}\rangle_c + \text{perm.}\Big)+... \tag{2.23}$$

Because of the δ-function, one can do one $\mathbf{k}$ integral. Combined with the primary term coming from $\hat{w}_2$ one finds:

$$\log Z = \cdots + \frac{z^2}{2}\int (d\mathbf{k}_1)(d\mathbf{k}_2)\, e^{-\beta(\omega_1+\omega_2)}\, \Big(1+sz(e^{-\beta\omega_1}+e^{-\beta\omega_2})\Big)\, \langle \mathbf{12}|\hat{U}|\mathbf{12}\rangle_c + \cdots \tag{2.24}$$

It is easy to see that the terms in the higher $\hat{w}_N$ that involve one $\hat{w}_2$ and $N-1$ $\hat{w}_1$'s contribute additional terms in the parentheses of the above equation that sum up to $\prod_{i=1}^2(1-sze^{-\beta\omega_i})^{-1}$. To summarize this result in the most convenient way, define $\sum'_N$ as the sum over $\hat{w}_N$ terms minus any terms involving the 1-particle factors $\hat{w}_1$. Then

$$\mathcal{F} = \mathcal{F}_0 - \frac{1}{\beta}\sum_{N\geq 2}{}' \frac{1}{N!}\int \left(\prod_{i=1}^N (d\mathbf{k}_i) f_0(\mathbf{k}_i)\right)\, w_N(\mathbf{k}_1,...,\mathbf{k}_N) \tag{2.25}$$

where $\mathcal{F}_0$ is the free contribution in eq. (2.21) and we have defined the free "filling fraction":

$$f_0(\mathbf{k}) \equiv \frac{z}{e^{\beta\omega_{\mathbf{k}}} - sz} \tag{2.26}$$

The functions w_N have many contributions built out of the connected matrix elements of $\hat{U}$. Define the vertex function $\mathcal{V}(\mathbf{k}'_1, \cdots, \mathbf{k}'_m; \mathbf{k}_1, \cdots, \mathbf{k}_n)$ as follows:

$$\langle \mathbf{k}'_1, ..., \mathbf{k}'_m | \hat{U} | \mathbf{k}_1, ..., \mathbf{k}_n \rangle_c = \beta (2\pi)^d \delta_{\mathbf{k},\mathbf{k}'} \, \mathcal{V}(\mathbf{k}'_1, ..., \mathbf{k}'_m; \mathbf{k}_1, ..., \mathbf{k}_n) \tag{2.27}$$

The vertices $\mathcal{V}$ have no temperature dependence and are essentially on-shell matrix elements of $\log S$. To lowest order in the scattering matrix T, this vertex is just the scattering amplitude: $\mathcal{V} \approx \mathcal{M}$.

Given our present interest in non-relativistic systems, only the matrix elements with $n = m$ are of concern here. We highlight this fact by attaching a subscript n to $\mathcal{V}$:

$$\mathcal{V}_n(\mathbf{k}'_1, ..., \mathbf{k}'_n; \mathbf{k}_1, ..., \mathbf{k}_n) \equiv \mathcal{V}(\mathbf{k}'_1, ..., \mathbf{k}'_n; \mathbf{k}_1, ..., \mathbf{k}_n) \tag{2.28}$$

Each term in the corrections $\mathcal{F} - \mathcal{F}_0$ can be represented graphically. We stress that this diagrammatic expansion as defined here, while being analogous to the usual Feynman diagrams, is completely unrelated to the (finite temperature) Feynman diagram approach. This is clear since each vertex in principle represents an exact zero-temperature quantity summed to all orders in perturbation theory. The correction $\mathcal{F} - \mathcal{F}_0$ is the sum of all connected "vacuum diagrams", made of oriented lines and vertices with n incoming and n outgoing lines attached, n being any positive integer. Note that there must be at least one vertex; i.e. the circle isn't allowed since it is already included as $\mathcal{F}_0$. A diagram is then evaluated according to the following rules and represents a contribution to $\mathcal{F}$:

1. Each line carries some momentum $\mathbf{k}$. To such a line is associated a factor of $f_0(\mathbf{k})$.

2. To each vertex, with the incoming set and the outgoing set of momenta being $\{\mathbf{k}_1, \ldots, \mathbf{k}_n\}$ and $\{\mathbf{k}'_1, \ldots, \mathbf{k}'_n\}$ respectively, associate a factor of the vertex function $(2\pi)^d \beta\, \mathcal{V}_n(\mathbf{k}'_1, ..., \mathbf{k}'_n; \mathbf{k}_1, ..., \mathbf{k}_n)$.

3. Enforce momentum conservation at each vertex.

4. Integrate over all unconstrained momenta with $d^d\mathbf{k}/(2\pi)^d$.

5. Divide by the symmetry factor of the diagram, defined as the number of permutations of the internal lines that do not change the topology of the graph, including relative positions. This factor is identical to the usual symmetry factor of a Feynman diagram.

6. For fermions, include one statistical factor $s = -1$ for each loop.

7. Divide the result by the volume of space $V = (2\pi)^d \delta(0)$ and by β. Note that this is equivalent to dividing the space-time volume $V\beta$ since at finite temperature, β is the circumference of compactified time.

To illustrate this diagrammatic expansion, we will now describe the first few terms. There is only one diagram that has two lines, as shown in Figure 2.1. This diagram corresponds to:

$$\mathcal{F} = ...\frac{1}{2}\int (d\mathbf{k}_1)(d\mathbf{k}_2) f_0(\mathbf{k}_1) f_0(\mathbf{k}_2) \mathcal{V}_2(\mathbf{k}_1, \mathbf{k}_2; \mathbf{k}_1, \mathbf{k}_2). \tag{2.29}$$

Comparing with the expression (2.25), we identify $w_2(\mathbf{k}_1, \mathbf{k}_2) = \beta \mathcal{V}_2(\mathbf{k}_1, \mathbf{k}_2; \mathbf{k}_1, \mathbf{k}_2)$.

At the next order, there is again only one diagram consisting of three lines, shown in Figure 2.1, and this implies $w_3(\mathbf{k}_1, \mathbf{k}_2, \mathbf{k}_3) = s\beta \mathcal{V}_3(\mathbf{k}_1, \mathbf{k}_2, \mathbf{k}_3; \mathbf{k}_1, \mathbf{k}_2, \mathbf{k}_3)$.

There are multiple diagrams with four lines, one of them includes $\mathcal{V}_4$, and the

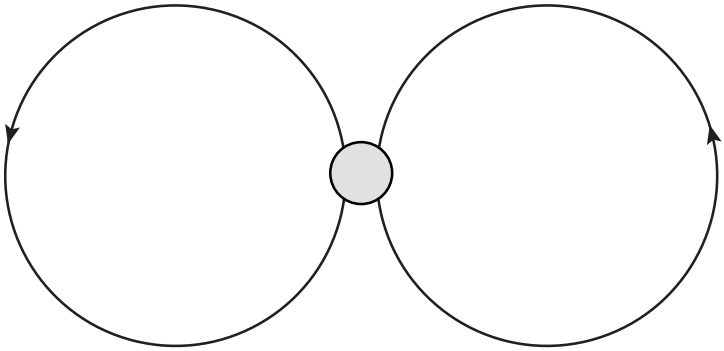

(a) Lowest contribution to w_2

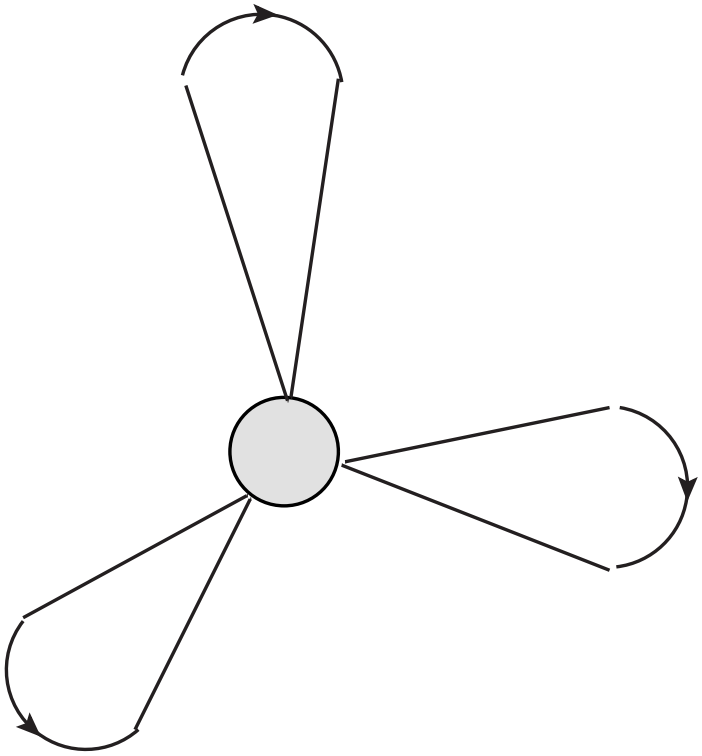

(b) Lowest contribution to w_3

Figure 2.1: Examples of contributions to two- and three-particle terms.

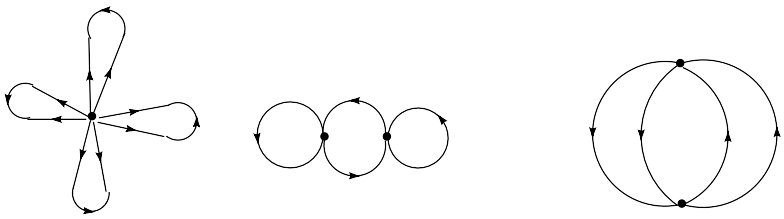

Figure 2.2: Diagrams contributing to w_4

others can be built from $\mathcal{V}_2$. They are shown in Figure 2.2. Their sum is

$$\begin{aligned}\mathcal{F} = \cdots + \int \left[\prod_{i=1}^{4}(d\mathbf{k}_i) f_0(\mathbf{k}_i)\right] \Big[&\frac{1}{4!}\mathcal{V}_4(\mathbf{k}_1,\dots\mathbf{k}_4;\mathbf{k}_1,\dots\mathbf{k}_4) \\ &+ \frac{s}{2}(2\pi)^d\delta^{(d)}(\mathbf{k}_2-\mathbf{k}_3)\beta\mathcal{V}_2(\mathbf{k}_1,\mathbf{k}_2;\mathbf{k}_1,\mathbf{k}_3)\mathcal{V}_2(\mathbf{k}_2,\mathbf{k}_4;\mathbf{k}_3,\mathbf{k}_4) \\ &+ \frac{s}{8}(2\pi)^d\delta(\sum_{i=1}^{4}\mathbf{k}_i)\beta^2\mathcal{V}_2(\mathbf{k}_1,\mathbf{k}_2;\mathbf{k}_3,\mathbf{k}_4)\mathcal{V}_2(\mathbf{k}_3,\mathbf{k}_4;\mathbf{k}_1,\mathbf{k}_2)\Big].\end{aligned} \tag{2.30}$$

From this expression, we can identify w_4, which is now a sum of terms built from the vertices $\mathcal{V}_4, \mathcal{V}_2$.

An interesting class of diagrams are the "ring-diagrams" shown in Figure 3, since they can be summed up in closed form. Let us define

$$G_2(\mathbf{k},\mathbf{k}') = \mathcal{V}_2(\mathbf{k},\mathbf{k}';\mathbf{k},\mathbf{k}') \tag{2.31}$$

A ring diagram with N external rings attached will have the following value according to the diagrammatic rules:

$$\begin{aligned}\frac{1}{\beta N}s^{N+1}\int(d\mathbf{k}_0)\prod_{i=1}^{N}(d\mathbf{k}_i)\left[\beta G_2(\mathbf{k}_0,\mathbf{k}_i)f_0(\mathbf{k}_i)\right]f_0(\mathbf{k}_0)^N \qquad &\text{if } N>1; \\ \frac{1}{2\beta}\int(d\mathbf{k}_0)(d\mathbf{k}_1)\beta G_2(\mathbf{k}_0,\mathbf{k}_1)f_0(\mathbf{k}_1)f_0(\mathbf{k}_0) \qquad &\text{if } N=1.\end{aligned} \tag{2.32}$$

Apart from the $N = 1$ term which has a different coefficient, all other terms can be identified with the power series for the logarithmic function. This class of diagrams are then resummed into:

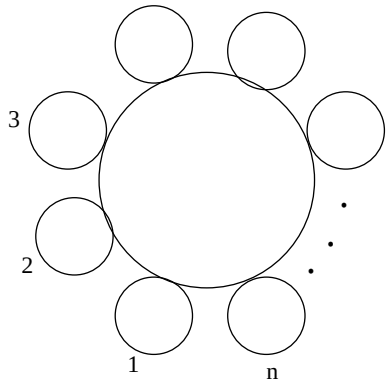

Figure 2.3: Ring diagrams.

$$\begin{aligned}\mathcal{F}_{\text{ring}} = -\frac{s}{\beta}\int (d\mathbf{k}_0)\log\left(1 - sf_0(\mathbf{k}_0)\int (d\mathbf{k}_1)\beta G_2(\mathbf{k}_0,\mathbf{k}_1)f_0(\mathbf{k}_1)\right)\\ -\frac{1}{2}\int (d\mathbf{k}_0)(d\mathbf{k}_1)G_2(\mathbf{k}_0,\mathbf{k}_1)f_0(\mathbf{k}_1)f_0(\mathbf{k}_0)\end{aligned} \tag{2.33}$$

CHAPTER 3

TBA-LIKE INTEGRAL EQUATION

We have formally developed an expansion for the free energy of a interacting system in the previous chapter. However, it is still very much a mathematical exercise at this stage. More work is clearly needed before we can apply the formalism on real problems.

There are in particular two loose ends: first, the diagrammatic expansion we developed earlier is still very much a weak-coupling expansion. A resummation scheme is needed in order to obtain results valid beyond the infinitesimal coupling regime. Second, the vertex functions $\mathcal{V}$, although formally defined, still lack explicit expressions.

In this chapter we devise a way to re-sum the terms in our diagrammatic expansion. The method resembles the resummation of self-energy insertions of the full propagator in the usual perturbative quantum field theory.

In practice, one of course still has to truncate the resummation at some point, corresponding to only resumming selected classes of diagrams. We shall introduce one such approximation that treats two-body interaction exactly but truncates all other terms.

And then we shall turn our attention to the four-point vertex function involved in this approximation, and derive its explicit expression in terms of the two-body scattering amplitude of the underlying filed-theoretic model.

The end result of all these will be an integral equation for the effective single-particle energy, which turns out to be closely related to the thermodynamic Bethe

ansatz of integrable system in one-dimension.

3.1 Legendre transformation

Given $\mathcal{F}(\mu)$, one can compute the thermally averaged number density n:

$$n = -\frac{\partial \mathcal{F}}{\partial \mu} \equiv \int (d\mathbf{k}) f(\mathbf{k}) \tag{3.1}$$

The dimensionless quantities f are called the filling fractions or occupation numbers. One can express $\mathcal{F}$ as a functional of f with a Legendre transformation. Define

$$G \equiv \mathcal{F}(\mu) + \mu\, n \tag{3.2}$$

Treating f and μ as independent variables, then using eq. (3.1) one has that $\partial_\mu G = 0$ which implies it can be expressed only in terms of f and satisfies $\delta G/\delta f = \mu$. Inverting the above construction shows that there exists a functional $F(f, \mu)$:

$$F(f, \mu) = G(f) - \mu \int (d\mathbf{k}) f(\mathbf{k}) \tag{3.3}$$

which satisfies eq. (3.1) and is a stationary point with respect to f:

$$\frac{\delta F}{\delta f} = 0 \tag{3.4}$$

The above stationary condition is to be viewed as determining f as a function of μ. The physical free energy is then $\mathcal{F} = F$ evaluated at the solution f to the above equation. We will refer to eq. (3.4) as the saddle point equation since it is suggestive of a saddle point approximation to a functional integral.

The function F is also required to satisfy

$$\frac{\partial F}{\partial \mu} = -\int (d\mathbf{k})\, f(\mathbf{k}) \tag{3.5}$$

In the sequel, it will be convenient to trade the chemical potential μ for the variable f_0. We will need:

$$\frac{\partial f_0}{\partial \mu} = \beta f_0(1 + s f_0) \tag{3.6}$$

In the free theory the functional $\mathit{\Gamma}_0$ is fixed only up to the saddle point equations, thus its explicit expression is not unique. As we will see, the appropriate choice that is consistent with the diagrammatic expansion is:

$$\mathit{\Gamma}_0(f, f_0) = -\frac{1}{\beta} \int (d\mathbf{k}) \left(s \log(1 + sf) - \left(\frac{f - f_0}{1 + s f_0} \right) \right) \tag{3.7}$$

The saddle point equation $\frac{\delta \mathit{\Gamma}_0}{\delta f} = 0$ implies $f = f_0$, and inserting this back into $\mathit{\Gamma}_0$ gives the correct free energy $\mathcal{F}_0$ for the free theory. Furthermore, $\mathit{\Gamma}_0$ satisfies eq. (3.5) if one uses the saddle point equation $f = f_0$.

Let us now include interactions by defining

$$\mathit{\Gamma} = \mathit{\Gamma}_0 + \mathit{\Gamma}_1 \tag{3.8}$$

where $\mathit{\Gamma}_0$ is given in eq. (3.7) and we define U as the "potential" which depends on f and incorporates interactions:

$$\mathit{\Gamma}_1 = -\frac{1}{\beta} \int (d\mathbf{k})\ U(f(\mathbf{k})) \tag{3.9}$$

3.2 Integral equation

The physical filling fraction f can be obtained by differentiating $\mathcal{F}$ in (2.25) with respect to the chemical potential μ, and the result is

$$f(\mathbf{k}) = f_0(\mathbf{k}) + f_0(\mathbf{k})\,(s f_0(\mathbf{k}) + 1) \sum_{N=1}^{\infty} \frac{1}{N!} \int \left[\prod_{i=1}^{N} (d\mathbf{k}_i) f_0(\mathbf{k}_i) \right]\ w_{N+1}(\mathbf{k}, \mathbf{k}_1, \ldots, \mathbf{k}_N). \tag{3.10}$$

Since f_0 is represented by a line in our graphical expansion, it is tempting to postulate that f would be a fully dressed line, but this interpretation isn't exactly correct.

Graphically, a dressed line is obtained by summing over all possible insertions due to interactions. The sum can be generated in the following way: take a (connected) vacuum diagram, cut an internal line into two external legs, and the resulting diagram contributes to the sum. If we sum over all possible ways of cutting an internal line from a vacuum diagram, and furthermore sum over all such diagrams, we have generated all correction terms to the so-called propagator.

Cutting a line and replacing it with two legs corresponds to replacing a factor of $f_0(\mathbf{k})$ by $sf_0(\mathbf{k})^2$. We have the extra factor of s because cutting one line removes one loop integral.

Recall that $\mathcal{F}-\mathcal{F}_0$ is the sum of all connected vacuum diagrams. The action of the derivative $\partial/\partial\mu$ makes sure that we've picked out every internal line in every diagram. However, it replaces f_0 by $f_0(1+sf_0)$. Consequently, we define the dressed line $\widetilde{f}(\mathbf{k})$ by

$$\widetilde{f}(\mathbf{k}) = f_0(\mathbf{k}) + \left(\frac{sf_0(\mathbf{k})}{sf_0(\mathbf{k})+1}\right)\left(f(\mathbf{k}) - f_0(\mathbf{k})\right). \tag{3.11}$$

It will be useful to define $\epsilon_{\mathbf{k}}$ as the single particle pseudo-energy at momentum $\mathbf{k}$ as follows:

$$f(\mathbf{k}) = \frac{1}{e^{\beta\epsilon_{\mathbf{k}}} - s} \tag{3.12}$$

Then the eq. (3.11) can be equivalently expressed in the simpler form:

$$\widetilde{f}(\mathbf{k}) = e^{\beta(\epsilon_{\mathbf{k}}-\omega_{\mathbf{k}}+\mu)} f(\mathbf{k}) \tag{3.13}$$

Figure 3.1: Graphical representation of the integral equation (3.15). The double line represents $\widetilde{f}$, and the single line represents f_0.

The following identity will be useful:

$$\frac{\delta \widetilde{f}(\mathbf{k})}{\delta f(\mathbf{k}')} = (2\pi)^d \delta(\mathbf{k}-\mathbf{k}') \frac{s f_0(\mathbf{k})}{1+s f_0(\mathbf{k})} \tag{3.14}$$

This fully dressed line should satisfy an equation analogous to the Dyson equation for the full propagator:

$$\widetilde{f}(\mathbf{k}) = f_0(\mathbf{k}) + s f_0(\mathbf{k}) \widetilde{f}(\mathbf{k}) \Sigma(\mathbf{k}), \tag{3.15}$$

where $\Sigma(\mathbf{k})$ is the sum of all (amputated) one-particle (1PI) insertions. Figure 3.1 represents this equation graphically.

Again we consider the analogy to Feynman diagrams. Take a two-particle irreducible (2PI) vacuum diagram with each internal line being fully dressed $\widetilde{f}$, and remove one internal line to form an amputated 1PI insertion. Summing over all ways of removing a line of a diagram, and then summing over all 2PI vacuum diagrams, the result is Σ.

Let $-\beta \mathit{\Gamma}_1$ be the sum of all 2PI vacuum diagrams, with internal lines being $\widetilde{f}$ instead of f_0. The operations above can be neatly summarized by the following:

$$\Sigma(\mathbf{k}) = -s\beta \left(\frac{s f_0(\mathbf{k})}{1+s f_0(\mathbf{k})} \right)^{-1} \frac{\delta \mathit{\Gamma}_1}{\delta f(\mathbf{k})}. \tag{3.16}$$

The factor of s is inserted by hand because the removal of one internal line decreases the loop count by one.

One correctly surmises that $\digamma_1$ turns out to be the interaction part of $\digamma$. Indeed, when there is no interaction, all vertex functions are zero and $\digamma_1$ vanishes. The "Dyson" equation now reads:

$$\widetilde{f}(\mathbf{k}) - f_0(\mathbf{k}) + \beta\widetilde{f}(\mathbf{k})(1 + sf_0(\mathbf{k}))\frac{\delta\digamma_1}{\delta f(\mathbf{k})} = 0. \tag{3.17}$$

and is actually an integral equation for f.

If we demand that the saddle point equation of the functional $\digamma$ leads to (3.17), then $\digamma_0$ can be uniquely fixed up to an additive constant and an overall scale. If we further demand that $\digamma_0$ reproduces the result of the free theory, then one can show that the only consistent choice is $\digamma = \digamma_0 + \digamma_1$, where $\digamma_0$ is given in eq. (3.7) and

$$\digamma_1 = \mathcal{F}^{2PI}(f_0 \to \widetilde{f}) \tag{3.18}$$

i.e. $\digamma_1$ is given by the 2PI diagrams with f_0 replaced by the fully dressed $\widetilde{f}$.

3.3 Two-body approximation

We shall now make the following approximations:

1. include only the four-vertex, i.e. $\mathcal{V}_2$, in our diagrammatic expansion;
2. consider only the foam diagrams, shown in Figure (3.2).

In practice, this approximation amounts to setting

$$\digamma_1 = -\frac{1}{2}\int (d\mathbf{k})(d\mathbf{k}')\tilde{f}(\mathbf{k})\tilde{f}(\mathbf{k}')G_2(\mathbf{k},\mathbf{k}'), \tag{3.19}$$

and truncating all terms with more $\tilde{f}$.

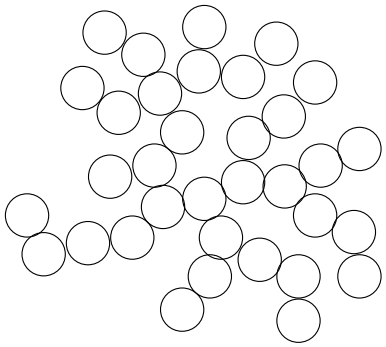

Figure 3.2: Foam diagrams.

Within this approximation, the integral equation (3.17) can be rewritten into a self-consistent equation for the single-particle pseudo-energy. With the expressions (3.19) and (3.14), the equation (3.17) reduces to

$$\tilde{f}(\mathbf{k}) = f_0(\mathbf{k}) + \tilde{f}(\mathbf{k}) \left(s\beta f_0(\mathbf{k}) \int (d\mathbf{k}') G_2(\mathbf{k}, \mathbf{k}') \tilde{f}(\mathbf{k}') \right). \tag{3.20}$$

In terms of the pseudo-energy $\epsilon_{\mathbf{k}}$ defined in eq. (3.12), using eq. (3.13) one can rewrite (3.20) as follows:

$$\epsilon_{\mathbf{k}} = \omega_{\mathbf{k}} - \mu - \frac{1}{\beta} \log \left(1 + \beta \int (d\mathbf{k}') G_2(\mathbf{k}, \mathbf{k}') \frac{e^{\beta(\epsilon_{\mathbf{k}'} - \omega_{\mathbf{k}'} + \mu)}}{e^{\beta \epsilon_{\mathbf{k}'}} - s} \right) \tag{3.21}$$

One may also want to find the free energy density of the system in terms of the physical filling fraction f. By using (3.20) and (3.11), it can be shown that

$$\begin{aligned} \mathcal{F}_1 &= -\frac{1}{2} \int (d\mathbf{k})(d\mathbf{k}') \tilde{f}(\mathbf{k}) \tilde{f}(\mathbf{k}') G_2(\mathbf{k}, \mathbf{k}') \\ &= -\frac{1}{2\beta} \int (d\mathbf{k}) \frac{\tilde{f}(\mathbf{k}) - f_0(\mathbf{k})}{s f_0(\mathbf{k})} \\ &= -\frac{1}{2\beta} \int (d\mathbf{k}) \frac{f(\mathbf{k}) - f_0(\mathbf{k})}{1 + s f_0(\mathbf{k})}. \end{aligned} \tag{3.22}$$

The free energy density then takes the simple form:

$$\begin{aligned} \mathcal{F} &= \mathcal{F}_0 + \mathcal{F}_1 \\ &= -\frac{1}{\beta} \int d\mathbf{k} \left(s \log(1 + sf) - \frac{1}{2} \left(\frac{f - f_0}{1 + s f_0} \right) \right) \end{aligned} \tag{3.23}$$

In summary, the two-body approximation consists of the integral equation (3.21) for the pseudo-energy defined in eq. (3.12), and the above expression (3.23) for the free energy. What is left is to give an explicit expression for the two-body kernel G_2.

3.4 Two-body kernel

In this section, we derive the two-body kernel $G_2(\mathbf{k}_1, \mathbf{k}_2)$ that enters the approximation of the last section. From the definition (2.27) and (2.31), we identify the kernel as the connected part of the diagonal matrix element of $\log S(E)$. In other words,

$$2\pi\delta\left(E - \frac{1}{2m}(\mathbf{k}_1^2 + \mathbf{k}_2^2)\right) V\, G_2(\mathbf{k}_1, \mathbf{k}_2) \equiv -i\langle \mathbf{k}_1, \mathbf{k}_2 | \log \hat{S}(E) | \mathbf{k}_1, \mathbf{k}_2 \rangle. \tag{3.24}$$

where V is the spatial volume.

Following the usual convention, we write the two-body S-matrix as the sum of the identity operator and the T-matrix, and then formally define $\log S$ as a power series of the T-matrix:

$$S(E) = 1 + i2\pi\delta(E - H_0)T(E) \tag{3.25}$$

$$\log S(E) = -\sum_{n=1}^{\infty} \frac{1}{n} \left(-i2\pi\delta(E - H_0)T(E)\right)^n \tag{3.26}$$

We shall now make two further assumptions that are rather general:

- The Hamiltonian is overall translationally invariant.
- The interaction potential V is isotropic in all direction.

The first assumption implies momentum conservation in all collision processes, while the second assumption is valid if we are in the low-energy, s-wave scattering regime.

In the graphical language, the T-matrix is the sum of all connected amputated Feynman diagrams with two incoming and two outgoing external legs.

Allowing the total energy E to go off-shell, the t-matrix element between an incoming and an outgoing two-particle states can be written as:

$$\langle \mathbf{k}_1, \mathbf{k}_2 | T | \mathbf{p}_1, \mathbf{p}_2 \rangle = (2\pi)^d \delta^{(d)}(\mathbf{p}_1 + \mathbf{p}_2 - \mathbf{k}_1 - \mathbf{k}_2) \mathcal{M}(E)_{\mathbf{p}_1, \mathbf{p}_2 \to \mathbf{k}_1, \mathbf{k}_2}, \tag{3.27}$$

where the scattering amplitude $\mathcal{M}$ is of course model-dependent.

We won't explicitly calculate $\mathcal{M}$ until the next chapter, but a general result follow immediately from the assumed translational and rotational invariances. When the energy E is on-shell, the S-matrix describes the actual physical process, and all the usual symmetries and conservation laws apply:

- Translational invariance means $\mathcal{M}$ can only depend on the differences of pair of momenta.
- Rotational invariance of the total Hamiltonian, as well as the interaction potential, cut the list of variables down to only $|\mathbf{k}_1 - \mathbf{k}_2|$ and $|\mathbf{p}_1 - \mathbf{p}_2|$.
- Finally, energy and momentum conservation implies $|\mathbf{k}_1 - \mathbf{k}_2| = |\mathbf{p}_1 - \mathbf{p}_2|$.

Therefore, when $E = \frac{1}{2m}(\mathbf{p}_1^2 + \mathbf{p}_2^2)$ is on-shell, the matrix elements of T can be

written as

$$\begin{aligned}
&\langle \mathbf{k}_1, \mathbf{k}_2 | \delta(E - H_0) T(E = \frac{\mathbf{p}_1^2}{2m} + \frac{\mathbf{p}_1^2}{2m}) | \mathbf{p}_1, \mathbf{p}_2 \rangle \\
&\quad = (2\pi)^d \delta \left(E - \frac{1}{2m}(\mathbf{k}_1^2 + \mathbf{k}_2^2) \right) \delta^{(d)}(\mathbf{p}_1 + \mathbf{p}_2 - \mathbf{k}_1 - \mathbf{k}_2) \mathcal{M}(|\mathbf{p}_1 - \mathbf{p}_2|) \\
&\quad = \frac{2m(2\pi)^d}{|\mathbf{p}_1 - \mathbf{p}_2|} \delta(|\mathbf{p}_1 - \mathbf{p}_2| - |\mathbf{k}_1 - \mathbf{k}_2|) \; \delta^{(d)}(\mathbf{p}_1 + \mathbf{p}_2 - \mathbf{k}_1 - \mathbf{k}_2) \mathcal{M}(|\mathbf{p}_1 - \mathbf{p}_2|)
\end{aligned} \tag{3.28}$$

With this, we set out to find the diagonal element of the nth power of $\delta(E - H_0)T(E)$:

$$\begin{aligned}
&\langle \mathbf{p}_1, \mathbf{p}_2 | (\delta(E - H_0) T(E))^n | \mathbf{p}_1, \mathbf{p}_2 \rangle \\
&\quad = \langle \mathbf{p}_1, \mathbf{p}_2 | \left[\delta(E - H_0) T(E) \right]^{n-1} \times \frac{1}{2\alpha} \int (d\mathbf{k_1})(d\mathbf{k_2}) |\mathbf{k}_1, \mathbf{k}_2\rangle \langle \mathbf{k}_1, \mathbf{k}_2| \times \\
&\quad \delta \left(\frac{\mathbf{p}_1^2}{2m} + \frac{\mathbf{p}_2^2}{2m} - H_0 \right) T \left(\frac{\mathbf{p}_1^2}{2m} + \frac{\mathbf{p}_2^2}{2m} \right) |\mathbf{p}_1, \mathbf{p}_2\rangle.
\end{aligned} \tag{3.29}$$

The left-most energy δ-function ensures that the right-most $T(E)$ is on-shell, and the on-shell matrix element has the form of (3.28). We have inserted a complete set of two-particle states, with the combinatoric factor α defined in (1.9).

Since the intermediate state $|\mathbf{k}_1, \mathbf{k}_2\rangle$ is constrained to have the same energy as the incoming state $|\mathbf{p}_1, \mathbf{p}_2\rangle$, the operator $T(E)$ acting on $|\mathbf{k}_1, \mathbf{k}_2\rangle$ is once again on-shell. Furthermore, given that $|\mathbf{p}_1 - \mathbf{p}_2| = |\mathbf{k}_1 - \mathbf{k}_2|$, the amplitude $\mathcal{M}$ is constant for every pair of allowed $(\mathbf{k}_1, \mathbf{k}_2)$.

Inserting more complete sets of states in between every factor of $\delta(E - H_0)T(E)$, we see that each matrix element becomes on-shell, and all amplitudes are identically equal to $\mathcal{M}(\mathbf{p}_1 - \mathbf{p}_2|)$.

Let $\mathcal{I}$ denotes the phase space volume accessible by each set of intermediate

states. It is defined as

$$\mathcal{I} = \frac{1}{2\alpha}\int (d\mathbf{k}_1)(d\mathbf{k}_2)(2\pi)^{d+1}\delta\left(\frac{\mathbf{p}_1^2}{2m}+\frac{\mathbf{p}_2^2}{2m}-\frac{\mathbf{k}_1^2}{2m}-\frac{\mathbf{k}_2^2}{2m}\right)\delta^d(\mathbf{p}_1+\mathbf{p}_2-\mathbf{k}_1-\mathbf{k}_2). \tag{3.30}$$

For definiteness, we give here expressions of $\mathcal{I}$ in dimension $d = 1, 2, 3$:

$$\mathcal{I} = \begin{cases} \frac{m^2}{2\sqrt{2}\alpha}\frac{1}{|\mathbf{p}_1-\mathbf{p}_2|} & d=1 \\ \frac{m}{4\alpha} & d=2 \\ \frac{m}{4\pi\alpha}|\mathbf{p}_1-\mathbf{p}_2| & d=3 \end{cases} \tag{3.31}$$

And we can now express the matrix element (3.29) in a compact form:

$$\begin{aligned} &\langle \mathbf{p}_1,\mathbf{p}_2|(\delta(E-H_0)T(E))^n|\mathbf{p}_1,\mathbf{p}_2\rangle \\ &\quad = \delta\left(E-\frac{\mathbf{p}_1^2}{2m}-\frac{\mathbf{p}_1^2}{2m}\right)(2\pi)^d\delta^d(0)\frac{1}{\mathcal{I}}\left(\frac{\mathcal{I}\mathcal{M}}{(2\pi)}\right)^n. \end{aligned} \tag{3.32}$$

Each of the $(n-1)$ intermediate sets of states leads to a factor of $\mathcal{I}$. The left-most momentum δ-function is saturated, leaving us with $(2\pi)^d\delta^{(d)}(0) = V$, the volume of space. The left-most energy δ-function stays intact. Now we are in the position to re-sum the power series in (3.26):

$$\langle \mathbf{p}_1,\mathbf{p}_2|\log S(E)|\mathbf{p}_1,\mathbf{p}_2\rangle = V2\pi\delta\left(E-\frac{\mathbf{p}_1^2}{2m}-\frac{\mathbf{p}_2^2}{2m}\right)\frac{1}{\mathcal{I}}\log\left[1+i\mathcal{I}\mathcal{M}(|\mathbf{p}_1-\mathbf{p}_2|)\right] \tag{3.33}$$

By comparing with (3.24), we obtain a closed-form expression for the two-body kernel:

$$G_2(\mathbf{p}_1,\mathbf{p}_2) = -\frac{i}{\mathcal{I}}\log\left(1+i\mathcal{I}\mathcal{M}(|\mathbf{p}_1-\mathbf{p}_2|)\right) \tag{3.34}$$

Also by looking at (3.24), we see that the kernel G_2 can be symbolically considered as

$$G_2 \sim \frac{-i\log S(E)}{(2\pi)\delta(E-H_0)}. \tag{3.35}$$

It is therefore sensible to identify the logarithm in (3.34) as the "phase shift" due to scattering. We make the definition:

$$\Theta(\mathbf{p}_1, \mathbf{p}_2) \equiv \log\left(1 + i\mathcal{I}\mathcal{M}(|\mathbf{p}_1 - \mathbf{p}_2|)\right). \tag{3.36}$$

This quantity Θ will appear again when we discuss the unitary limit of a quantum gas.

3.5 Extension to multi-component gases

The extension of the above formalism to a multi-component gas is very straightforward. Even though our work here primarily focuses on quantum gas with one species of particles, a fermion with spin-1/2 necessarily has two spin components, making this extension relevant to our work.

Let $a = 1, 2, \ldots N$ labels the N species of particles. In general, they may have different masses, experience different chemical potentials, or even obey different statistics. One can nevertheless formally define an $SU(N)$ group that transform these species into each other. We can then say that the masses, chemical potentials, and statistical factors s all carries an $SU(N)$ index a and transform as vectors.

By the same token, the filling fractions f and pseudo energy ϵ are also $SU(N)$ vectors.

Much of the derivation in chapter II remains valid. The only modification needed is that, in addition to the momentum, each particle is also labeled by its species. In the diagrammatic expansion, each line now carries an additional species label, and the vertex function $\mathcal{V}_n$ carries n species indices, matching the $2n$ lines

that are joined by the vertex. A summation over the species index is implied for each closed loop.

The Legendre transformation goes through similarly. The free energy functional $\digamma$ once again consists of the non-interacting part $\digamma_0$, and $\digamma_1$, the part due to interaction.

The non-interacting part $\digamma_0$ is simply a sum over all particle species:

$$\digamma_0 = -\sum_a \frac{1}{\beta} \int (d\mathbf{k}) \left(s_a \log(1 + s_a f_a) - \left(\frac{f_a - f_{a0}}{1 + s_a f_{a0}} \right) \right); \tag{3.37}$$

while the interacting part is the sum of all 2PI vacuum diagrams, with the dressed $\widetilde{f}_a$ as its internal lines. In particular, the two-body approximation now yields a set of N coupled integral equations.

A two-particle state now carries two species labels. Since the two particles can in general be distinguished by their momenta, we do not assume any symmetry property for these two species indices. The species label for a two-particle state may hence take N^2 distinct values. The two-particle scattering amplitude can then be regarded as an $N^2 \times N^2$ matrix.

The two-body kernel follows straightforwardly:

$$G_{2,ab}(\mathbf{p}_1, \mathbf{p}_2) = -\left[\frac{i}{\mathcal{I}} \log \left(1 + i\mathcal{I}\mathcal{M}(|\mathbf{p}_1 - \mathbf{p}_2|) \right) \right]_{ab,ab}. \tag{3.38}$$

Here the logarithm of an $N^2 \times N^2$ matrix is defined by its Taylor series as usual. The accessible phase space volume $\mathcal{I}$ is itself an $N^2 \times N^2$ diagonal matrix, its components given by:

$$\mathcal{I}_{ab,ab} = \frac{1}{2} \int (d\mathbf{k}_1)(d\mathbf{k}_2)(2\pi)^{d+1} \delta \left(E - \frac{\mathbf{k}_1^2}{2m_a} - \frac{\mathbf{k}_2^2}{2m_b} \right) \delta^d(\mathbf{p}_1 + \mathbf{p}_2 - \mathbf{k}_1 - \mathbf{k}_2), \tag{3.39}$$

where E denotes the total initial energy.

Instead of (3.20), we have

$$\tilde{f}_a(\mathbf{k}) = f_{a0}(\mathbf{k}) + \tilde{f}_a(\mathbf{k}) \left(s_a \beta f_{a0}(\mathbf{k}) \sum_b \int (d\mathbf{k}') G_{2,ab}(\mathbf{k}, \mathbf{k}') \tilde{f}_b(\mathbf{k}') \right). \tag{3.40}$$

The pseudo-energy becomes

$$\epsilon_{a,\mathbf{k}} = \omega_{a,\mathbf{k}} - \mu_a - \frac{1}{\beta} \log \left(1 + \beta \int (d\mathbf{k}') G_{2,ab}(\mathbf{k}, \mathbf{k}') \frac{e^{\beta(\epsilon_{b,\mathbf{k}'} - \omega_{b,\mathbf{k}'} + \mu_b)}}{e^{\beta \epsilon_{b,\mathbf{k}'}} - s_b} \right). \tag{3.41}$$

We now work out the special case of the spin-1/2 fermion gas, with the species index $a = 1, 2$. We have $s_1 = s_2 = -1$ and $m_1 = m_2 = m$, but potentially $\mu_1 \neq \mu_2$ in the presence of a magnetic filed. Barring a symmetry-breaking field, the $SU(2)$ group is an actual symmetry of the action in this case.

The Pauli exclusion principle, along with the assumption of a *delta*-function potential (see Chapter IV,) ensures that scattering can only take place between two fermions of opposite spins. Angular momentum conservation further demands that the two outgoing particles have opposite spins. We may write

$$\mathcal{M}_{12,12} = \mathcal{M}_{12,21} = \mathcal{M}_{21,12} = \mathcal{M}_{21,21} = \mathcal{M}, \tag{3.42}$$

while all other components are zero.

The summation over the matrix indices (ab) effectively yields a factor of 2 each time it is performed. One may absorb this factor into $\mathcal{I}$. The integral equations and pseudo energy are then

$$\begin{aligned} \tilde{f}_1(\mathbf{k}) &= f_{1,0}(\mathbf{k}) + \tilde{f}_1(\mathbf{k}) \left(-\beta f_{1,0}(\mathbf{k}) \sum_2 \int (d\mathbf{k}') G_2(\mathbf{k}, \mathbf{k}') \tilde{f}_2(\mathbf{k}') \right) \\ \epsilon_{1,\mathbf{k}} &= \omega_{\mathbf{k}} - \mu - \frac{1}{\beta} \log \left(1 + \beta \int (d\mathbf{k}') G_2(\mathbf{k}, \mathbf{k}'); \frac{e^{\beta(\epsilon_{\mathbf{k}'} - \omega_{\mathbf{k}'} + \mu_2)}}{e^{\beta \epsilon_{\mathbf{k}'}} + 1} \right), \end{aligned} \tag{3.43}$$

together with equations in which spin indices are exchanged. The kernel G_2 is as given in (3.34).

CHAPTER 4

FIELD THEORIES FOR QUANTUM GASES

After developing the S-matrix formulation of quantum statistical mechanics, and a practical way of carrying out calculation under the frame work, we want to apply the machinery to the problem of quantum gases.

Before jumping into the problem, however, we wish to present a quick review of the model we are interested in.

4.1 Actions and Feynman rules

We consider two different models: a single-component boson gas, and a spin-1/2 fermion gas.

The bosonic action is

$$S = \int dt\, d^d\mathbf{x} \left(\phi^\dagger \left[i\partial_t - \frac{\nabla^2}{2m} + \mu \right] \phi - \frac{g}{4} \phi^\dagger \phi^\dagger \phi \phi \right) \tag{4.1}$$

The chemical potential μ is necessary because we will allow thermal fluctuation in particle density. However, all vertex functions of our S-matrix formulation are always associated with scattering in the vacuum.

The field operator $\phi(\mathbf{x}, t)$ has the usual interpretation of an particle annihilation operator: it annihilates a boson at position $\mathbf{x}$ at time t. Its Hermitian conjugate $\phi^\dagger$ is the corresponding creation operator. Due to the Bose statistics, they obey the equal-time commutation relation:

$$\left[\phi(\mathbf{x}, t), \phi^\dagger(\mathbf{x}', t) \right] = \delta^{(d)}(\mathbf{x} - \mathbf{x}'). \tag{4.2}$$

One can read off the free-particle propagator in momentum space from the quadratic part of the action (4.1):

$$G_0^R(\omega, \mathbf{k}) = \lim_{\eta \to 0^+} \frac{1}{\omega - \mathbf{k}^2/2m + \mu + i\eta}. \tag{4.3}$$

The infinitesimal $i\eta$ prescription is added to ensure the convergence of the path integral of e^{iS}.

Since we are only interested in scattering processes at $T = 0$ in the vacuum, we can take the chemical potential μ to be zero. Note that the advance propagator is absent as a result. As the "backward propagation" of a particle is really the forward propagation of a hole in the background of pre-existing particles, such process cannot take place in the vacuum.

The quartic interaction term in (4.1) implies that these bosons interact with a δ-function potential. This is a good low-energy description for any finite-ranged potential. But, being a low-energy approximation, we shall see that an ultraviolet cut-off will be necessary. This term gives a four-particle vertex in the perturbation theory.

The fermionic action is:

$$S = \int dt\, d^d\mathbf{x} \left(\sum_{a=\uparrow,\downarrow} \psi_a^\dagger \left[i\partial_t - \frac{\nabla^2}{2m} + \mu_a \right] \psi_a - \frac{g}{2} \psi_\uparrow^\dagger \psi_\downarrow^\dagger \psi_\downarrow \psi_\uparrow \right) \tag{4.4}$$

The two spin states of the fermion can be regarded as two distinct species of particles. Note that the chemical potential μ may be different for each spin, corresponding to an external magnetic field breaking the spin rotational symmetry.

The field operators ψ_a and $\psi_a^\dagger$, $a = \uparrow, \downarrow$, are the annihilation and creation operators of the fermion respectively. They obey the equal-time anticommutation

relation:

$$\left\{\psi_a(\mathbf{x},t),\psi_b^\dagger(\mathbf{x}'t,t)\right\}=\delta_{a,b}\delta^{(d)}(\mathbf{x}-\mathbf{x}'). \tag{4.5}$$

For our choice of coefficients, the bosonic four-vertex is proportional to $-ig$, while the fermionic version is $-ig/2$. Recall the definition of α in (1.9), we have here $\alpha=1$ for bosons and $\alpha=1/2$ for fermions, and the four-vertex can be expressed generally as $i\alpha g$.

4.2 Two-body scattering in vacuum

Central to our integral equation is the two-body scattering process in vacuum, and we shall look at it in some depth in this section.

The exact two-body scattering amplitude $\mathcal{M}$ can be obtained by resumming the so-called ladder diagrams, as depicted in figure 4.1. Algebraically this is a geometric series, and can be resummed as such:

$$\begin{aligned} i\mathcal{M} &= (-i\alpha g)+\frac{1}{2}(-ig\alpha)^2\frac{1}{2\alpha}\int(\text{loop})+\frac{1}{4}(-ig\alpha)^3\left(\frac{1}{2\alpha}\int(\text{loop})\right)^2+\dots \\ &= -ig\alpha\left(1+\frac{ig}{2}\int(\text{loop})\right)^{-1}. \end{aligned} \tag{4.6}$$

Attention is drawn to the extra factor of $(2\alpha)^{-1}$ in front of each loop integral. A boson loop carries a combinatoric factor $1/2$ since both legs of the loop are identical, while a fermion loop does not have this factor since the two legs have opposite spins. The upshot is, regardless of statistics, each additional loop contributes a factor of $-igs/2\int(\text{loop})$.

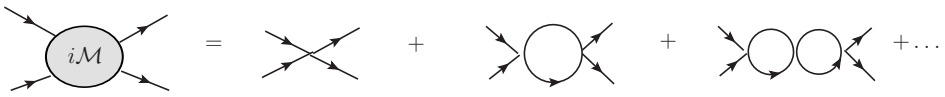

Figure 4.1: Ladder diagram resummation of the two-body scattering amplitude.

Assuming that the two incoming particles have a total energy E and total momentum $\mathbf{P}$, the loop integral $\int(\text{loop})$ is given as

$$\int(\text{loop}) = \int(d\omega)(d\mathbf{k}) \left(\frac{i}{\omega - k^2/2m + i\epsilon}\right) \left(\frac{i}{(E-\omega) - (\mathbf{P}-\mathbf{k})^2/2m + i\epsilon}\right) \tag{4.7}$$

4.2.1 $d = 2$

By simple power counting, it is easy to see that the integral (4.7) is ultraviolet-divergent is two spatial dimensions. We regulate this divergence by cutting off the momentum integral at UV cut-off Λ, and retain only the universal terms proportional to a non-negative power of Λ. The result is:

$$\begin{aligned} \int(\text{loop}) &= -\frac{im}{8\pi} \log\left(\frac{\Lambda^2 - i\eta}{-\left(mE - \frac{\mathbf{P}^2}{4}\right) - i\eta}\right) \\ &= -\frac{mi}{8\pi}\left[\log\left(\frac{mE - \frac{\mathbf{P}^2}{4}}{\Lambda^2}\right) + i\pi\right] \end{aligned} \tag{4.8}$$

When the total energy of the incoming particles is on-shell, the quantity $(mE - \frac{\mathbf{P}^2}{4})$ is positive. So it is necessary to keep the infinitesimal $i\eta$ until the last step to pick out the correct branch of the logarithm function.

When this expression is plugged into equation (4.6), we get the result:

$$i\mathcal{M} = \frac{-i\alpha}{\frac{1}{g} + \frac{m}{8\pi}\left[\log\left(\frac{mE - \frac{\mathbf{P}^2}{4}}{\Lambda^2}\right) + i\pi\right]}. \tag{4.9}$$

4.2.2 $d = 3$

Once again the integral (4.7) is diverging in the ultraviolet, and the UV momentum cut-off Λ is needed. The amplitude (4.6) becomes:

$$\begin{aligned} i\mathcal{M} &= \frac{-\alpha}{\frac{1}{ig} + \frac{m}{4\pi^2}\left(\frac{\Lambda}{i} + \frac{\pi}{2}\sqrt{mE - \frac{\mathbf{P}^2}{4}}\right)} \\ &= \frac{-i\alpha}{\frac{1}{g_R} + \frac{im}{4\pi}\sqrt{mE - \frac{\mathbf{P}^2}{4}}} \end{aligned} \tag{4.10}$$

The cutoff Λ in the last line is absorbed completely into the definition of renormalized coupling constant g_R:

$$\frac{1}{g_R} = \frac{1}{g} + \frac{m}{4\pi^2}\Lambda. \tag{4.11}$$

In the zero-momentum limit, the amplitude (4.10) reduces to simply

$$i\mathcal{M} \to i\alpha g_R. \tag{4.12}$$

We note that the differential cross-section of scattering process is given by:

$$\frac{d\sigma}{d\Omega} = \frac{m^2 k^{d-3}}{4(2\pi)^{d-1}}|(k)\mathcal{M}|^2. \tag{4.13}$$

At $d = 3$, the s-wave scattering length a is defined by $\sigma = \pi a^2$ at the zero momentum limit, where σ is the total cross-section. Since we have $\mathcal{M} = g_R$ at zero momentum, the scattering length is related to g_R by

$$a = \frac{m g_R}{2\pi} \tag{4.14}$$

CHAPTER 5

CRITICAL POINT OF THE TWO-DIMENSIONAL BOSE GAS

As the first application of our new formalism, we shall investigate the critical point of the two-dimensional weakly-interacting Bose gas. Although we find results that are similar to the known results [41, 12, 18, 42], we find our treatment to be considerably simpler and transparent and doesn't rely on an effective description of vortices.

The interacting Bose gas in 2 spatial dimensions is defined by the action (4.1) and taking $d = 2$.

In terms of the yet-to-be-specified two-body kernel G_2, the integral equation (3.20) gives the pseudo-energy of the Bose gas $\epsilon(\mathbf{k})$. The interacting gas behaves as if it were non-interacting, with $\epsilon(\mathbf{k})$ being the single-particle energy eigenvalues. The number density n of the gas is then

$$n = \int \frac{d^2\mathbf{k}}{(2\pi)^2} \frac{1}{e^{\beta\epsilon(\mathbf{k})} - 1} \tag{5.1}$$

where β is the inverse temperature T.

We consider the weakly-interacting limit of the two-body kernel (3.34). Assuming that the coupling constant g is small, the scattering amplitude is simply $\mathcal{M} = g$ to leading order of g, and is independent of the particle momenta. By expanding the logarithm in (3.34) to leading order in g, we end up with the simple result

$$G_2 \approx -g \tag{5.2}$$

for small g.

Since when $g = 0$, $\epsilon(\mathbf{k}) = \omega_{\mathbf{k}} - \mu$, at weak coupling an approximate solution

to (3.20) is obtained by substituting $\epsilon(\mathbf{k}) = \omega_{\mathbf{k}} - \mu$ on the right hand side. As in Bose-Einstein condensation, the critical point is defined to occur at the value of the chemical potential μ_c where the occupation number at zero momentum diverges, i.e. $\epsilon(\mathbf{k} = 0) = 0$. This gives the following integral equation for μ_c:

$$\mu_c = -\int \frac{d^2\mathbf{k}}{(2\pi)^2} G_2(0, \mathbf{k}) \frac{1}{e^{\beta(\omega_{\mathbf{k}} - \mu_c)} - 1} \tag{5.3}$$

Furthermore, we shall make the approximation $G_2 \approx -g$ as reasoned above. Consider first the case where the interaction is attractive, i.e. $g < 0$. The equation (5.3) becomes

$$\beta\mu_c = -\frac{mg}{2\pi} \log\left(1 - e^{\beta\mu_c}\right). \tag{5.4}$$

For negative g, the above equation has negative μ_c solutions, which makes physical sense since energy is released when a particle is added. Here the attractive interaction makes a critical point possible at finite temperature and density. The critical density $n_c \approx \mu_c/g$.

Suppose now the interaction is repulsive, i.e. $g > 0$. The equation (5.4) now has no real solutions for μ_c. This can be traced to the infra-red divergence of the integral when μ_c changes sign. Let us therefore introduce a low-momentum cut-off k_0, i.e. restrict the integral to $|\mathbf{k}| > k_0$. The equation (5.3) now becomes

$$\beta\mu_c = \frac{mg}{2\pi} \left[\beta\epsilon_0 - \beta\mu_c - \log\left(e^{\beta(\epsilon_0 - \mu_c)} - 1\right)\right] \tag{5.5}$$

where $\epsilon_0 = k_0^2/2m$. The above equation now has solutions at positive μ_c, however for arbitrary k_0 there are in general two solutions. If k_0 is chosen appropriately to equal a critical value k_c, then there is a unique solution μ_c. This is shown in Figure 5.1, where the right and left hand sides of equation (5.5) are plotted against μ_c for two values of k_0, one being the critical value k_c.

Since the slopes of the right and left hand sides of eq. (5.5) are equal at the critical point, taking the derivative with respect to μ_c of both sides gives the additional equation:

$$\beta(\epsilon_c - \mu_c) = \log\left(1 + \frac{mg}{2\pi}\right) \tag{5.6}$$

where $\epsilon_c = k_c^2/2m$. The two equations (5.5, 5.6) determine μ_c and ϵ_c:

$$\begin{aligned} \mu_c &= \frac{mgT}{2\pi}\log\left(1 + \frac{2\pi}{mg}\right) \\ \epsilon_c &= \frac{k_c^2}{2m} = T\left(1 + \frac{mg}{2\pi}\right)\log\left(1 + \frac{mg}{2\pi}\right) + \frac{mgT}{2\pi}\log\left(\frac{2\pi}{mg}\right) \end{aligned} \tag{5.7}$$

Note that ϵ_c goes to zero as g goes to zero. Finally, making the approximation $\epsilon(\mathbf{k}) \approx \omega_{\mathbf{k}} - \mu_c$ in eq. (5.1) and using eq. (5.5) one obtains the critical density $n_c \approx \mu_c/g$:

$$n_c \approx \frac{mk_BT}{2\pi\hbar^2}\log\left(1 + \frac{2\pi}{mg}\right) \tag{5.8}$$

The above can be expressed as $n_c\lambda^2 = \log(1+2\pi/mg)$ where $\lambda = \hbar\sqrt{2\pi/mk_BT}$ is the thermal wavelength. As expected, at fixed temperature, the critical density goes to infinity as g goes to zero.

In obtaining the above result we have only kept the leading term in the kernel G_2 at small coupling, which is momentum-independent. Systematic corrections to the above results may be obtained by keeping higher order terms in the kernel. However since the kernel involves $\log \mathbf{k}^2$, at small coupling these corrections are quite small, as we have verified numerically.

In numerical simulations of the critical point, it was found that $\mu_c \sim \frac{mgT}{2\pi}\log(2C/mg)$ where C is a constant[42]. This form agrees with our result (5.7) in the limit of small g, however, whereas we find $C = \pi$, numerically one finds a significantly higher value $C \approx 13.2$.

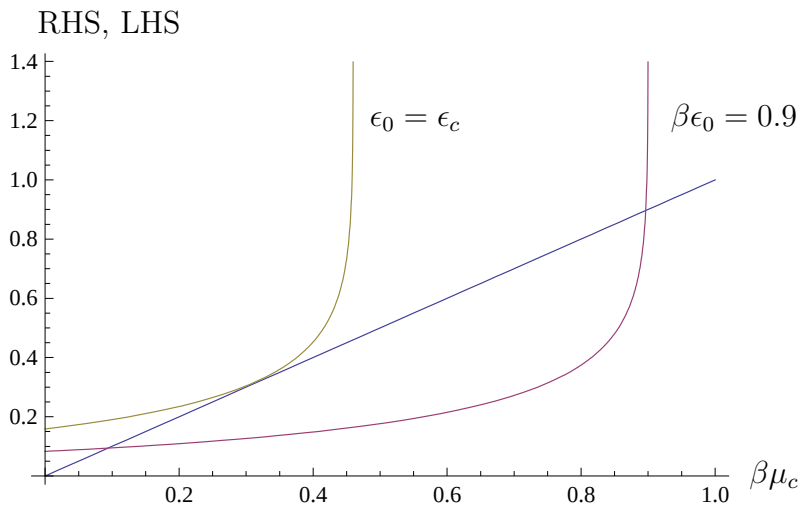

Figure 5.1: Left and right hand sides of eq. (5.5) as a function of $\beta\mu_c$ at two values of the infra-red cut-off ϵ_0, one being the critical value ϵ_c.

Assuming that C was not overestimated numerically, one possible explanation for this discrepancy is based on the renormalization group. The beta-function for g can be found by requiring that the kernel G_2 in eq. (7.1) be independent of the ultra-violet cut-off Λ. To lowest order this gives:

$$\Lambda \frac{dg}{d\Lambda} = \frac{mg^2}{4\pi} \tag{5.9}$$

which implies the coupling decreases at low energies. Integrating this equation leads to the cut-off dependent coupling $g(\Lambda)$:

$$\frac{2\pi}{mg(\Lambda)} = \frac{2\pi}{mg_0}\left(1 + \frac{mg_0}{4\pi}\log(\Lambda_0/\Lambda)\right) \tag{5.10}$$

where $g_0 = g(\Lambda_0)$. Thus at low energies where $\Lambda < \Lambda_0$, the combination $2\pi/mg$ grows. However since the dependence on the cut-off is only logarithmic, it is not clear that this could explain the large C discrepancy. This seems to imply that higher N-body interactions are important.

CHAPTER 6

RENORMALIZATION GROUP AND THE UNITARY LIMIT

With the knowledge of scattering amplitudes, we can now discuss the renormalization group flow of our models under scaling transformations.

Let us first consider the free-field case by setting the coupling constant $g \to 0$. By inspection, the actions (4.1) and (4.4) possess a scale invariance with dynamical exponent $z = 2$, i.e. they are invariant under:

$$t \to \Lambda^{-2} t, \mathbf{x} \to \Lambda^{-1} \mathbf{x}.$$

We shall now proceed to show that the actions (4.1) and (4.4) are also scale-invariant in the so-called unitary limit, where the s-wave scattering length of the model diverges.

It is customary to define the scaling dimension of a field X, $\dim[X]$, in unit of inverse length. In this notation, we have $\dim[\mathbf{k}] = 1$, $\dim[t] = -2$, and so on.

Requiring that the action be dimensionless yields $\dim[\phi] = \dim[\psi] = d/2$ and $\dim[g] = 2 - d$.

6.1 The 3d case

The renormalization group behavior can be inferred from the coupling constant dependence of the S-matrix. Consider first the particular case of $d = 3$ dimensions. The cut-off dependence of the scattering amplitude is completely absorbed into the definition of renormalized coupling g_R in equation (4.11). Two theories, with different bare coupling constant g and cut-off Λ, would appear to have the exact

same low-energy behavior if they have the same g_R.

Define the dimensionless coupling $\hat{g} = g\Lambda^{-1}$. If we require the low-energy behavior of the model be independent of the cut-off Λ, which represents the high-energy or short-distance detail of the actual physical system which we don't want to deal with, we arrive at the following beta-function:

$$\frac{d\hat{g}}{dl} = -\hat{g} - \frac{m}{4\pi^2}\hat{g}^2, \tag{6.1}$$

where $l = -\log[\Lambda]$.

This beta-function goes to zero for two different values of $\hat{g}$. The first, trivial case is $\hat{g} = 0$, corresponding to the free-field case. We shall show that the other zero at $\hat{g} = \hat{g}_* \equiv -4\pi^2/m$ corresponds to the unitary limit.

At this renormalization group fixed point, the renormalized coupling g_R takes value

$$\frac{1}{g_R} = \frac{\Lambda}{\hat{g}_*} + \frac{m}{4\pi^2}\Lambda = 0. \tag{6.2}$$

As g_R is proportional to the scattering length, we have shown that the unitary limit of the model, characterized by an infinite scattering length, is this scale-invariant fixed point. This should not come as a surprise, because the scattering length is the only length scale in the low-energy effective theory, and the only cases where it can be invariant under a scale transformation are zero and infinity.

The bare coupling $\hat{g}_*$ is *negative* at the fixed point, implying an *attractive* potential between each pair of particles. A gas of bosons with mutual attractive may be thermodynamically unstable and prone to collapse. On the other hand, the attractive interaction in a fermion gas may be balanced by the Fermi pressure, and the gas stable against collapse.

The bare coupling can approach this non-trivial fixed point from either side of the $\hat{g}$-axis. From (4.11) it is easy to see that g_R and $(\hat{g} - \hat{g}_*)$ have opposite signs.

To the right of the fixed point, the scattering length is positive, indicating attraction at low energy. For a fermionic gas, it is well-known that an effective attraction leads to Cooper pairing and the BCS instability at low temperature.

On the other hand, the scattering length is negative on the left side of the fixed point, indicating an effective repulsion at low energy. The amplitude (4.10) has a pole at $k = 16\pi i/mg_R$ (which corresponds to a negative center-of-mass energy), indicating the presence of a bound state. The position of the pole gives the binding energy of the pair, and it is:

$$E_{\text{bind}} = -\frac{128\pi^2}{m^3 g_R^2}. \tag{6.3}$$

This bound state is only present for $\hat{g} < \hat{g}_*$. The fermion pairs are bosonic, and would presumably undergo Bose-Einstein condensation at a low enough temperature.

We therefore identify the fixed point $\hat{g}_*$ with the BCS-BEC crossover, at which the inverse of the scattering length $1/a$ changes sign. We also note that the binding energy (6.3) goes to zero as the system approaches the crossover from the BEC side, and then the bound state ceases to exist on the BCS side. Nevertheless, the crossover is expected to be smooth if one includes the bound states in the thermodynamic of the BEC side.

As the model approaches its fixed point $g_R \to 0$, the phase shift (3.36) becomes:

$$\Theta(\mathbf{p}_1, \mathbf{p}_2) = \log\left(-1 + \frac{i}{g_R}\,\frac{8\pi}{m|\mathbf{p}_1 - \mathbf{p}_2|}\right) \tag{6.4}$$

As $g_R \to \pm\infty$, the phase shift becomes independent from the momenta of

the particles, and takes value of $\pm i\pi$. The interaction is infinitely strong in the low-energy regime that the phase shift of the two-particle scattering is always saturated at the largest possible value (any phase shift larger than π is physically indistinguishable from a smaller negative shift.)

There is a closed parallel in the one-dimensional thermodynamic Bethe Ansatz of interacting bosons. By simple power counting, the two-boson interaction is a relevant perturbation in the sense of renormalization group, and would grow in strength as the model flows to the infrared. And in the Bethe Ansatz solution, these bosons behave as if they are fermions due to their strong interaction. More specifically, since the exchange phase and scattering phase can't be separated in one-dimension, the phase change due to interaction has the effect of altering particle statistics.

We shall adopt the saturation of scattering phase shift at $\pm i\pi$ as an alternative definition of the unitary limit.

6.2 The case of a generic $d \neq 2$

The loop integral (4.7) can be evaluated for a general d. The ω integral can always be done by closing the contour in the upper-half plane and picking up the pole at $\omega = \mathbf{k}^2/2m - i\epsilon$. The loop integral then become

$$\begin{aligned} \int (\text{loop}) &= i \int (d\mathbf{k}) \frac{1}{\left(E - \frac{\mathbf{k}^2}{2m}\right) - \frac{(\mathbf{p}-\mathbf{k})^2}{2m} - 2i\epsilon} \\ &= -i\, m \int (d\mathbf{k}) \frac{1}{\mathbf{k}^2 - (m\, E - \frac{\mathbf{p}^2}{4}) - i\epsilon} \end{aligned} \tag{6.5}$$

Note that, to get to the last line, we have shifted the integration variable $(\mathbf{k} - \mathbf{p}/2) \to \mathbf{k}$.

If $2 < d < 3$, the integral is ultraviolet divergent and in need of regularization. Let us write $d = 2 + \eta$, and introduce the UV cut-off Λ:

$$\begin{aligned}\int (\text{loop}) &= -i\, m \frac{\Omega_d}{(2\pi)^d} \int_0^\Lambda \frac{k^{1+\eta}\, dk}{\mathbf{k}^2 - (m\, E - \frac{\mathbf{p}^2}{4}) - i\epsilon} \\ &= -i\, m \frac{\Omega_d}{(2\pi)^d} \int_0^\Lambda dk\, \left(k^{\eta-1} + \dots\right) \\ &= -i\, m \frac{\Omega_d}{(2\pi)^d} \frac{\Lambda^\eta}{\eta} + \dots\end{aligned} \tag{6.6}$$

where $\Omega_d = 2\pi^{d/2}/\Gamma(d/2)$ is the volume of the unit $(d-1)$-sphere. The terms that are omitted are either cutoff-independent or proportional to some inverse power of Λ, and can be dropped in the low-energy limit.

Define the dimensionless coupling $\hat{g} = g\Lambda^\eta$. By requiring the amplitude (4.6) to be scale-invariant, we see that the combination:

$$\frac{1}{g_R} \equiv \frac{\Lambda^\eta}{\hat{g}} + m\, \frac{\Omega_d}{(2\pi)^d} \frac{\Lambda^\eta}{\eta} \tag{6.7}$$

must be cutoff-independent. This leads to the beta-function:

$$\frac{d\hat{g}}{dl} = -(d-2)\hat{g} - m\, \frac{\Omega_d}{(2\pi)^d} \hat{g}^2. \tag{6.8}$$

By requiring the beta-function to vanish, we can solve for the non-trivial fixed point:

$$\hat{g}_* = (2-d) \frac{m\,(2\pi)^d}{\Omega_d} \tag{6.9}$$

For the present case, we see that the renormalization group flow is qualitatively similar to the case of $d = 3$, which we just worked out explicitly. Apart from the infrared-stable fixed point $\hat{g} = 0$, there exists a ultraviolet-stable fixed point $\hat{g} = \hat{g}_*$ at which the renormalized coupling g_R diverges. The renormalization group flow is depicted in Figure 6.1(a).

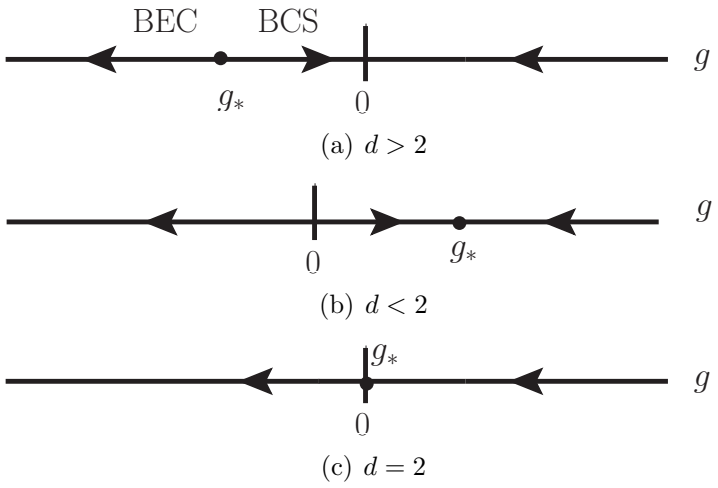

Figure 6.1: Renormalization group flow for space dimension d. The arrow indicates flow to the IR.

For $d < 2$, the loop integral is convergent. However, the zero-momentum limit of the amplitude is not well-defined, and we need an IR cutoff if we wish to speak of the scattering length in the infrared. The computation leading to the beta-function is identical to the $2 < d < 3$ case and giving identical result as in (6.8).

This time, however, the non-trivial fixed point is infrared stable. The renormalization group flow is also depicted in Figure 6.1(b).

6.3 $d = 2$

The loop integral (4.7) is logarithmic divergent at $d = 2$. Equivalently, the two-particle interaction is marginal in the sense of renormalization group flow. This fact makes the $d = 2$ case more subtle.

The running of the coupling g can be derived from requiring the amplitude

(4.9) to be independent of the cutoff Λ. This condition leads to the requirement:

$$\frac{1}{g} - \frac{m}{8\pi}\log(\Lambda^2) = \text{constant}, \tag{6.10}$$

and from here we get the beta-function:

$$\frac{dg}{dl} = -\frac{m}{4\pi}g^2. \tag{6.11}$$

This is indeed the same as (6.8) with $d = 2$. There is only one fixed point at $g_* = 0$, corresponding to the free-field theory, thus there is no analogue of the BCS/BEC crossover. The renormalization group flow is depicted in Figure 6.1(c).

One can nevertheless formally define the unitary limit as the scattering phase shift approaching $\pm i\pi$, parallel to the $3d$ case. In this section we shall explore this possibility, and interpret it using the renormalization group. As we'll see, this limit occurs at $g = \pm\infty$, and the scattering length diverges.

First let us begin with the beta function above (6.11). Let $g = g_0$ at some arbitrary scale Λ_0. Integrating the beta function one finds:

$$g(\Lambda) = \frac{g_0}{1 - \frac{mg_0}{4\pi}\log(\Lambda/\Lambda_0)}. \tag{6.12}$$

Note that g diverges at the scale:

$$\Lambda_* = \Lambda_0 e^{4\pi/mg_0}. \tag{6.13}$$

This is the familiar Landau pole. Whereas in for example the relativistic ϕ^4 theory in $d = 3$ where the Landau pole is unphysical due to higher order corrections, here the beta function (6.11) is exact [32], thus this divergence is physical.

There are two cases to consider:

1. *Attractive case:* If g_0 is negative, $\Lambda_* < \Lambda_0$, and thus $g = -\infty$ occurs in the infra-red.

2. *Repulsive case:* If g_0 is positive, $\Lambda_* > \Lambda_0$, and $g = +\infty$ occurs in the ultra-violet.

Both cases are consistent with the flows depicted in Figure 6.1.

In fact, the scale $\Lambda_* = \Lambda e^{4\pi/mg}$ is an RG invariant:

$$\frac{d\Lambda_*}{d\log\Lambda} = 0 \tag{6.14}$$

and is the natural coupling constant in this problem that physical quantities are expressed in terms of. The amplitude (4.9) becomes:

$$\begin{aligned} -i\mathcal{M} &= \frac{-i\alpha}{\frac{m}{8\pi}\log\left(\frac{\Lambda_*^2}{mE-\frac{1}{4}(\mathbf{p}_1+\mathbf{p}_2)^2}\right) + i\pi\,\frac{m}{8\pi}} \\ &= \frac{-i\alpha}{\frac{m}{4\pi}\log\left(\frac{2\Lambda_*}{|\mathbf{p}_1-\mathbf{p}_2|}\right) + i\frac{\pi}{2}\frac{m}{4\pi}}. \end{aligned} \tag{6.15}$$

where in the last line we have assumed that the momenta $\mathbf{p}_1$ and $\mathbf{p_2}$ are on-shell. From here we obtain the scattering phase shift:

$$\Theta(\mathbf{p}_1,\mathbf{p}_2) = \log\left(\frac{\log\left(\frac{2\Lambda_*}{|\mathbf{p}_1-\mathbf{p}_2|}\right) - i\frac{\pi}{2}}{\log\left(\frac{2\Lambda_*}{|\mathbf{p}_1-\mathbf{p}_2|}\right) + i\frac{\pi}{2}}\right) \tag{6.16}$$

Near the fixed point $g(\Lambda) = 0^-$, $\Lambda_* = 0$ from (6.13), and the phase shift $\Theta = 0$, consistent with the free theory. The same applies to the other side of the fixed point $g(\Lambda) = 0^+$, where $\Lambda_* = +\infty$.

On the other hand, consider the low energy limit of the attractive case where $g(\Lambda) = -\infty$. Here $\Lambda_* = \Lambda$, and this scale is effectively an infra-red cutoff. Thus at low energies $|\mathbf{p}_1 - \mathbf{p}_2| \gtrapprox 2\Lambda_*$ and the phase shift $\Theta = +i\pi$. One must keep the positive infinitesimal $\log(|\mathbf{p}_1 - \mathbf{p}_2|/\Lambda_*)$ in order to pick out the correct branch of the logarithmic function.

Similar arguments apply to the high energy limit of the repulsive case $g(\Lambda) = +\infty$, and the phase shift turns out to be $\Theta = -i\pi$. It is clear that, unlike in $3d$, this definition of the unitary limit does not correspond to a renormalization group fixed point in the usual sense of a zero of the beta function and is somewhat engineered; nevertheless it defines a scale-invariant theory.

Let us turn now to the scattering length. Using the scattering amplitude (6.15), for $|\mathbf{p}_1 - \mathbf{p}_2| = \Delta p$, the cross section is:

$$\begin{aligned} \sigma(k) &= \frac{m^2 g^2}{4\Delta p} \frac{1}{(1 + \frac{mg}{4\pi} \log(2\Lambda/\Delta p))^2 + \pi^2} \\ &= \frac{4\pi^2}{\Delta p} \frac{1}{\log^2(2\Lambda_*/\Delta p) + 16\pi^4/m^2 g^2} \end{aligned} \tag{6.17}$$

Near the scale $\Delta p = 2\Lambda_*$:

$$\sigma(\Lambda_*) = \frac{2}{\Lambda_*} \left(\frac{mg}{4\pi}\right)^2 \tag{6.18}$$

Equating σ with a scattering length a, as appropriate to $2d$, one sees that a diverges in the unitary limit $g \to \pm\infty$.

Because of the logarithmic dependence on $|\mathbf{p}_1 - \mathbf{p}_2|$, the S-matrix does not have a pole. However the denominator is zero when $|\mathbf{p}_1 - \mathbf{p}_2| = 2i\Lambda_*$, which is a remnant of the bound state pole in $3d$. The energy of this quasi-bound state is $-2\Lambda_*^2/m$. Note that this quasi-bound state disappears as $g_0 \to 0^-$, since in this limit $\Lambda_* \to 0$, and this is analogous to the situation in $3d$. We thus expect that the "attractive" case of the unitary limit should be better behaved since this bound state disappears, in contrast to the repulsive case where $\Lambda_* \to \infty$ as $g_0 \to 0^+$, and this will be born out of our subsequent analysis.

6.4 Thermodynamic scaling functions at the quantum critical point

At a quantum critical point, the only length scales of the quantum gas are the thermal wavelength $\lambda_T = \sqrt{2\pi/mT}$ and the length scale $n^{1/d}$ set by the density n. Equivalently, one can express physical properties in terms of the only two energy scales, the temperature T and the chemical potential μ, since the density is a function of T, μ.

In order to fix normalizations in a meaningful way, it is useful to consider the simplest theories with $z = 2$ scale invariance: free, non-relativistic bosons and fermions. The free energy density is given by the well-known expression for each particle:

$$\mathcal{F} = \frac{s}{\beta} \int (d^d\mathbf{k}) \, \log\left(1 - se^{-\beta(\omega_\mathbf{k} - \mu)}\right) \tag{6.19}$$

where $\beta = 1/T$, $\omega_\mathbf{k} = \mathbf{k}^2/2m$ and $s = 1, -1$ corresponds to bosons, fermions respectively.

The integrals over wave-vectors can be expressed in terms of polylogarithms $\mathrm{Li}_\nu(z)$, where $z = e^{\beta\mu}$ is a fugacity, using $\int d^d\mathbf{k} = 2\pi^{d/2}/\Gamma(d/2) \int dk k^{d-1}$ and the integrals

$$\begin{aligned} \int_0^\infty dx \, \frac{zx^{\nu-1}}{e^x - z} &= \Gamma(\nu) \, \mathrm{Li}_\nu(z) \\ \int_0^\infty dx \, \frac{zx^{\nu-1}}{e^x + z} &= -\Gamma(\nu) \, \mathrm{Li}_\nu(-z) \end{aligned} \tag{6.20}$$

valid for $\Re(\nu) > 0$. The result, as expected, is of the form of T/λ_T^d, multiplied by a dimensionless scaling function:

$$\mathcal{F} = -sT \left(\frac{mT}{2\pi}\right)^{d/2} \mathrm{Li}_{(d+2)/2}(sz) \tag{6.21}$$

There are two important limits to consider. For Bose gases near Bose-Einstein condensation, physically the interesting limit is $\mu/T \to 0$. Physically this corresponds to either the high-temperature, or the low-density limit. Since $\mathrm{Li}_\nu(1) = \zeta(\nu)$, where ζ is Riemann's zeta function, this leads us to define the scaling functions $c_d(\mu/T)$:

$$\begin{aligned} \mathcal{F} &= -\frac{\pi m T^2}{12}\, c_2(\mu/T) && (d=2) \\ \mathcal{F} &= -\frac{\zeta(5/2) m^{3/2} T^{5/2}}{(2\pi)^{3/2}}\, c_3(\mu/T) && (d=3) \end{aligned} \tag{6.22}$$

where we have used $\zeta(2) = \pi^2/6$. With the above normalizations, $c_d = 1$ for a single free boson when $\mu/T = 0$.

The above formulas are also well-defined for fermions at zero chemical potential. Using

$$-\mathrm{Li}_\nu(-1) = \left(1 - \frac{1}{2^{\nu-1}}\right)\zeta(\nu) \tag{6.23}$$

one finds as $\mu/T \to 0$:

$$c_2 = \frac{1}{2}, \qquad c_3 = 1 - \frac{1}{2\sqrt{2}} \qquad \text{(free fermions)} \tag{6.24}$$

It should be pointed out that the coefficients c_d are analogous to the Virasoro central charge for relativistic systems in $d = 1$, as discussed in [28].

The other interesting limit is $T/\mu \to 0$, i.e. $z \to \infty$ or $z \to 0$. Physically this corresponds to the zero-temperature limit, with or without a non-zero particle density in the ground state, depending on the sign of the chemical potential. (For bosons, clearly one can only take $z \to 0$, as a non-zero density at zero temperature requires the presence of a Bose-Einstein condensate. The ground state, and the Hilbert space on top of it, are qualitatively different from a free gas on which our analysis is based. But a Fermi gas admits both limits.)

Here the scaling forms are naturally based on the zero temperature degenerate free fermion gas, where $\mu > 0$ is the Fermi energy. In fact, the function $\mathrm{Li}_\nu(z)$ has a branch cut along the real axis from $z = 1$ to ∞ and the bosonic free energy is ill-defined at $z = \infty$, in contrast with fermions. Using the analytic continuation of the asymptotic behavior

$$-\mathrm{Li}_\nu(-z) \approx \frac{\log^\nu(z)}{\Gamma(\nu+1)} \qquad \text{as } z \to \infty \tag{6.25}$$

from positive integer ν to half-integer values, we define the scaling functions b_d as follows:

$$\begin{aligned} \mathcal{F} &= -\frac{m\mu^2}{4\pi}\, b_2(T/\mu) && (d=2) \\ \mathcal{F} &= -\frac{2\sqrt{2}m^{3/2}\mu^{5/2}}{15\pi^2}\, b_3(T/\mu) && (d=3) \end{aligned} \tag{6.26}$$

The above normalizations are defined such that $b_d(0) = 1$ for a single free fermion. One can verify that the above $d = 3$ expression is the standard result for a zero temperature, single component, degenerate fermion gas where μ is the Fermi energy.

Other thermodynamic quantities follow from the free energy. The pressure $p = -\mathcal{F}$. The density is $n = -\partial\mathcal{F}/\partial\mu$ and the entropy density is $s = -\partial\mathcal{F}/\partial T$. Using the scaling form in (6.26), one obtains for $d = 3$:

$$\begin{aligned} n &= \frac{2\sqrt{2}}{15\pi^2}(m\mu)^{3/2}\left(\frac{5}{2}b_3 - \frac{T}{\mu}b_3'\right) \\ s &= \frac{2\sqrt{2}}{15\pi^2}(m\mu)^{3/2}\, b_3'(T/\mu) \end{aligned} \tag{6.27}$$

where b' is the derivative with respect to its argument T/μ. (Henceforth, g' will always refer to the derivative of the function g with respect to it's argument μ/T or T/μ as defined above.) The analogous formulas in 2 dimensions are:

$$\begin{aligned} n &= \frac{m\mu}{4\pi}\left(2b_2 - \frac{T}{\mu}b_2'\right) \\ s &= \frac{m\mu}{4\pi}\, b_2' \end{aligned} \tag{6.28}$$

The energy density ϵ follows from the relation $\epsilon = Ts + \mu n + \mathcal{F}$:

$$\epsilon = -\frac{d}{2}\mathcal{F} \tag{6.29}$$

It is interesting to note that the above result, which in terms of the pressure is simply $\epsilon = pd/2$, is a consequence of the mechanics of *free* gases. This shows that this relation continues to hold for interacting gases at a quantum critical point, as pointed out by Ho[16].

Also of interest is the energy per particle $\epsilon_1 = \epsilon/n$:

$$\epsilon_1 = -\frac{d}{2}\frac{\mathcal{F}}{n} \tag{6.30}$$

Consider first the limit $T/\mu \to 0$, with μ positive. In this limit, if b is a smooth function of T/μ as $T/\mu \to 0^+$, then the b' terms in the density vanish and one simply obtains

$$\lim_{T/\mu \to 0^+} \epsilon_1 = \frac{d}{d+2}\mu \tag{6.31}$$

which is the same result as for a free gas, where for fermions μ is equal to the Fermi energy ϵ_F. The above formula is usually not appropriate to the $T \to 0$ limit when μ is negative. For the interacting gas $\mu \neq \epsilon_F$, so this leads us to define the scaling functions ξ:

$$\xi_d(T/\mu) = \frac{d+2}{d}\frac{\epsilon_1}{\epsilon_F} \tag{6.32}$$

As $T/\mu \to 0^+$, the functions ξ_d should become universal constants, and for free fermions $\xi_d(0^+) = 1$. The Fermi energy ϵ_F can be defined based on its relation to density in the zero temperature free fermion gas. For bosons, one can formally use the same definition. For $d = 2$, $\epsilon_F = 2\pi n/m$, whereas for $d = 3$, $\epsilon_F = (3\pi^2 n/\sqrt{2})^{2/3}/m$. This leads to the definitions:

$$\begin{aligned} \xi_2 &= \left(\frac{m\mu}{2\pi n}\right)^2 b_2(T/\mu) \\ \xi_3 &= \left(\frac{\sqrt{2}}{3\pi^2 n}\right)^{5/3} (m\mu)^{5/2}\, b_3(T/\mu) \end{aligned} \tag{6.33}$$

Next consider the energy per particle in the limit $\mu/T \to 0$. Here it is more appropriate to use the form in eq. (6.22), which gives

$$\epsilon_1 = \frac{d}{2}\frac{c_d}{c'_d}\,T \tag{6.34}$$

The expression for ϵ_1 for free fermions in the limit $\mu/T \to 0$ in $d = 3$ leads us now to define $\tilde{\xi}$:

$$\epsilon_1 = \frac{3}{2}\left(\frac{2\sqrt{2}-1}{2\sqrt{2}-2}\right)\frac{\zeta(5/2)}{\zeta(3/2)}\,T\;\tilde{\xi}_3(\mu/T) \tag{6.35}$$

With this normalization, for free fermions, as $\mu/T \to 0$, $\tilde{\xi}_3 = 1$.

In two dimensions, ϵ_1 goes to zero for free bosons as $\mu/T \to 0$ since it is proportional to $1/\zeta(1)$. However ϵ_1 is finite for fermions in this limit. Using $\lim_{d\to 2}(2^{d/2}-2)\zeta(d/2) = 2\log 2$, we define

$$\epsilon_1 = \frac{\pi^2 T}{12\log 2}\;\tilde{\xi}_2(\mu/T) \qquad\qquad (d=2) \tag{6.36}$$

With the above normalization, $\tilde{\xi}_2(0) = 1$ for free fermions.

CHAPTER 7

THE TWO-DIMENSIONAL QUANTUM GAS AT UNITARY LIMIT

7.1 Two-body kernal, integral equation, and scaling functions

We begin with writing down the two-dimensional version of the kernel introduced in (3.34), using (4.9) and the appropriate expression from (3.31):

$$\begin{aligned} G_2(\mathbf{k}_1,\mathbf{k}_2) &= -\frac{4i\alpha}{m}\log\left(\frac{1+\frac{mg}{4\pi}\left(\log\left(\frac{2\Lambda}{|\mathbf{k}_1-\mathbf{k}_2}\right)-i\pi/2\right)}{1+\frac{mg}{4\pi}\left(\log\left(\frac{2\Lambda}{|\mathbf{k}_1-\mathbf{k}_2}\right)+i\pi/2\right)}\right) \\ &= -\frac{8\alpha}{m}\arctan\left(\frac{2\pi}{\log\left(\frac{2\Lambda_*}{|\mathbf{k}_1-\mathbf{k}_2|}\right)}\right). \end{aligned} \tag{7.1}$$

Here Λ_* is as defined in (6.13).

In the unitary limit as defined in the previous chapter, $g \to \pm\infty$ and the theory is at the scale Λ_*. The difference in momenta $|\mathbf{k}_1 - \mathbf{k}_2| \sim 2\Lambda_*$ and the logarithmic function in the kernel (7.1) diverges. We therefore have

$$G_2(\mathbf{k}_1,\mathbf{k}_2) \to \mp\frac{4\pi\alpha}{m}. \tag{7.2}$$

For the attractive case, $|\mathbf{k}_1 - \mathbf{k}_2|$ approaches $2\Lambda_*$ from above as $g \to -\infty$. This thus corresponds to the positive sign in (7.2). Conversely, the repulsive case corresponds to the negative sign of (7.2).

With the kernel reduced to a constant in the unitary limit, the analysis in two dimensions is considerably simpler. It is convenient to define

$$\begin{aligned} \delta(\mathbf{k}) &\equiv \epsilon(\mathbf{k}) - (\omega_{\mathbf{k}} - \mu); \\ y(\mathbf{k}) &\equiv e^{-\beta\delta(\mathbf{k})}. \end{aligned} \tag{7.3}$$

The free energy (3.23) becomes:

$$\mathcal{F} = -\frac{1}{\beta}\int (d\mathbf{k}) \left[-s\log(1 - se^{-\beta\epsilon(\mathbf{k})}) - \frac{1}{2}\frac{(1 - y^{-1}(\mathbf{k}))}{e^{\beta\epsilon(\mathbf{k})} - s} \right]. \tag{7.4}$$

Since the kernel is independent of $\mathbf{k}$, one can infer from (3.21) that δ must also be independent of $\mathbf{k}$. With this knowledge, it is now possible to carry out the integration on the right hand side of (3.21) explicitly. The end result is an algebraic transcendental equation, instead of an integral equation:

$$y = 1 \pm \frac{2\alpha}{sy}\log(1 - syz). \tag{7.5}$$

The integrals in (7.4) can also be carried out explicitly. The result agrees with the scaling form (6.22), with the scaling function

$$c_2 = -\frac{6s}{\pi^2}\left(\mathrm{Li}_2(syz) + \frac{1}{2}(1 - y^{-1})\log(1 - syz) \right). \tag{7.6}$$

Simple algebra leads to the other scaling function defined in (6.26):

$$b_2 = \frac{\pi^2}{3\log^2 z} c_2. \tag{7.7}$$

For the remainder of this chapter we shall drop the subscript $2d =$ in all scaling functions, as we are specializing in the two-dimensional case.

The number density can either be derived from the thermodynamic relation $n = -\partial\mathcal{F}/\partial\mu$, or from integrating the filling fraction $f(\mathbf{k})$:

$$n = -\frac{smT}{2\pi}\log(1 - syz) \tag{7.8}$$

The total energy per particle scaling function $\tilde{\xi}$, as defined in (6.36), is also expressed in terms of c:

$$\tilde{\xi} = \left(\frac{2\log 2}{\log(1 - syz)} \right) c. \tag{7.9}$$

Finally ξ takes the form:

$$\xi = \left(\frac{\log z}{\log(1 - syz)} \right)^2 b. \tag{7.10}$$

7.2 Attractive fermions

For fermions, the parameters $s = -1$ and $\alpha = 1/2$. The Kernel (7.2) takes the positive sign.

The equation for pseudo-energy (7.5) becomes

$$y = 1 + \frac{1}{y}\log(1 + yz) \tag{7.11}$$

and a solution exists for any positive z, i.e. for $-\infty < \mu/T < \infty$. The density is plotted in Figure 7.1. It takes on all positive values and approaches ∞ as $\mu/T \to \infty$. As $T/\mu \to 0^+$, the density approaches the free field value $n = m\mu/2\pi$. However at high temperatures there is a departure from the free field value:

$$\lim_{\mu/T \to 0} n = 0.9546\frac{mT}{2\pi} \tag{7.12}$$

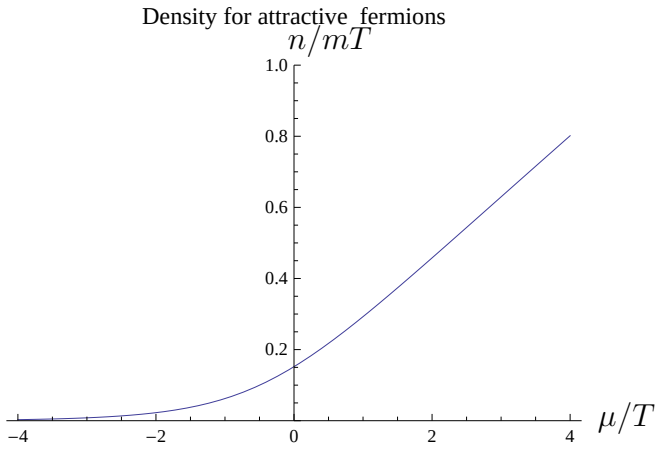

Figure 7.1: Attractive fermions in 2d: density as a function of μ/T.

The filling fraction f is plotted in Figure 7.2. The scaling function c is shown in Figure 7.3. One finds:

$$\lim_{\mu/T \to 0} c = 0.624816 \tag{7.13}$$

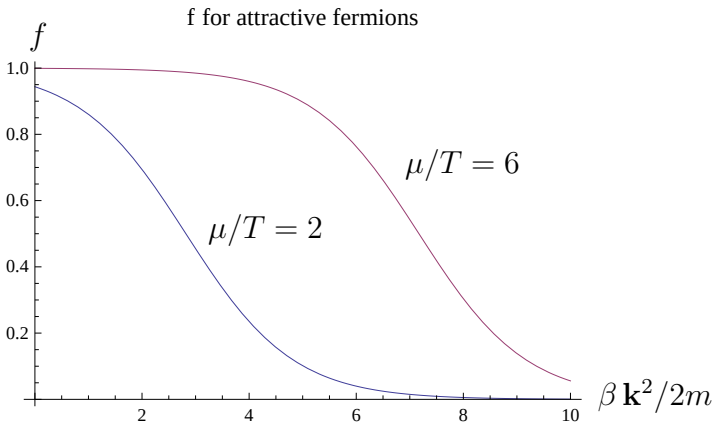

Figure 7.2: Attractive fermion in 2d: filling fraction f at two different values of μ/T.

which is higher than the free field value $c = 1/2$. From these results, one obtains the equation of state:

$$p = 1.077\, nT, \qquad (\mu/T \to 0) \tag{7.14}$$

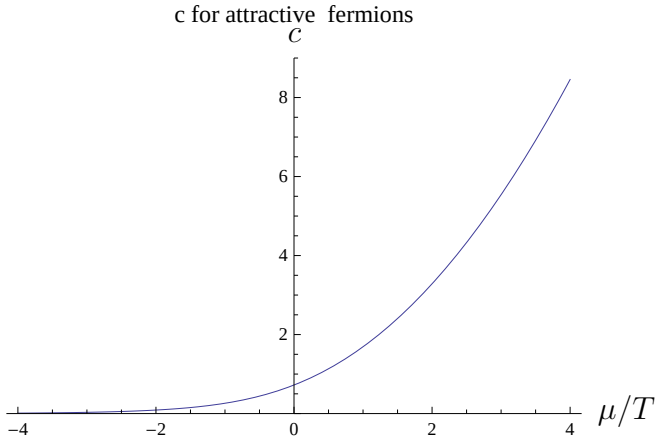

Figure 7.3: Attractive fermion in 2d: the scaling function c as a function of μ/T.

One needs to make sure that all regions of μ/T are physical, and not for instance metastable. In particular, the entropy must increase with temperature, otherwise the specific heat is negative. In Figure 7.4 we plot the entropy density s, and one

sees that $\partial s/\partial T < 0$ when $\mu/T > 11.7$.

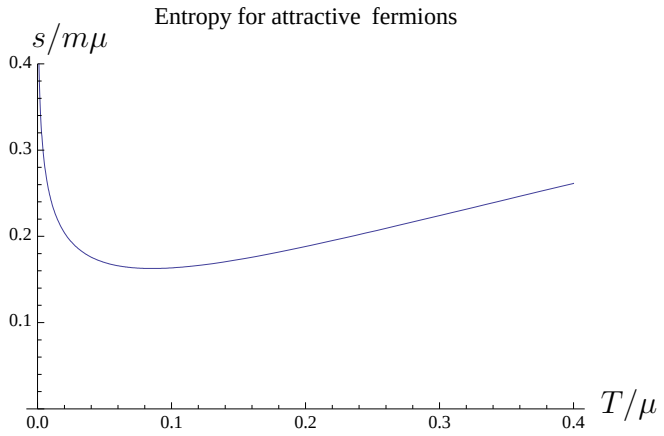

Figure 7.4: Attractive fermion in 2d: the entropy density s divided by $m\mu$ as a function of T/μ.

One must bear in mind that our formalism, though non-perturbative in some respects, is still an approximation, and such a feature could be an artifact that disappears once the corrections are incorporated. Since it is beyond the scope of this work to systematically explore these corrections, we will instead try and interpret our results as they are, for this and subsequent cases.

The above feature of the entropy density could signify a phase transition at $\mu/T = 11.7$, where the density and temperature are related by:

$$n = 13.1\,\frac{mT}{2\pi} \qquad \Longleftrightarrow \qquad T_c = 0.076\,T_F \tag{7.15}$$

where T_F is the Fermi temperature ϵ_F/k_B, where ϵ_F is defined in section III, and T_c is the critical temperature for this hypothetical phase transition. The above value is comparable to the prediction $T_c \approx 0.1\,T_F$ in [38] for quasi 2d (trapped) systems. In all other regions, and for all other cases considered below, $\partial s/\partial T > 0$.

7.3 Attractive bosons

With the bosonic values $s = +1$, $\alpha = 1$, the integral equation (7.5) becomes

$$y = 1 \pm \frac{2}{y} \log(1 - zy) \tag{7.16}$$

where the $+$ $(-)$ sign refers to repulsive (attractive) interactions. The scaling function c is now

$$c = \frac{6}{\pi^2} \left(\mathrm{Li}_2(zy) + \frac{1}{2}(1 - y^{-1} \right) \log(1 - zy) \tag{7.17}$$

The scaling function b has the same expression as in eq. (7.7), with the above c. The density now is

$$n = -\frac{mT}{2\pi} \log(1 - zy). \tag{7.18}$$

The energy per particle scaling functions now take the form:

$$\tilde{\xi} = -\frac{2 \log(2) c}{\log(1 - zy)} \tag{7.19}$$

and

$$\xi = \left(\frac{\log z}{\log(1 - zy)} \right)^2 b \tag{7.20}$$

For this bosonic case, there is only a solution to eq. (**??**) for $z \leq z_c \approx .34$, or $\mu/T \leq -1.08$. The density is shown in Figure 7.5, and note that it has a maximum. The filling fractions are shown for several μ/T up to $\log z_c$ in Figure 7.6. From these plots, it appears that f is diverging at $\mathbf{k} = 0$ as z approaches z_c, suggestive of condensation to a superfluid. Let us refer to the maximum density then as the critical density

$$n_c \approx 1.24 \frac{m\, k_B T}{2\pi\hbar^2} \quad \Longleftrightarrow \quad T_c \approx 0.81\, T_F \tag{7.21}$$

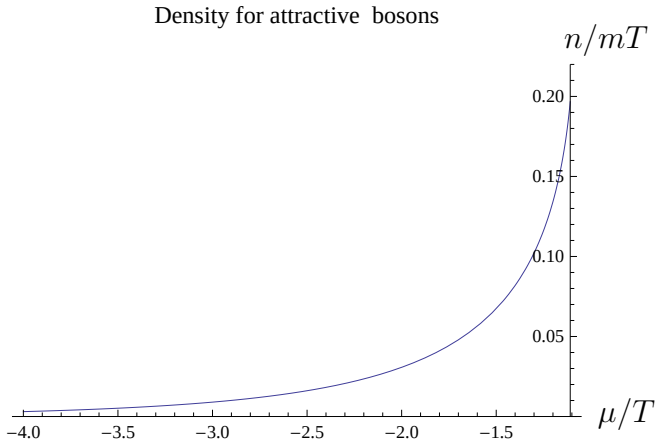

Figure 7.5: Attractive boson in 2d: density as a function of μ/T. The origin of the axes is at $(\log z_c, 0)$.

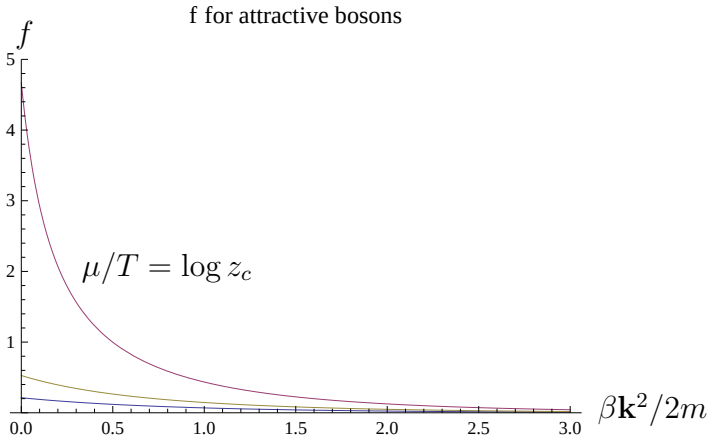

Figure 7.6: Attractive boson in 2d: the filling fraction f for $\mu/T = -2, -1.5, -1.08 = \log z_c$.

The scaling function c is shown in Figure 7.7. The limiting value is

$$c(z_c) \approx 0.35 \tag{7.22}$$

which is considerably less than for a free boson with $c = 1$. The function b decreases to zero at $T/\mu \to 0$, and the limiting value is

$$b(z_c) \approx 0.94 \tag{7.23}$$

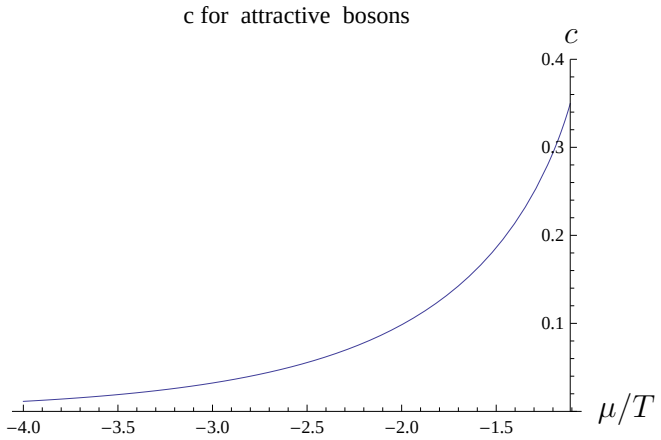

Figure 7.7: Attractive boson in 2d: the scaling function c as a function of μ/T. The origin of the axes is at $(\log .33, 0)$.

The energy per particle scaling functions ξ and $\tilde{\xi}$ are shown in Figures 7.8, 7.9. The limiting values are

$$\lim_{\mu/T\to-\infty} \tilde{\xi} = 0.842766, \qquad \tilde{\xi}(z_c) \approx 0.39 \tag{7.24}$$

and

$$\lim_{T/\mu\to 0^-} \xi = \infty, \qquad \xi(z_c) \approx 2.3 \tag{7.25}$$

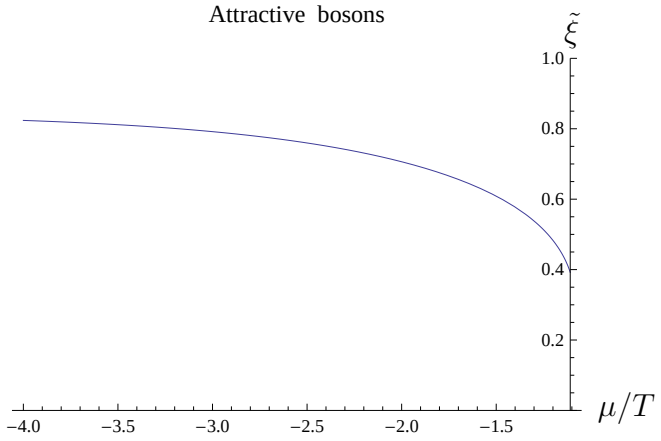

Figure 7.8: Attractive bosons in 2d: the energy per particle scaling function $\tilde{\xi}$ as a function of μ/T.

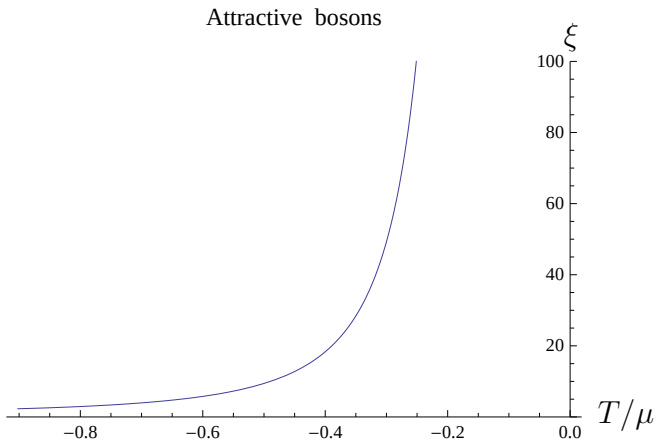

Figure 7.9: Attractive boson in 2d: the energy per particle scaling function ξ as a function of T/μ.

As for the fermionic case, the value $\tilde{\xi} = 0.842766 = 12 \log 2/\pi^2$ implies the energy per particle $\epsilon_1 = T$, which means the gas is in the classical limit.

7.4 Repulsive fermions and bosons

For the repulsive fermions, there are solutions to (7.5) for all $\mu/T < 0$, and the density is positive in this range. A plot of the density is shown in Figure 7.10. The density maximizes at $\mu/T \approx -0.56$, where $n/mT \approx 0.04$. This seems physically reasonable given the strong repulsion in the unitary limit.

In contrast, for small coupling g, the kernel $G \approx -g$, and there are solutions for positive chemical potential. In the bosonic case, our formalism leads to a critical density of $n_c = \frac{mT}{2\pi} \log(2\pi/mg)$ for the Kosterlitz-Thouless transition. The filling fractions are shown in Figure 7.11. Note that they are considerably smaller than in the attractive case, as expected. The scaling function c is shown in Figure 7.12.

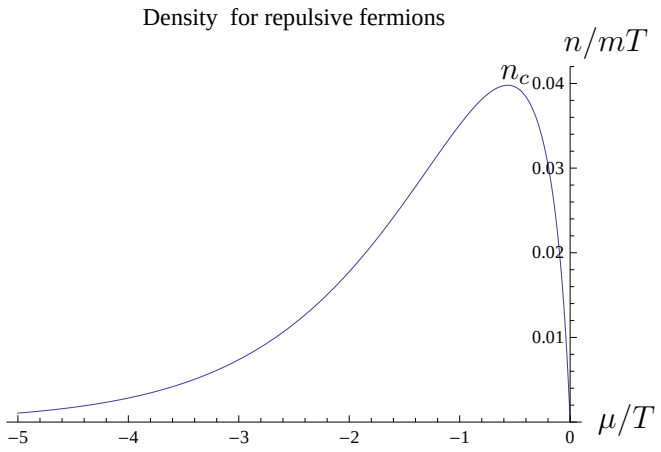

Figure 7.10: Repulsive fermion in 2d: density as a function of μ/T.

It has the limiting value

$$\lim_{\mu/T \to 0} c = 0.303964, \tag{7.26}$$

which is considerably less than the free field value $c = 1/2$.

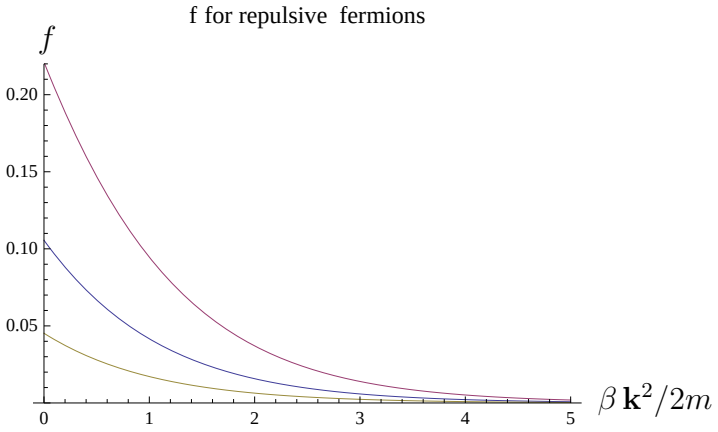

Figure 7.11: Repulsive fermion in 2d: filling fraction f for $\mu/T = -3, -2, -0.55$. The top curve corresponds to the critical density in eq. (7.27).

The scaling function b has the limiting values $\lim_{T/\mu \to 0^-} b = 0$, and $\lim_{T/\mu \to -\infty} b = \infty$.

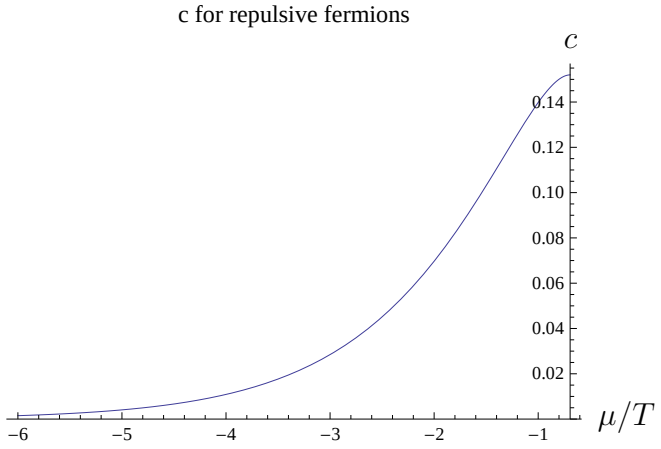

Figure 7.12: Repulsive fermion in 2d: the scaling function c as a function of μ/T.

Since the pressure is proportional to c, the same density occurs at two different pressures. One sees that for $\mu/T < -0.56$, the density increases with pressure as it should. For $\mu/T > -0.56$ the density decreases with increasing pressure, violating $dp/dV < 0$, and should thus be viewed as an unphysical region. We interpret this as a phase transition occurring at $z_c = e^{-0.56} = 0.57$, where the critical density

$$n_c = 0.25\,\frac{mk_BT}{2\pi\hbar^2} \qquad \Longleftrightarrow \qquad T_c \approx 4.0\,T_F \tag{7.27}$$

At this critical point $c(-0.56) = 0.24$. This perhaps corresponds to a transition to a crystalline phase. We cannot prove this, since we have not calculated the shear modulus for instance, and it could simply be an artifact of our approximation, but let us take it as a hypothesis. Whereas a Wigner crystal phase occurs at low density in three dimensions, it occurs at high density in two dimensions[7]. The possibility of crystal phases for repulsive bosons was studied in [24]. For Coulomb repulsion with strength e^2, the thermodynamic state of a classical Coulomb system is determined by $\Gamma = \sqrt{\pi n}\,e^2/k_BT$, where n is the density. Experimentally it was

found that $\Gamma \approx 137$[15], which gives a critical density

$$n_c \approx 2.15 \times 10^9 \, T^2 \, \frac{1}{\mathrm{cm}^2 K^2} \tag{7.28}$$

On the other hand, since our model has point-like interactions, and is in the unitary limit, the conditions for a crystal phase are expected to be different. In particular our formula eq. (7.27) has no e^2 dependence, and this leads to a linear in T dependence. For m equal to the electron mass

$$n_c \approx 4.5 \times 10^9 \, T \, \frac{1}{\mathrm{cm}^2 K} \tag{7.29}$$

It is interesting to note that for T of order 1, which is where the data in [15] was taken, the two densities (7.28) and (7.29) are comparable.

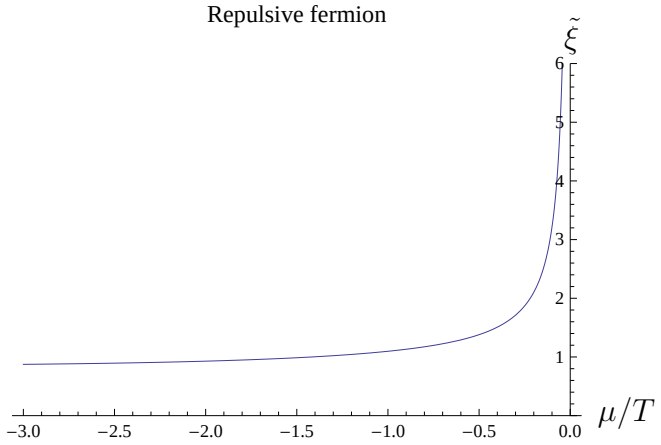

Figure 7.13: Repulsive fermion in 2d: the energy per particle scaling function $\tilde{\xi}$ as a function of μ/T.

The energy per particle function $\tilde{\xi}$ is shown in Figure 7.13. The limiting values are:

$$\lim_{\mu/T \to -\infty} \tilde{\xi} = 0.842766, \qquad \tilde{\xi}(z_c) = 1.32 \tag{7.30}$$

As in previous cases, the above value of $\tilde{\xi}$ implies $\epsilon_1 = T$ as $\mu/T \to -\infty$ and the gas is thus in the classical limit.

Beyond the critical point where the density increases, $\lim_{\mu/T\to 0}\tilde{\xi} = \infty$. Note that $\tilde{\xi}$ starts to diverge around the proposed phase transition at $\mu/T = -0.56$.

Finally the other energy per particle function ξ is less interesting, as it diverges at both endpoints of the density range where the density goes to zero. At the critical point it is still quite large: $\xi(z_c) = 12.6$.

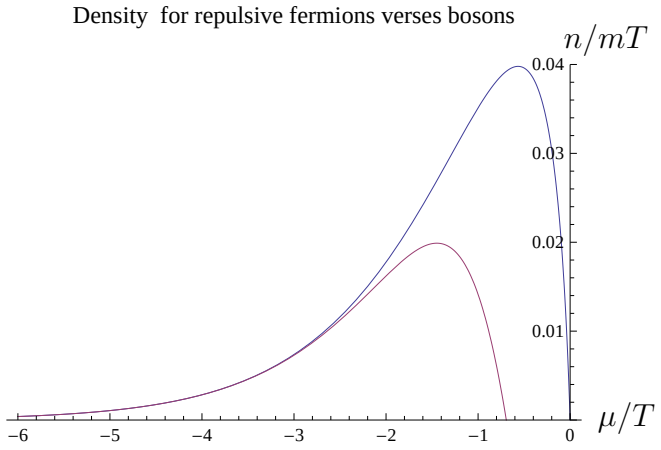

Figure 7.14: Density of repulsive bosons (bottom curve) verses fermions as a function of μ/T.

The repulsive boson case is similar to the repulsive fermion, except that now there are only positive density solutions to the eq. (7.5) for $\mu/T < -\log 2$. Figure 7.14 compares the density for bosons verses fermions. The maximum density for bosons, which could again possibly signify a critical point at $z_c \approx e^{-1.45} = 0.235$, is half that of the fermion case:

$$n_c = 0.125\,\frac{mk_BT}{2\pi\hbar^2} \qquad \Longleftrightarrow \qquad T_c \approx 8.0\,\epsilon_F \tag{7.31}$$

At this point $c(-1.3) \approx 0.11$.

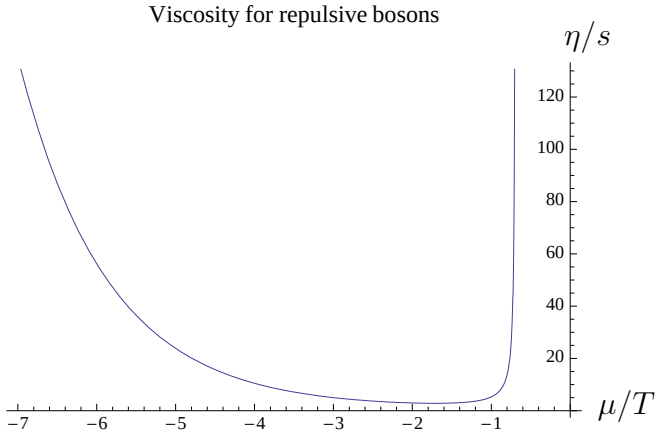

Figure 7.15: Repulsive boson in 2d: the ratio η/s as a function of μ/T.

CHAPTER 8

THE THREE-DIMENSIONAL QUANTUM GAS AT UNITARY LIMIT

8.1 Two-body kernal and integral equation

Parallel to the $d = 2$ case, we take the kernel from (3.34), and insert appropriate expressions from (3.31) and (4.10), to get the two-body kernel:

$$\begin{aligned} G(\mathbf{k}_1, \mathbf{k}_2) &= -\frac{i4\pi\alpha}{m|\mathbf{k}_1 - \mathbf{k}_2|} \log\left(\frac{\frac{1}{g_R} - \frac{im}{8\pi}|\mathbf{k}_1 - \mathbf{k}_2|}{\frac{1}{g_R} + \frac{im}{8\pi}|\mathbf{k}_1 - \mathbf{k}_2|}\right) \\ &= \frac{-8\pi\alpha}{m|\mathbf{k}_1 - \mathbf{k}_2|} \arctan\left(\frac{\frac{m}{8\pi}|\mathbf{k}_1 - \mathbf{k}_2|}{\frac{1}{g_R}}\right) \end{aligned} \tag{8.1}$$

The unitary limit is $\frac{1}{g_R} \to 0^{\pm}$. The plus sign is the repulsive case, where the scattering length is positive, and can be associated with the BEC side of the BCS-BEC crossover. The negative sign is associated with the attractive interaction, negative scattering length, and the BCS side of the crossover.

Recall that on the BEC side of the fixed point, there is a two-particle bound state in the spectrum of the theory, with binding energy given by (6.3). For the reminder of this chapter we shall work on the BCS side of the fixed point, so that the bound state does not need to be incorporated in the thermodynamics.

Taking the limit, the kernel is reduced to

$$G_2(\mathbf{k}_1, \mathbf{k}_2) \to \mp\frac{8\pi^2\alpha}{m|\mathbf{k}_1 - \mathbf{k}_2|}. \tag{8.2}$$

Unlike the $d = 2$ case, the kernel remains dependent on the momenta of the particles. The pseudo-energy shift $\delta_{\mathbf{k}}$ is therefore not a constant. The integral

equation is

$$y(\mathbf{k}) = 1 + \beta \int (d^3\mathbf{k}')\, G(\mathbf{k}, \mathbf{k}') \frac{y(\mathbf{k}')^{-1}}{e^{\beta\epsilon(\mathbf{k}')} - s} \tag{8.3}$$

and does not reduce to an algebraic equation.

The angular part of the integral in (8.3) can be easily performed and lead to some simplification. Defining the dimensionless variable $\kappa = \mathbf{k}^2/2mT$, the integral equation becomes

$$y(\kappa) = 1 + 4\alpha \int_0^\infty d\kappa' \left[\Theta(\kappa - \kappa')\sqrt{\kappa'/\kappa} + \Theta(\kappa' - \kappa)\right] \frac{z}{e^{\kappa'} - szy(\kappa')} \tag{8.4}$$

where $z = e^{\mu/T}$ is the fugacity and Θ is the Heaviside step function.

The free energy, followed from (3.23), has the same form as (7.4) and is reproduced below:

$$\mathcal{F} = -T \int (d^3\mathbf{k}) \left[-s \log(1 - se^{-\beta\epsilon}) - \frac{1}{2} \frac{(1 - y^{-1})}{e^{\beta\epsilon} - s}\right] \tag{8.5}$$

8.2 The scaling functions

The scaling function c_3, as defined in (6.22), does not admit an analytic close form expression. It can only be determined numerically from the solution of the integral equation (8.3) (itself numerical.)

We shall henceforth drop all the subscripts $d = 3$ of the scaling functions in this chapter, since we will deal with the three-dimensional case exclusively.

It is also convenient to define the scaling function q, which is a measure of the quantum degeneracy, in terms of the density as follows:

$$n\lambda_T^3 = q, \tag{8.6}$$

where λ_T is the thermal wavelength $\sqrt{2\pi/mT}$.

The two scaling functions c and q are of course related since $n = -\partial\mathcal{F}/\partial\mu$, which leads to

$$q = \zeta(5/2)c' \tag{8.7}$$

where c' is the derivative of c with respect to $x \equiv \mu/T$. Henceforth g' will always denote the derivative of g with respect to x.

Recall from (6.30) that the energy per particle, ϵ_1, is proportional to the free energy per particle. One may compare this with the result of a free fermion at zero temperature, $\epsilon_1 = 3\epsilon_F/3$, with ϵ_F the Fermi energy. This leads us to the scaling function ξ, as defined in the equation (6.32):

$$\xi(x) = \frac{5\zeta(5/2)}{3}\left(\frac{6}{\pi}\right)^{1/3}\frac{c}{q^{5/3}} \tag{8.8}$$

This scaling function is meaningful at the limit $x \to \infty$, or equivalently $T \to 0$.

Another important limit would be $x \to 0$. The relevant scaling function $\tilde{\xi}$ was defined in (6.35), and it can be rewritten in terms of c and q introduced here:

$$\tilde{\xi}(x) = \frac{\zeta(3/2)(2\sqrt{2}-2)}{(2\sqrt{2}-1)}\frac{c}{q} \tag{8.9}$$

The entropy density is $s = -\partial\mathcal{F}/\partial T$, and the entropy per particle takes the form

$$\frac{s}{n} = \zeta(5/2)\left(\frac{5c/2 - xc'}{q}\right) \tag{8.10}$$

Next consider the specific heat per particle at constant volume and particle number, i.e. constant density. One needs $\partial x/\partial T$ at constant density. Using the fact that $n \propto T^{3/2}q$, at constant density $q \propto T^{-3/2}$. This gives

$$T\left(\frac{\partial x}{\partial T}\right)_n = -\frac{3}{2}\frac{q}{q'} \tag{8.11}$$

The specific heat per particle is then:

$$\frac{C_V}{N} = \frac{1}{N}\left(\frac{\partial E}{\partial T}\right)_{N,V} = \frac{\zeta(5/2)}{4}\left(15\frac{c}{q} - 9\frac{c'}{q'}\right) \tag{8.12}$$

The isothermal compressibility is defined as

$$\kappa = -\frac{1}{V}\left(\frac{\partial V}{\partial p}\right)_T \tag{8.13}$$

where the pressure $p = -\mathcal{F}$. Since $n = N/V$ and N is kept fixed,

$$\kappa = -n\left(\frac{\partial n^{-1}}{\partial p}\right)_T = \frac{1}{nT}\frac{q'}{q} = \frac{1}{T}\left(\frac{mT}{2\pi}\right)^{3/2}\frac{q'}{q^2} \tag{8.14}$$

Finally the equation of state can be expressed parametrically as follows. Given n and T, one uses (8.6) to find x as a function of n, T. The pressure can then be written as

$$p = \left(\frac{\zeta(5/2)c(x(n,T))}{q(x(n,T))}\right)nT \tag{8.15}$$

In order to compare with numerical simulations and experiments, it will be useful to plot various quantities as a function of q or T/T_F:

$$\frac{T}{T_F} = \left(\frac{4}{3\sqrt{\pi}q}\right)^{2/3} \tag{8.16}$$

8.3 Analysis of fermions

The integral equation (8.4) is then solved numerically by iteration. One first substitutes $y_0 = 1$ on the right hand side and this gives the approximation y_1 for y. One then substitutes y_1 on the right hand side to generate y_2, etc. For regions of z where there are no critical points, this procedure converges rapidly, and as little as 5 iterations are needed. For fermions, as one approaches zero temperature,

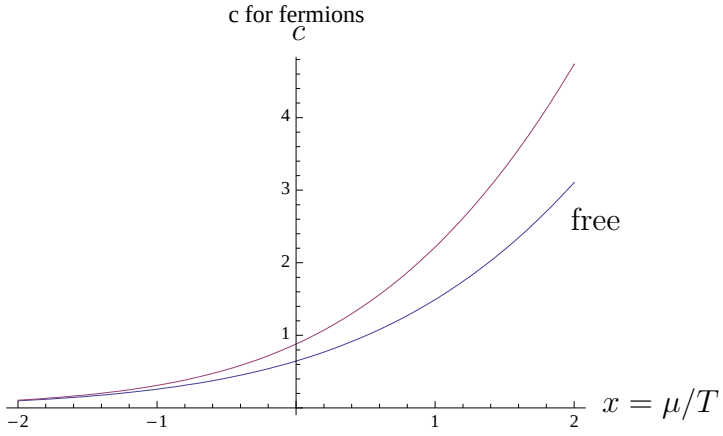

Figure 8.1: Attractive fermion in 3d: $c(x)$ and its equivalent for a free theory as a function of $x = \mu/T$.

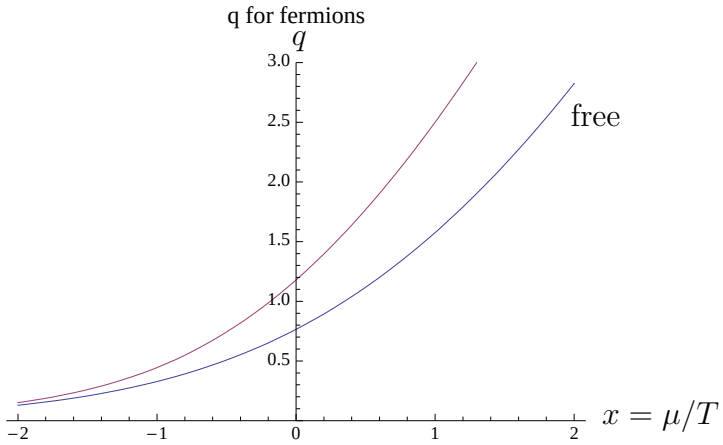

Figure 8.2: Attractive fermion in 3d: $q(x)$ and its equivalent for a free theory as a function of $x = \mu/T$.

i.e. x large and positive, more iterations are needed for convergence. The results presented in this chapter are based on 50 iterations.

When $z \ll 1$, $y \approx 1$, and the properties of the free ideal gas are recovered, since the gas is very dilute. There are solutions to equation (8.4) for all $-\infty < x < \infty$. $(x = \mu/T)$. The scaling function c, and it's comparison with a free theory, are shown in Figure 8.1 as a function of x. The corrections to the free theory become

appreciable when $x > -2$. At $x = 0$:

$$c(0) = 0.880, \qquad \tilde{\xi} = 0.884, \tag{8.17}$$

compared to the free gas values of $c(0) = 0.646$ and $\tilde{\xi} = 1$.

The scaling function q for the density is shown as function of x in Figure 8.2. Note that the density in the interacting case is always higher than for a free gas, due to the attractive interactions. At $x = 0$, $q(0) = 1.18$, whereas for a free gas $q = 0.765$. At low temperatures and high densities, $\mu/T \gg 1$, the occupation numbers resemble that of a degenerate Fermi gas, as shown in Figure 8.3.

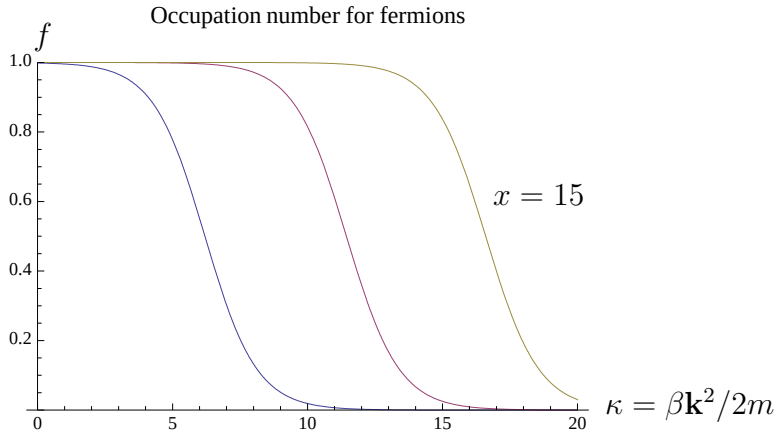

Figure 8.3: Attractive fermion in 3d: the occupation numbers as a function of κ for $x = 5, 10, 15$.

Whereas c and q are nearly featureless, other quantities seem to indicate a critical point, or phase transition, at large density. For instance, the entropy per particle decreases with decreasing temperature up to $x < x_c \approx 11.2$, as shown in Figure 8.4. Beyond this point the entropy per particle has the unphysical behavior of increasing with temperature.

A further indication that the region $x > x_c$ is unphysical is that the specific heat per particle becomes negative, as shown in Figure 8.5. When $x \ll 0$, C_V/N

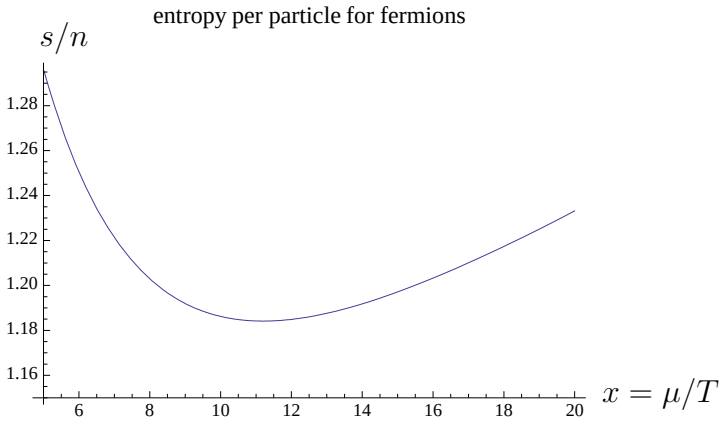

Figure 8.4: Attractive fermion in 3d: entropy per particle as a function of x.

approaches the classical value 3/2. This leads us to suggest a phase transition, at $x = x_c$, corresponding to the critical temperature $T_c/T_F \approx 0.1$.

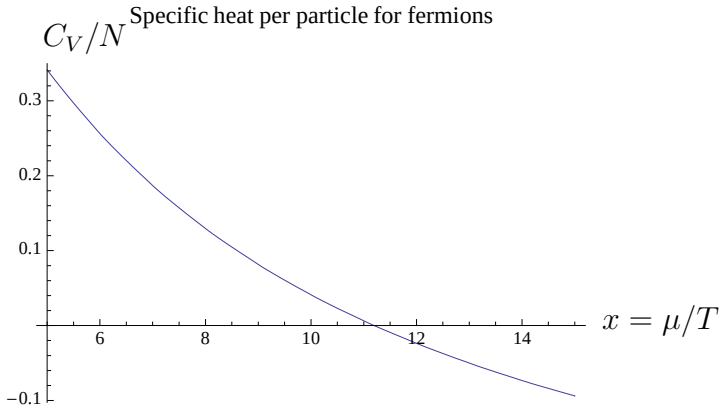

Figure 8.5: Attractive fermion in 3d: specific heat per particle as a function of x.

As we will show, our analysis of the viscosity to entropy-density ratio suggests a higher T_c/T_F. There have been numerous estimates of T_c/T_F based on various approximation schemes, mainly using Monte Carlo methods on the lattice [36, 29, 2, 22, 3], quoting results for T_c/T_F between 0.05 and 0.23. The work [29] puts an upper bound $T_c/T_F < 0.14$, and the most recent results of Burovski et. al. quote $T_c/T_F = 0.152(7)$. Our result is thus consistent with previous work.

The equation of state at this point follows from eq. (8.15):

$$p = 4.95nT \tag{8.18}$$

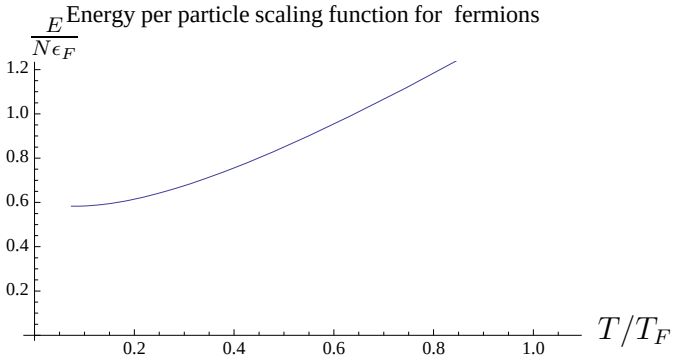

Figure 8.6: Attractive fermion in 3d: energy per particle normalized to ϵ_F as a function of T/T_F.

The energy per particle, normalized to the Fermi energy ϵ_F, i.e. $E/N\epsilon_F = 3\xi/5$, and the entropy per particle, are shown in Figures 8.6,8.7 as a function of T/T_F, where $k_B T_F = \epsilon_F$. At high temperatures it matches that of a free Fermi gas, in agreement with the Monte Carlo simulations in [2, 3]. Note that there is no sign of pair-breaking at $T^*/T_F = 0.5$ predicted in [36], and this also agrees with the Monte Carlo simulations.

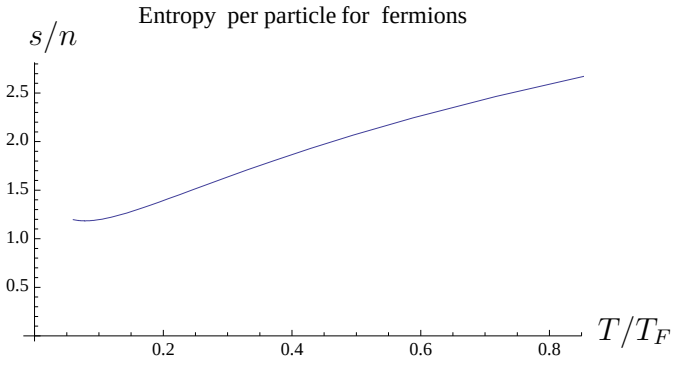

Figure 8.7: Attractive fermion in 3d: entopy per particle as a function of T/T_F.

However at low temperatures in the vicinity of T_c, the agreement is not as good. This suggests our approximation is breaking down for very large z, i.e. the limit of zero temperature. The same conclusion is reached by examining μ/ϵ_F, displayed in Figure 8.8, since the zero temperature epsilon expansion and Monte Carlo give $\mu/\epsilon_F \approx 0.4 - 0.5$[47, 3].

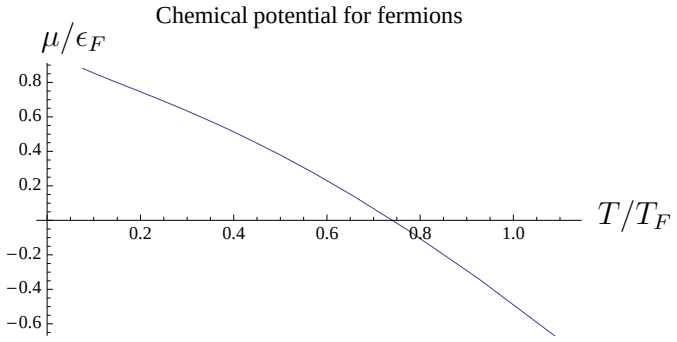

Figure 8.8: Attractive fermion in 3d: chemical potential normalized to ϵ_F as a function of T/T_F.

8.4 Analysis of bosons

For bosons we again solved the integral equation (8.4) by iteration, starting from $y = 1$. Since the occupation numbers decay quickly as a function of κ, we introduced a cut-off $\kappa < 10$. For x less than approximately -2, the gas behaves nearly classically.

The main feature of the solution to the integral equation is that for $x > x_c \equiv -1.2741$, there is no solution that is smoothly connected to the classical limit $x \to -\infty$. Numerically, when there is no solution the iterative procedure fails to converge. The free energy scaling function is plotted in Figure 8.9. Note that $c < 1$, where $c = 1$ is the free field value. We thus take the physical region to be

$x < x_c$.

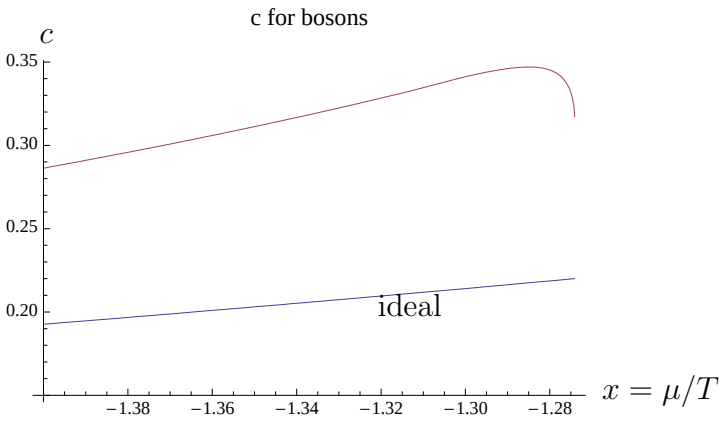

Figure 8.9: Attractive boson in 3d: the free-energy scaling function c as a function of μ/T compared to the ideal gas case.

We find strong evidence that the gas undergoes BEC at $x = x_c$. In Figure 8.10, we plot $\epsilon(\mathbf{k} = 0)$ as a function of x, and ones sees that it goes to zero at x_c. This implies the occupation number f diverges at $\mathbf{k} = 0$ at this critical point. One clearly sees this behavior in Figure 8.11.

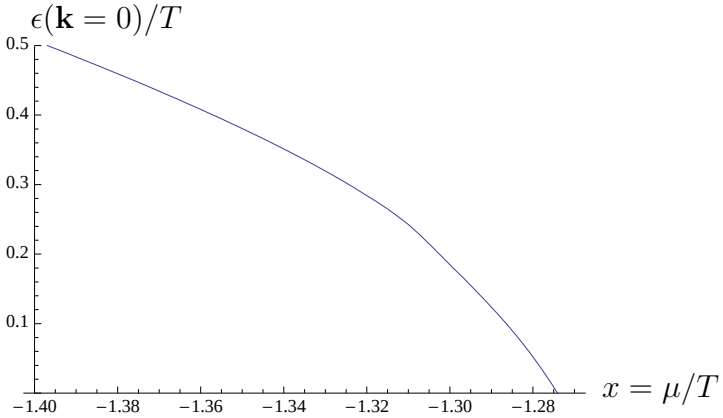

Figure 8.10: Attractive boson in 3d: the pseudo-energy ϵ at $\mathbf{k} = 0$ as a function of $x = \mu/T$.

The compressibility is shown in Figure 8.12, and diverges at x_c, again consistent with BEC. We thus conclude that there is a critical point at x_c which a strongly

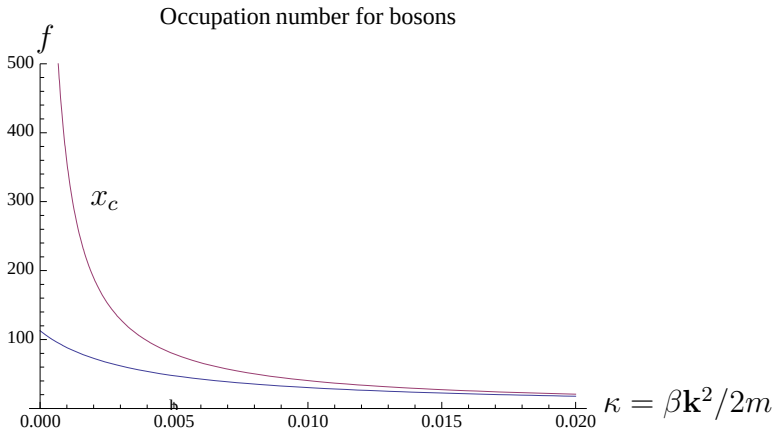

Figure 8.11: Attractive boson in 3d: the occupation number $f(\kappa)$ for $x = -1.275$ and $x_c = -1.2741$.

interacting, scale invariant version of the ideal BEC. In terms of the density, the critical point is:

$$n_c \lambda_T^3 = 1.325, \qquad (\mu/T = x_c = -1.2741) \tag{8.19}$$

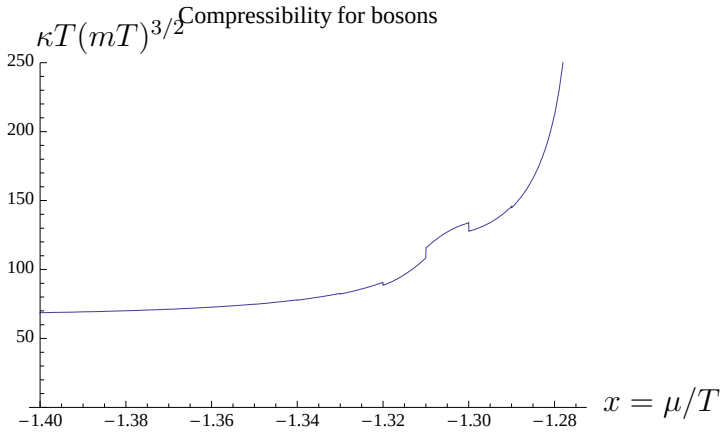

Figure 8.12: Attractive boson in 3d: the compressibility κ as a function of μ/T.

The negative value of the chemical potential is consistent with the effectively attractive interactions. The above should be compared with the ideal BEC of the free theory, where $x_c = 0$ and $n_c \lambda_T^3 = \zeta(3/2) = 2.61$, which is higher by a factor of

2. At the critical point the equation of state is

$$p = 0.318nT \tag{8.20}$$

compared to $p = 0.514nT$ for the free case. $(0.514 = \zeta(5/2)/\zeta(3/2))$.

A critical exponent ν characterizing the diverging compressibility can be defined as

$$\kappa \sim (T - T_c)^{-\nu} \tag{8.21}$$

A log-log plot of the compressibility verses $T - T_c$ shows an approximately straight line, and we obtain $\nu \approx 0.69$. This should be compared with BEC in an ideal gas, where $\nu \approx 1.0$. Clearly the unitary gas version of BEC is in a different universality class.

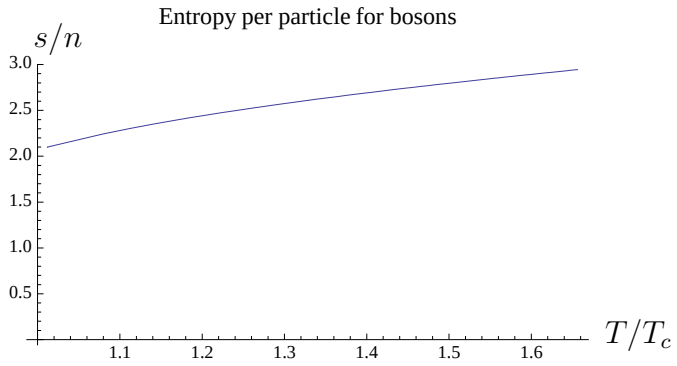

Figure 8.13: Attractive boson in 3d: the entropy per particle as a function of T/T_c.

The energy per particle scaling function $\tilde{\xi}$ at the critical point is $\tilde{\xi}(x_c) = 0.281$ compared to $0.453 = (2\sqrt{2} - 2)/(2\sqrt{2} - 1)$ for the free case. The entropy per particle and specific heat per particle are plotted in Figures 8.13, 8.14 as a function of T/T_c. At large temperatures, as expected $C_V/N = 3/2$, i.e. the classical value. It increases as T is lowered, however in contrast to the ideal gas case, it then begins to decrease as T approaches T_c.

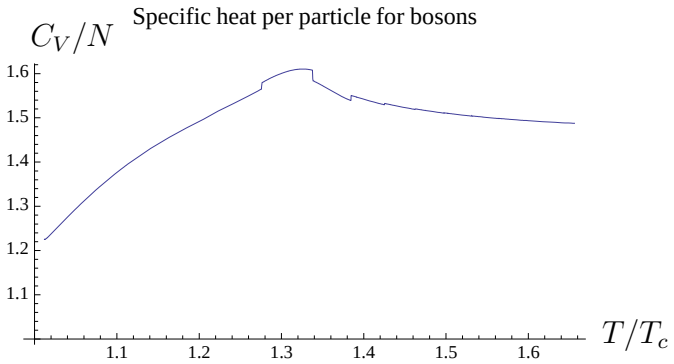

Figure 8.14: Attractive boson in 3d: the specific heat per particle as a function of T/T_c.

CHAPTER 9

ENTROPY-TO-VISCOSITY RATIO OF QUANTUM GASES

The ratio of the shear viscosity η to the entropy density s has units of $\hbar/k_B$ in any dimension. A lower bound was conjectured for 3d relativistic systems[26]:

$$\frac{\eta}{s} \geq \frac{\hbar}{4\pi k_B} \tag{9.1}$$

based on the AdS/CFT correspondence. The bound is saturated in certain strongly coupled supersymmetric gauge theories. It is therefore interesting to study this ratio for non-relativistic, strongly interacting systems, in 3 and lower dimensions, since it is unknown whether there really is a lower bound. This ratio was studied for $3d$ unitary Fermi gases in [4, 30, 13, 46, 45].

9.1 2d

In two dimensions,the attractive fermion is the most interesting and well-behaved case in our formalism, as was evident in chapter 6, so we study the issue in this case in detail.

Consider first a gas with a single species of particle of mass m. For a non-relativistic system in 2 spatial dimensions:

$$\eta = \frac{1}{2} n \bar{v} m l_{\text{free}} \tag{9.2}$$

where $\bar{v}$ is the average speed and l_{free} the mean free path. The mean free path is $l_{\text{free}} = 1/(\sqrt{2} n \sigma)$ where σ is the total cross-section. The $\sqrt{2}$ comes from the ratio of the mean speed to the mean relative speed [43].

Recall that we defined the unitary limit for a repulsive gas as the case where the scattering phase shift (3.36) taking value of $-\pi$. This implies the scattering

amplitude $\mathcal{M} = 2i/\mathcal{I}$. The accessible phase space volume $\mathcal{I}$ is $m/4\alpha$, as given in (3.31). Using the formula for differential cross-section (4.13), one can integrate over all angle and get

$$\sigma = \frac{16}{|\mathbf{k}|} \tag{9.3}$$

in the unitary limit, where $\mathbf{k}$ is the difference of momenta of the two scattering particles. This gives

$$\eta = \frac{m}{16\sqrt{2}} \left(\frac{1}{2} m \bar{v}^2 \right) \tag{9.4}$$

Since the pressure is determined by the average kinetic energy, and the ideal gas relation eq. (6.29) still holds for a unitary gas, the average kinetic energy per particle is just $\epsilon_1 = -\mathcal{F}/n$, eq. (6.30). Finally we obtain:

$$\frac{\eta}{s} = \frac{m}{16\sqrt{2}} \frac{\mathcal{F}}{n} \left(\frac{\partial \mathcal{F}}{\partial T} \right)^{-1} \tag{9.5}$$

where all the quantities in the above formula are the single component values.

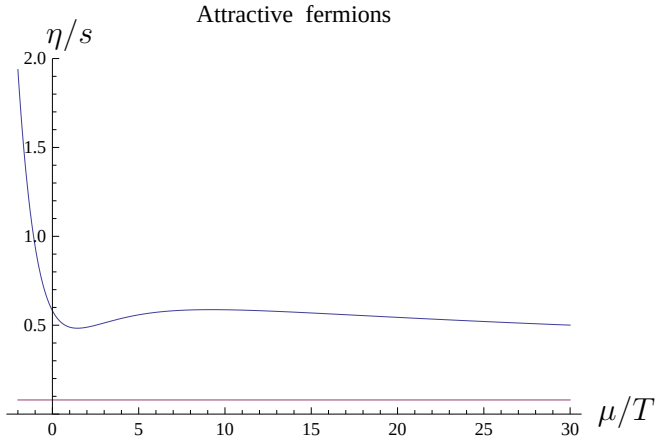

Figure 9.1: The ratio η/s as a function of μ/T. The horizontal line is $1/4\pi$.

In terms of the scaling functions:

$$\frac{\eta}{s} = \frac{3}{4\sqrt{2}\pi} \frac{c}{c'} \frac{}{(2c - \frac{\mu}{T} c')} = \frac{\pi}{4\sqrt{2}} \frac{b}{b'} \frac{}{(2b - \frac{T}{\mu} b')} \tag{9.6}$$

For two-component fermions the available phase space $\mathcal{I}$ is doubled, reflected by α taking the value $1/2$ instead of 1. The cross-section is then halved, since spin up particles only scatter with spin down. And the entropy is doubled, assuming symmetry of the two spin components. This gives

$$\left(\frac{\eta}{s}\right)_{\text{fermi}} = 4\left(\frac{\eta}{s}\right)_{\text{bose}} \tag{9.7}$$

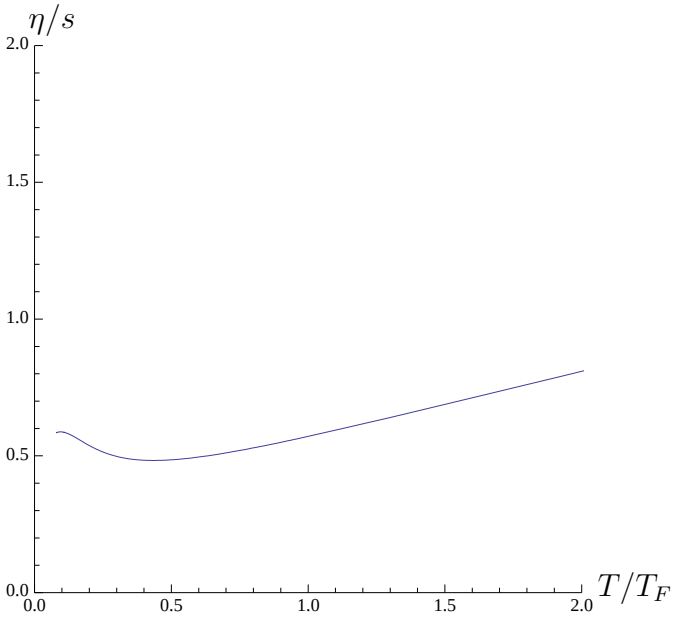

Figure 9.2: The ratio η/s as a function of T/T_F for attractive fermions.

The above expression is easily evaluated numerically using the expressions from Chapter 6. The result is displayed for small values of μ/T in Figure 9.1. In this regime, η/s is well above the conjectured bound, and comparable to the $3d$ values extracted from the experimental data[46]. We find

$$\lim_{\mu/T\to 0} \frac{\eta}{s} = 7.311\frac{\hbar}{4\pi k_B} \tag{9.8}$$

This is well-below the values for common substances like water, however it is comparable to values for liquid helium, which is about 9 times the bound[26]. In

the region shown:

$$\frac{\eta}{s} \geq 6.07 \frac{\hbar}{4\pi k_B} \tag{9.9}$$

In Figure 9.2 we plot η/s as a function of T/T_F, and one observes a behavior quite similar both qualitatively and quantitatively to the 3d data summarized in[46], where the minimal value is about 6 times the bound.

Recall that, in Chapter 6, it was argued that the region $\mu/T > 11.7$ is unphysical, or perhaps metastable, since the entropy increases with decreasing temperature there. Thus for the regions that are surely physical, the bound (9.9) holds.

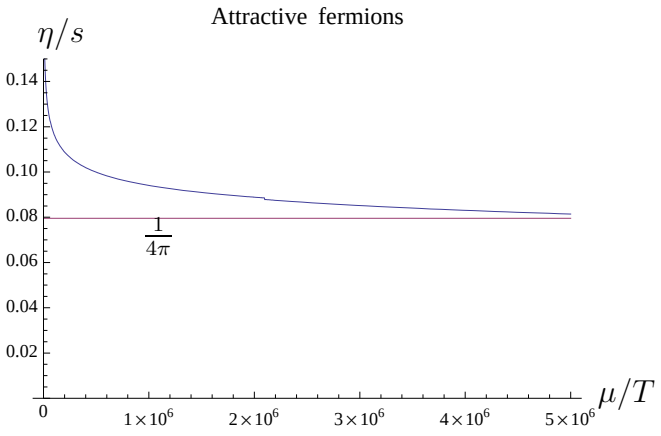

Figure 9.3: The ratio η/s as a function of μ/T as μ/T gets very large.. The horizontal line is $1/4\pi$.

It is nevertheless interesting to study the viscosity in this unphysical region. In the zero temperature limit, i.e. $T/\mu \to 0^+$, η/s slowly decreases and seems to approach the bound. See Figure 9.3. However it eventually dips below it. See Figure 9.4.

This behavior can be understood analytically as follows. For $x = \mu/T$ very large, the solution to the equation (7.5) is approximately:

$$y(x) \approx \sqrt{x} + 1/2 + (\log x - 1)/4\sqrt{x}. \tag{9.10}$$

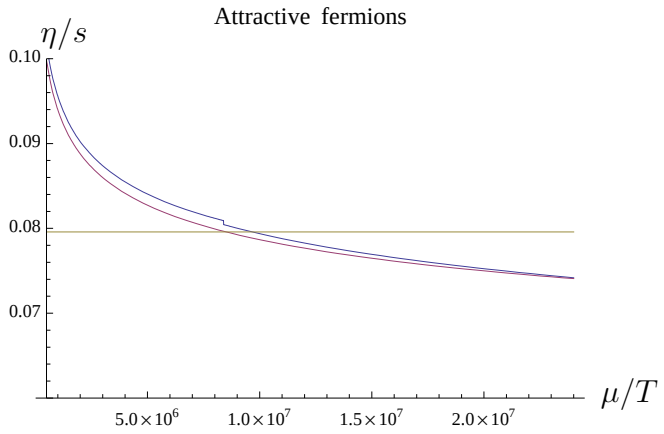

Figure 9.4: The ratio η/s as a function of μ/T in the limit of very low temperatures (top curve). The horizontal line is $1/4\pi$. The bottom curve is the approximation eq. (9.12).

This leads to the asymptotic expansions:

$$\begin{aligned} c &\approx 3(x^2 + x\log x - x)/\pi^2 \\ n &\approx \frac{mT}{2\pi}(x + \log(x)/2) \end{aligned} \tag{9.11}$$

and

$$\frac{\eta}{s} \approx \frac{\pi}{2\sqrt{2}}\left(1/(\log(\mu/T) - 2) + T/2\mu\right) \tag{9.12}$$

In terms of the density:

$$\lim_{\mu/T\to\infty}\frac{\eta}{s} = \frac{\pi}{2\sqrt{2}\log(2\pi n/mT)} \tag{9.13}$$

It is important to note that although the energy per particle scaling function ξ approaches the free field value at low temperatures, the above behavior is very different from the free field case. In the latter, the scaling function $c = -6\,\mathrm{Li}_2(-z)/\pi^2$, which gives the diverging behavior at very low temperature:

$$\frac{\eta}{s} \approx \frac{3}{4\sqrt{2\pi}}\frac{\mu}{T}, \qquad \text{(free fermions)} \tag{9.14}$$

Finally, as $\mu/T \to -\infty$, $y \approx 1 + z$, and $c \approx 6z/\pi^2$ and $n \approx mTz/2\pi$. This

leads to exponential growth:

$$\lim_{\mu/T\to-\infty}\frac{\eta}{s}=-\frac{\pi T}{2\sqrt{2}\mu}e^{-\mu/T}=-\frac{mT}{4\sqrt{2}}\frac{1}{n\log(2\pi n/mT)} \tag{9.15}$$

9.2 3d

We shall first extract the viscosity of a single-component quantum gas at the unitary limit in a way similar to the previous two-dimensional case.

In kinetic theory, the shear viscosity can be expressed as

$$\eta=\frac{1}{3}n\bar{v}ml_{\text{free}} \tag{9.16}$$

where $\bar{v}$ is the average speed and l_{free} is the mean free path. (Note that the numerical prefactor is different from the two-dimensional case (9.2).)

The mean free path is related to the total cross-section σ by $l_{\text{free}}=1/(\sqrt{2}n\sigma)$ [43].

In the unitary limit the phase shift (3.36) is $\Theta=\pm i\pi$. The scattering amplitude is then

$$i\mathcal{M}=-\frac{8\pi\alpha}{m|\Delta\mathbf{k}|}. \tag{9.17}$$

This leads to

$$\sigma=\frac{m^2|\mathcal{M}|^2}{4\pi}=\frac{16\pi}{|\mathbf{k}|^2} \tag{9.18}$$

where $|k|$ is the momentum of one of the particles in the center of mass frame, i.e. $|\mathbf{k}_1-\mathbf{k}_2|=2|\mathbf{k}|$. This gives

$$\eta=\frac{m^3\bar{v}^3}{48\sqrt{2}\pi} \tag{9.19}$$

Since the equation (6.30) is the same relation between the pressure and energy of a free gas, and the pressure is due to the kinetic energy, this implies

$$\frac{1}{2}m\bar{v}^2 = E/N = \frac{3}{2}\frac{c}{c'}T. \tag{9.20}$$

Since the entropy density $s = -\partial\mathcal{F}/\partial T$, one finally has

$$\frac{\eta}{s} = \frac{\sqrt{3\pi}}{8\zeta(5/2)}\left(\frac{c}{c'}\right)^{3/2}\frac{1}{5c/2 - xc'} \tag{9.21}$$

For two-component fermions, the same considerations as those in the two-dimensional case apply, and the entropy-to-viscosity ratio is four times that of single-component bosons.

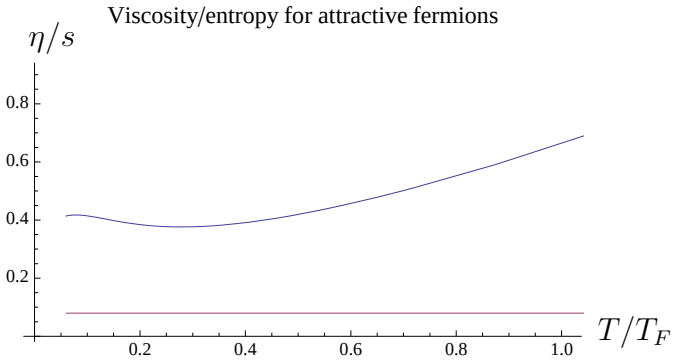

Figure 9.5: The viscosity to entropy-density ratio as a function of T/T_F for fermions. The horizontal line is $1/4\pi$.

The ratio η/s for fermions as a function of T/T_F is shown in Figure 9.5, and is in good agreement both quantitatively and qualitatively with the experimental data summarized in [46]. The lowest value occurs at $x = 2.33$, which corresponds to $T/T_F = 0.28$, and

$$\frac{\eta}{s} > 4.72\frac{\hbar}{4\pi k_B} \tag{9.22}$$

The experimental data has a minimum that is about 6 times this bound. In the free fermion theory the minimum occurs at $\mu/T \approx 2.3$, which gives $\eta/s > 7.2\hbar/4\pi k_B$.

More recently, Cao *et. al.* [4] reported that the η/s ratio about five times the conjectured lower bound, which is in good agreement with our result here.

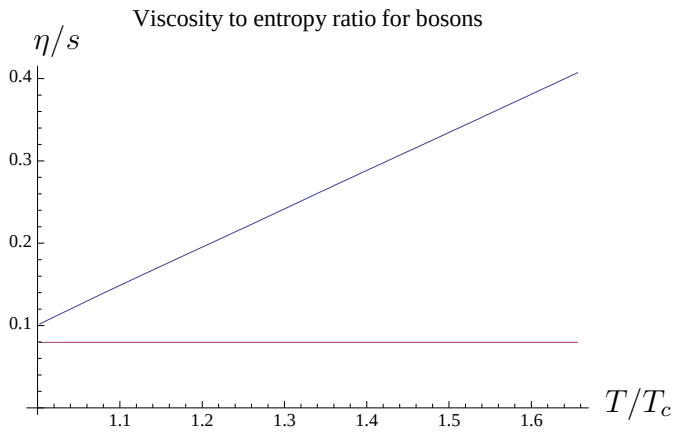

Figure 9.6: The viscosity to entropy-density ratio as a function of T/T_c for bosons. The horizontal line is $1/4\pi$.

For bosons, the ration η/s is plotted in Figure 9.6 as a function of T/T_c. One sees that it has a minimum at the critical point, where

$$\frac{\eta}{s} > 1.26\frac{\hbar}{4\pi k_B} \tag{9.23}$$

Thus the bosonic gas at the unitary critical point is a more perfect fluid than that of fermions. On the other hand, the ideal Bose gas at the critical point has a lower value:

$$\left.\frac{\eta}{s}\right|_{\text{ideal}} = \frac{\sqrt{3\pi\zeta(5/2)}}{20\zeta(3/2)^{3/2}} = 0.53\frac{\hbar}{4\pi k_B} \tag{9.24}$$

CHAPTER 10

SUMMARY AND CONCLUSION

Building on the original result due to Dashen [8], we have derived the S-matrix formulation of quantum statistical mechanics. By resumming all two-body terms, we arrive at the integral equation (3.20), reproduced below:

$$\tilde{f}(\mathbf{k}) = f_0(\mathbf{k}) + \tilde{f}(\mathbf{k}) \left(s\beta f_0(\mathbf{k}) \int (d\mathbf{k}') G_2(\mathbf{k}, \mathbf{k}') \tilde{f}(\mathbf{k}') \right), \tag{10.1}$$

which mimics the Yang-Yang equation of the Thermodynamic Bethe Ansatz (TBA).

This integral equation is first applied to an weakly interacting Bose gas in two dimensions. In Chapter 5 the critical chemical potential and density at a fixed temperature is obtained for an *attractive* Bose gas:

$$\begin{aligned} n_c &\approx \frac{mk_BT}{2\pi\hbar^2} \log\left(1 + \frac{2\pi}{mg}\right) \\ \mu_c &\approx \frac{mgT}{2\pi} \log\left(1 + \frac{2\pi}{mg}\right) \end{aligned} \tag{10.2}$$

In the weak coupling limit, the form of critical chemical potential is in agreement with numerical simulation in [42], which is $\mu_c = mgT/2\pi \log(2C/mg)$ where $C \approx 13.2$ numerically. Our result indicated that $C = \pi$. The discrepancy may be attributed to the renormalization group running of g, which causes the effective $1/g$ to grow in the low-momentum end.

In Chapter 6, we have identified the unitary limit of a quantum gas as the limit where the two-body scattering phase taking the maximal values of $\pm\pi$. This corresponds to the same $g \to \infty$ limit in three dimensions, while for two dimensions the same limit arises if an infrared cutoff is given, for example coming from a

finite system size. Anticipating that the quantum gas is scale-invariant at the unitary limit, we have also defined various thermodynamics scaling functions. The numerical solutions to our integral equation at the unitary limit in two and three dimensions are presented in Chapter 7 and 8, respectively.

For the three dimensional fermion gas, we report a critical temperature $T_c/T_F \approx 0.1$ for the superfluid transition at finite temperature. For the three dimensional boson gas, we present evidence that the gas undergoes a strongly interacting version of BEC at critical density $n_c\lambda_T^3 \approx 1.3$.

Chapter 9 is devoted to the calculation of the ratio of shear viscosity to entropy density η/s, which has a conjecture lower bound of

$$\eta/s \geq \hbar/4\pi k_B \tag{10.3}$$

based on the relativistic AdS/CFT correspondence in three dimensions [26]. We calculated this ratio of unitary quantum gas in two and three dimensions using our integral equation.

In two dimensions, this ratio of attractive bosons drops below the bound by a factor of 0.4, however this could be an artifact of our approximation. For attractive fermions, the conjectured lower bound is reached at very large $\mu/T \approx 10^7$, however this was argued to occur in an unphysical or metastable region; in the physical regions, $\eta/s \geq 6.07\,\hbar/4\pi k_B$.

In three dimensions, we report ratios that are above the bound for both boson and fermion gases. The fermionic ratio is 4.72 times the bound, while the bosonic one is 1.26 times the bound. The recent finding by Cao *et. al.* [4] put the experimental value for the fermionic ratio in the range of 0.4-0.5, in good agreement with our result.

APPENDIX A

S-MATRIX AND RESOLVANT

In this section we shall review some elements of scattering theory, with the ultimate goal of proving the relationship (2.5). For a more thorough introduction, please see [44].

We restate here the definition of resolvants:

$$\begin{aligned} G(E) &= \frac{1}{E - H + i\eta} \\ G_0(E) &= \frac{1}{e - H_0 + i\eta}, \end{aligned} \tag{A.1}$$

where η is a real positive infinitesimal, and the full Hamiltonian H can be split into a free part H_0 and an interaction part H_1. We have full knowledge of the eigenstate and eigenvalues of H_0.

In addition, we shall assume that the eigenvalues of H_0 are densed, and (without loss of generality) the ground state energy is zero. So for any given $E > 0$, there exists an eigenstate with energy E. Also we assume that the perturbation H_1 connects the free and interacting Hilbert spaces adiabatically, so that there is a one-to-one correspondence of states.

The interaction H_1 may shift the ground-state energy. If the exact ground-state energy of the full Hamiltonian H is $\Delta E \neq 0$, we make the following modifications so that the ground states of H_0 and H have the same energy:

$$\begin{aligned} H_0 &\to H_0 + \Delta E \\ H_1 &\to H_1 - \Delta E \end{aligned} \tag{A.2}$$

We want to solve the full time-independent Schroedinger's equation for H:

$$H|\Psi_a\rangle = E_a|\Psi_a\rangle, \tag{A.3}$$

where a represents all necessary labels. A good starting point is to build $|\Psi_a\rangle$ from its free counterpart $|\Phi_a\rangle$, which satisfies:

$$H_0|\Phi_a\rangle = E_a|\Phi_a\rangle. \tag{A.4}$$

Subtracting (A.4) from (A.3), using $H = H_0 + H_1$, and doing some rearrangement, one may formally write:

$$|\Psi_a\rangle = |\Phi_a\rangle - \frac{1}{H_0 - E_a} H_1|\Psi_a\rangle \tag{A.5}$$

Since the operator $(H_0 - E_a)^{-1}$ has poles along the real axis, we add to the denominator the infinitesimal $\pm i\eta$. Depending on our choice of the sign, two sets of states emerges from two equations:

$$\begin{aligned} |\Psi_a^+\rangle &= |\Phi_a\rangle + G_0(E_a)H_1|\Psi_a^+\rangle \\ |\Psi_a^-\rangle &= |\Phi_a\rangle + G_0^*(E_a)H_1|\Psi_a^-\rangle. \end{aligned} \tag{A.6}$$

These equations (A.6) are known as the Lippmann-Schwinger equations. The state $|\Psi^+\rangle$ corresponds to the *incoming* state, while $|\Psi^-\rangle$ is the *outgoing* state. These equations have formal solutions:

$$\begin{aligned} |\Psi_a^+\rangle &= (1 + G(E_a)H_1)\,|\Phi_a\rangle \\ |\Psi_a^-\rangle &= (1 + G^*(E_a)H_1)\,|\Phi_a\rangle \end{aligned} \tag{A.7}$$

To see that the assignment of incoming and outgoing states make sense, we consider the case of $|\Psi^+\rangle$, and define a wave packet localized in time:

$$|\Psi_a^+(t)\rangle \equiv \sum_\kappa c_\kappa e^{-iE_\kappa t}|\Psi_\kappa^+\rangle, \tag{A.8}$$

where the coefficient c_κ is sharply centered around $\kappa = a$. It's non-interacting counterpart is

$$|\Phi_a(t)\rangle \equiv \sum_\kappa c_\kappa e^{-iE_\kappa t}|\Phi_\kappa\rangle \tag{A.9}$$

Using the Lippmann-Schwinger equation (A.6), we can formally write (A.8) in terms of the free eigenstates:

$$\begin{aligned} |\Psi_a^+(t)\rangle &= |\Phi_a(t)\rangle + \sum_n f_n(t)|\Phi_n\rangle \ ; \\ f_n(t) &\equiv \sum_\kappa c_\kappa \frac{e^{-iE_\kappa t}}{E_\kappa - E_n + i\eta}\langle\Phi_n|H_1|\Psi_\kappa^+\rangle. \end{aligned} \tag{A.10}$$

The label κ contains energy and possibly other quantum numbers. Let us explicitly display the energy dependences:

$$\begin{aligned} c_\kappa &\to c_K(E) \ , \\ R_{n\kappa} \equiv \langle\Phi_n|H_1|\Psi_\kappa^+\rangle &\to R_{nK}(E), \end{aligned} \tag{A.11}$$

where K denotes all the other labels necessary to specify a quantum state. Then the coefficient $f_n(t)$ is

$$f_n(t) = \sum_K \int dE\, c_K(E) R_{nK}(E) \frac{e^{-iEt}}{E - E_n + i\eta} \tag{A.12}$$

Assuming $c_K(E)$ and $R_{nK}(E)$ do not contain poles in E, we see that $f_n(t) = 0$ as $t \to -\infty$. In the far-past, the wave packet $|\Psi_a^+(t)\rangle$ coincides with the non-interacting $|\Phi_a(t)\rangle$. We may thus identify the "+"-states with the incoming states in a scattering process.

Similarly, one identifies the "−"-states with the outgoing states by using the same argument as above. The only difference is that in (A.12) the sign of η is reversed, reducing the state to the non-interacting version in the far-future instead.

The scattering matrix is defined to be the overlap of in- and out-states:

$$S_{fi} = \langle\Psi_f^-|\Psi_i^+\rangle. \tag{A.13}$$

With (A.6) and (A.7), we can formally rewrite the inner product as:

$$\begin{aligned}\langle\Psi_f^-|\Psi_i^+\rangle &= \langle\Phi_f|\Psi_i^+\rangle + \langle\Phi_f|H_1G(E_f)|\Psi_i^+\rangle \\ &= \langle\Phi_f|\Phi_i\rangle + \langle\Phi_f|G_0(E_i)H_1|\Psi_i^+\rangle + \langle\Phi_f|H_1G(E_f)|\Psi_i^+\rangle \\ &= \delta_{fi} + \left(\frac{1}{E_f - E_i + i\eta} + \frac{1}{E_i - E_f + i\eta}\right)\langle\Phi_f|H_1|\Psi_i^+\rangle.\end{aligned} \tag{A.14}$$

To get to the last line, we made use of the fact that the free eigenstates form an orthonormal set of basis, so that $\langle\Phi_f|\Phi_i\rangle = \delta_{fi}$. Also the operators G and G_0 can be replaced by their respective eigenvalues when acting on their eigenstates $|\Psi_i^+\rangle$ and $\langle\Phi_f|$.

Making use of the identity $(x+i\eta)^{-1} - (x-i\eta)^{-1} = 2\pi i\delta(x)$, we can now recast (A.14) into the familiar form:

$$\begin{aligned}S_{fi} &= \delta_{fi} + 2\pi i\,\delta(E_f - E_i)\,T_{fi}\ ; \\ T_{fi} &\equiv \langle\Phi_f|H_1|\Psi_i^+\rangle = \langle\Phi_f|\,(H_1 + H_1G(E_i)H_1)\,|\Phi_i\rangle\end{aligned} \tag{A.15}$$

Now we are free to take the energy of the initial state off-shell by the introduction of the operators $\hat{S}(E)$ and $\hat{T}(E)$:

$$\begin{aligned}\hat{S}(E) &\equiv 1 + 2\pi i\delta(E - H_0)\,\hat{T}(E)\ , \\ \hat{T}(E) &\equiv H_1G(E)H_1\ , \\ S_{fi} &= \langle\Phi_f|\hat{S}(E_i)|\Phi_i\rangle.\end{aligned} \tag{A.16}$$

We are now in the position to derive the equation (2.5), reproduced below:

$$\hat{S} = G_0^*(G^*)^{-1}GG_0^{-1}. \tag{A.17}$$

To begin with, we make use of the following identities to rewrite (A.17), both easily proven from the definition (A.1):

$$\begin{aligned}(G^*)^{-1}G &= 1 - 2i\eta\,G\ , \\ G_0^*G_0^{-1} &= 1 + 2i\eta\,G_0^*.\end{aligned} \tag{A.18}$$

The right hand side of (A.17) then becomes:

$$\begin{aligned} G_0^*(G^*)^{-1}GG_0^{-1} &= G_0^*\,(1-2i\eta\,G)\,G_0^{-1} \\ &= (1+2i\eta\,G_0^*) - 2i\eta\,G_0^*GG_0^{-1} \\ &= 1+2i\eta\,G_0^*(G_0-G)G_0^{-1} \end{aligned} \tag{A.19}$$

Next, we use $G_0 - G = -G_0H_1G$ to get:

$$G_0^*(G^*)^{-1}GG_0^{-1} = 1 - 2i\eta\,(G_0^*G_0)(H_1GG_0^{-1}) \tag{A.20}$$

Finally, we can show that $-2i\eta\,G_0^*(E)G_0(E) = 2\pi i\delta(E-H_0)$, and that $GG_0^{-1} = 1 + GH_1$. Substitute these identities into last equation, and we get:

$$G_0^*(G^*)^{-1}GG_0^{-1} = 1 + 2\pi i\,\delta(E-H_0)H_1(1+GH_1) = \hat{S}(E) \tag{A.21}$$

as required.

BIBLIOGRAPHY

[1] T. Bourdel, J. Cubizolles, L. Khaykovich, K. M. F. Magalhães, S. J. J. M. F. Kokkelmans, G. V. Shlyapnikov, and C. Salomon. Measurement of the interaction energy near a feshbach resonance in a ^6li fermi gas. *Physical Review Letters*, 91(2):020402, Jul 2003.

[2] A. Bulgac, Joaquín E. D., and P. Magierski. Spin 1/2 fermions in the unitary regime: A superfluid of a new type. *Physical Review Letters*, 96(9):090404, Mar 2006.

[3] E. Burovski, N. Prokof'ev, B. Svistunov, and M. Troyer. Critical temperature and thermodynamics of attractive fermions at unitarity. *Physical Review Letters*, 96(16):160402, Apr 2006.

[4] C. Cao, E. Elliott, J. Joseph, H. Wu, J. Petricka, T. Schäfer, and J. E. Thomas. Universal quantum viscosity in a unitary fermi gas. *Science*, 331(6013):58–61, 2011.

[5] Cheng Chin, Rudolf Grimm, Paul Julienne, and Eite Tiesinga. Feshbach resonances in ultracold gases. *Reviews of Modern Physics*, 82(2):1225–1286, Apr 2010.

[6] S. L. Cornish, N. R. Claussen, J. L. Roberts, E. A. Cornell, and C. E. Wieman. Magnetic field dependence of ultracold inelastic collisions near a feshbach resonance. *Physical Review Letters*, 85:1795, 2000.

[7] R. S. Crandall and R. Williams. Crystallization of electrons on the surface of liquid helium. *Physics Letters A*, 34(7):404–405, 1971.

[8] R. Dashen, S.-K. Ma, and H. Bernstein. S-matrix formulation of statistical mechanics. *Physical Review*, 187(1):345, 1969.

[9] K. Dieckmann, C. A. Stan, S. Gupta, Z. Hadzibabic, C. H. Schunck, and W. Ketterle. Decay of an ultracold fermionic lithium gas near a feshbach resonance. *Physical Review Letters*, 89(20):203201, Oct 2002.

[10] D. M. Eagles. Possible pairing without superconductivity at low carrier concentrations in bulk and thin-film superconducting semiconductors. *Physical Review*, 186(2):456–463, Oct 1969.

[11] A. L. Fetter and J. D. Walecka. *Quantum Theory of Many-Particle Systems*. Dover Publications, 1971.

[12] D. S. Fisher and P. C. Hohenberg. Dilute bose gas in two dimensions. *Physical Review B*, 37(10):4936–4943, Apr 1988.

[13] B. A. Gelman, E. V. Shuryak, and I. Zahed. Ultracold strongly coupled gas: A near-ideal liquid. *Physical Review A*, 72(4):043601, Oct 2005.

[14] M. Greiner, C. A. Regal, and D. S. Jin. Emergence of a molecular bose-einstein condensate from a fermi gas. *Nature*, 426:537, 2003.

[15] C. C. Grimes and G. Adams. Evidence for a liquid-to-crystal phase transition in a classical, two-dimensional sheet of electrons. *Physical Review Letters*, 42(12):795–798, Mar 1979.

[16] T.-L. Ho. Universal thermodynamics of degenerate quantum gases in the unitarity limit. *Physical Review Letters*, 92(9):090402, Mar 2004.

[17] P. C. Hohenberg. Existence of long-range order in one and two dimensions. *Physical Review*, 158(2):383–386, Jun 1967.

[18] M. Holzmann, G. Baym, J. P. Blaizot, and F. Laloë. The kosterlitz-thouless-berezinskii transition of homogeneous and trapped bose gases in two dimensions. *Proceeding of National Academic of Science USA*, 104:1476, 2007.

[19] P.-T. How and A. LeClair. Critical point of the two-dimensional bose gas: an s-matrix approach. *Nuclear Physics B*, 824:415, 2010.

[20] P.-T. How and A. LeClair. S-matrix approach to quantum gases in the unitary limit i: the two-dimensional case. *Journal of Statistical Mechanics: Theory and Experiment*, pages –03025, 2010.

[21] P.-T. How and A. LeClair. S-matrix approach to quantum gases in the unitary limit ii: the three-dimensional case. *Journal of Statistical Mechanics: Theory and Experiment*, pages –07001, 2010.

[22] H. Hu, X. J. Liu, and P. D. Drummond. Equation of state of a superfluid fermi gas in the bcs-bec crossover. *EPL (Europhysics Letters)*, 74(4):574, 2006.

[23] S. Inouye, M. R. Andrews, J. Stenger, H. J. Miesner, D. M. Stamper-Kurn,

and W. Ketterle. Observation of feshbach resonances in a bose–einstein condensate. *Nature*, 392:151, 1998.

[24] E. B. Kolomeisky and J. P. Straley. Renormalization-group analysis of the ground-state properties of dilute bose systems in d spatial dimensions. *Physical Review B*, 46(18):11749–11756, Nov 1992.

[25] V. E. Korepin, N. M. Bogoliubov, and A. G. Izergin. *Quantum Inverse Scattering Method and Correlation Functions*. Cambridge Monographs on Mathematical Physics. Cambridge University Press, 1997.

[26] P. K. Kovtun, D. T. Son, and A. O. Starinets. Viscosity in strongly interacting quantum field theories from black hole physics. *Physical Review Letters*, 94(11):111601, Mar 2005.

[27] M. Le Bellac. *Thermal Field Theory*. Cambridge University press, 1996.

[28] A. LeClair. Interacting bose and fermi gases in low dimensions and the riemann hypothesis. *International Journal of Modern Physics*, A23:1371, 2008.

[29] D. Lee and T. Schäfer. Cold dilute neutron matter on the lattice. ii. results in the unitary limit. *Physical Review C*, 73(1):015202, Jan 2006.

[30] P. Massignan, G. M. Bruun, and H. Smith. Viscous relaxation and collective oscillations in a trapped fermi gas near the unitarity limit. *Physical Review A*, 71(3):033607, Mar 2005.

[31] N. D. Mermin and H. Wagner. Absence of ferromagnetism or antiferromagnetism in one- or two-dimensional isotropic heisenberg models. *Physical Review Letters*, 17(22):1133–1136, Nov 1966.

[32] P. Nikolićand S. Sachdev. Renormalization-group fixed points, universal phase diagram, and $1/n$ expansion for quantum liquids with interactions near the unitarity limit. *Physical Review A*, 75(3):033608, Mar 2007.

[33] Y. Nishida and D. T. Son. Fermi gas near unitarity around four and two spatial dimensions. *Physical Review A*, 75(6):3617, 2007.

[34] P. Nozières and S. Schmitt-Rink. Bose condensation in an attractive fermion gas: From weak to strong coupling superconductivity. *Journal of Low Temperature Physics*, 59(195), 1985.

[35] K. M. O'Hara, S. L. Hemmer, M. E. Gehm, S. R. Granade, and J. E. Thomas. Observation of a strongly interacting degenerate fermi gas of atoms. *Science*, 298(5601):2179–82, 2002.

[36] A. Perali, P. Pieri, L. Pisani, and G. C. Strinati. Bcs-bec crossover at finite temperature for superfluid trapped fermi atoms. *Physical Review Letters*, 92(22):220404, Jun 2004.

[37] E. M. Peskin and V. D. Schroeder. *An Introduction to Quantum Field Theory*. Westview Press, 1995.

[38] D. S. Petrov, M. A. Baranov, and G. V. Shlyapnikov. Superfluid transition in quasi-two-dimensional fermi gases. *Physical Review A*, 67(3):031601, Mar 2003.

[39] P. Phillips. *Advanced Solid State Physics*. Westview Press, 2002.

[40] W. D. Phillips. Laser cooling and trapping of neutral atoms. *Reviews of Modern Physics*, 70:721, 1998.

[41] V. N. Popov. *Functional Integrals in Quantum Field Theory and Statistical Physics*. Reidel, Drodrecht, 1983.

[42] N. Prokof'ev, O. Ruebenacker, and B. Svistunov. Critical point of a weakly interacting two-dimensional bose gas. *Physical Review Letters*, 87:270402, 2001.

[43] F. Reif. *Fundamentals of Statistical and Thermal Physics*. McGraw-Hill, 1965.

[44] P. Roman. *Advanced Quantum Theory*. Addison-Wesley Series in Advanced Physics. Addison-Wesley, 1965.

[45] G. Rupak and T. Schäfer. Shear viscosity of a superfluid fermi gas in the unitarity limit. *Physical Review A*, 76(5):053607, Nov 2007.

[46] T. Schäfer. Ratio of shear viscosity to entropy density for trapped fermions in the unitarity limit. *Physical Review A*, 76(6):063618, Dec 2007.

[47] D. T. Son. Toward an ads/cold atoms correspondence: A geometric realization of the schrödinger symmetry. *Physical Review D*, 78(4):046003, Aug 2008.

[48] H. B. Thacker. Many-body scattering processes in a one-dimensional boson system. *Physical Review D*, 14(12):3508–3519, Dec 1976.

[49] H. B. Thacker. Statistical mechanics of a (1 + 1)-dimensional quantum field theory at finite density and temperature. *Physical Review D*, 16(8):2515–2525, Oct 1977.

[50] S. Weinberg. *Quantum Theory of Fields*, volume 1. Cambridge University PRess, 1995.

[51] C. N. Yang and C. P. Yang. Thermodynamics of a one-dimensional system of bosons with repulsive delta-function interaction. *Journal of Mathematical Physics*, 10pages, 1969.